Comparing hardness tests to estimate, evaluate, and analyse the mechanical properties of structural steel

Govind Gopi

A thesis submitted in fulfillment of the requirements

for the degree of Master of Engineering

Main supervisor: Dr Zhiyuan (Arthur) Fang

Co-supervisors: Prof James Lim and Dr Kris Roy

School of Engineering

The University of Waikato

New Zealand

2024

Abstract

The paper investigates the mechanical properties of structural steels, focusing on hardness and toughness, which are important indicators used in industrial applications. In total, four major hardness testing methods were analysed: Vickers, Rockwell, Brinell, and Leeb, and the Charpy impact test was used to measure toughness. The hardness tests evaluated the precision with which steel resistance to deformation can be determined under different conditions, and the Charpy test examined their energy absorption capacity in case of sudden fractures and tensile testing was estimated on them to study the range of yield strength and ultimate tensile strength. This research has conducted 288 experimental tests to evaluate the correlation between various hardness testing methods (Brinell, Vickers, Rockwell, and Leeb) and the mechanical properties of the structural steel samples. Further, 42 experimental tests were performed for the Charpy impact test to evaluate a correlation between Charpy impact values and mechanical properties of the structural steel samples. 330 samples were prepared for the respective tests, representing various structural steel grades (Grade 300, 350, and 400). Among different grades of steel samples, 350-grade steel exhibited a higher impact energy of 94.4 J. Both Charpy Impact Values and Hardness Test Values were plotted against ultimate tensile strength and yield strength to determine if there is a correlation between the properties. The results reveal a better accuracy of Vickers and Rockwell tests as they revealed only an error percentage of 2.5% and 1.9%, respectively, especially for fine-grained materials, while Leeb is characterized by good convenience in large-scale testing at the site. Although the Brinell test is very effective for coarse structures, it was not as precise as martensite in more complex microstructures. Both hardness and tensile strength showed a strong correlation, indicating that hardness may accurately predict the material strength. The study also highlights the reverse relationship between hardness and toughness.

This research contributes to structural steel testing by proposing methods to predict mechanical properties using non-destructive testing techniques. It sets the stage for future improvements

in hardness testing models by incorporating factors like microstructural variations, strain hardening, and heat treatment, which can enhance the accuracy of predictions. Furthermore, the research underscores the importance of portable hardness testing methods and emphasizes the need for improved calibration protocols to ensure more accurate in-situ measurements.

Acknowledgements:

I would like to express my heartfelt gratitude to my esteemed professors, Dr Arthur Fang, my chief supervisor, James Lim, and Dr Kris Roy, for their invaluable help, support, and guidance on the research. I am also immensely grateful to Kaveh Andisheh, General Manager of Structural Systems at HERA, for guiding me in a valuable research topic and supporting me at every step.

I sincerely thank Kurt Hatchard, the Workshop Supervisor from Grayson Engineering, for providing the samples needed for my research. Additionally, I would like to thank Shannon McMurray for arranging the Charpy impact machine from Wurth, Dr Leandro Bolzoni for his ongoing support, and always answering my questions about the project. I appreciate the technical assistance provided by Dr Sophia Rodriguez, Peter Higgins, Jonathan Van Harselaar, Duncan Barnard, and Giss George in the laboratory. I must also thank Cole Dawson for his prompt assistance in setting up the Charpy machine. I also would like to express my appreciation for all the help from Mohammed Al-Adawi, Yi Xao, and Anusharan Poudyal throughout my experiments and for sharing ideas.

Special thanks to the University of Waikato; School of Engineering for providing experimental equipment and research assistance. Finally, I want to express my profound gratitude to my family and friends for their unwavering support.

Declaration of Authorship:

I, Govind Gopi, declare that this dissertation is my own work. Any materials, ideas, or submissions from other authors have been properly cited and appropriately acknowledged wherever they have been used.

Table of Contents

List of Figures

List of Tables

1. Introduction

Structural steel is a cornerstone of modern structural engineering. It is renowned for its exceptional mechanical properties, including hardness, toughness, and remarkable tensile strength. These qualities enable structural steel to endure significant stresses throughout its lifecycle across various applications. Additionally, its recyclability and durability make it an environmentally sustainable choice in contemporary construction, fully aligning with the principles of sustainable development. Structural steel is distinguished by its strength, ductility, fracture toughness, and weldability—attributes crucial for creating resilient infrastructure such as buildings and bridges. Steel's closed-loop material cycling allows it to be recycled without compromising quality, making it indispensable for its mechanical benefits and positive environmental impact. There have been sufficient studies on the relationship between hardness tests and steel's mechanical properties, so many correlations have already been developed. Hardness tests (Vickers and Brinell) are often used as a fast and inexpensive alternative to determine mechanical properties, e.g., yield strength and tensile strength. It has been shown that hardness values can be used to provide a linear relationship between yield stress and tensile strength for a variety of steel samples, indicating that hardness may be a generally reliable tool for approximating these material properties independent of the specific steel composition and treatment [1,2]. It has also been successful in predicting limits of fatigue, often with increases in hardness corresponding to increases in the resistance to fatigue. Hardness tests are a convenient way to measure the mechanical properties of steel, and exhibit a good correlation with yield strength, tensile strength, and fatigue strength[3].

Engineers commonly conduct coupon tests to assess the mechanical properties of structural steel. These tests involve extracting small, standardized samples—known as coupons—from the steel. Although coupon tests are efficient, they have notable limitations. They are performed on small, isolated samples, which may not accurately reflect the material's performance in realworld applications. Furthermore, since these tests are typically conducted off-site in controlled environments, they do not adequately account for the conditions the steel will face in actual use. As a result, engineers often struggle to understand the material's behaviour under complex, in-situ conditions, highlighting the need for rapid and reliable field-testing methods for timely design assessments and construction decisions.

Current methods to correlate hardness testing results and Charpy impact values with yield and tensile strength are limited. While hardness testing offers a quick, non-destructive assessment, it often requires separate, resource-intensive tensile testing to accurately determine yield and tensile strength. Preparing tensile specimens involves precise machining, which is resource-intensive and may require advanced equipment [4]. This complexity adds time, cost, and logistical challenges, particularly when field samples need transportation to laboratories.

This research aims to enhance the correlation between hardness testing, Charpy impact measurements, and the tensile properties of structural steel. The study seeks to determine whether these tests can reliably predict tensile properties without the need for separate tensile testing. By bridging the gap between different testing methodologies, this research aims to offer a more efficient mechanical property evaluation method, particularly for on-site assessments. This integrated approach can potentially reduce costs and improve the speed of evaluations, ensuring that steel used in critical infrastructure meets necessary performance standards under varying environmental conditions, including seismic events.

The mechanical properties of materials, especially steel, are the prime features that govern their accomplishment in engineering service [5]. The steel grades within the range of 300-400 grades cover carbon steel and alloy steel types that have good acceptance in structural applications in construction, manufacturing, or other process industries because of their favourable strength, hardness, and toughness[5,6]. The prediction and evaluation of these mechanical properties are of utmost importance in material reliabilities with respect to service safety. In the list of different important properties of the materials to be determined are hardness and toughness, as both of them are directly proportional to the resistance of any material to deformation, wear, and fracture[7]. In order to evaluate the hardness of materials, testing has been performed by evaluating resistance of the surface against deformation under load. In this context there are different types of hardness tests used for different materials and applications. Such hardness tests include Vickers, Rockwell, Brinell, and Leeb hardness tests[8]. Each test uses different indenters, loads, and methodologies to characterize material hardness. Besides from hardness, another major indication of material performance, especially in steel under a sudden force, is toughness[6]. Material toughness is usually measured by energy absorption at the time of fracture by the Charpy impact test, widely used.

Thus, it is inferred that hardness and impact tests are the two major tests of materials that need to be explored in a better manner. Therefore, the present paper discusses the comparative analysis by performing the Vickers, Rockwell, Brinell, and Leeb hardness testing methods[9] and the Charpy impact test in predicting the mechanical properties of steel grades within the range of 300 to 400. Therefore, in the succeeding section, complete discussion of different hardness and impact testing are briefly discussed, which are given below[7].

1.1 Hardness testing

Hardness is a basic property that characterizes the resistance of a material to indentation, abrasion, or scratching. The hardness testing methods are used to predict other mechanical properties such as tensile strength, wear resistance, and machinability. The value of hardness can often give a better indication of the structural adequacy of the material and its load-carrying capacity before its failure[10]. The characteristics of the four most common hardness testing methods—Vickers, Rockwell, Brinell, and Leeb—offer many different ways to measure hardness under many conditions and load applications.

1.1.1 Vicker's hardness testing:

The Vickers hardness (HV) test is a microhardness test that uses a diamond indenter in a square-based, pyramidal shape[11]. The schematic image is shown in Figure 1[12]. It is particularly useful in testing surface layers and thin sections of steel. In the Vickers hardness test, the hardness number is calculated by dividing the applied load by the surface area of the indentation produced[11]. The formula used for calculating the hardness is available in equation (1)[12]. This test has the advantage of giving precise measures irrespective of the level of hardness of the material. Besides, the Vickers test can be conducted on any material, with no need for big samples.

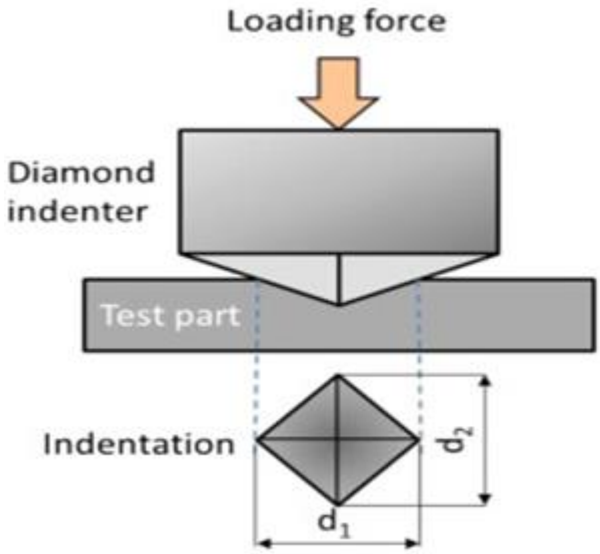

Figure 1: Schematic diagram of Vicker's Hardness tester.

$$HV = 1.8544 \frac{P}{d^2} \quad \dots\dots\dots\dots\dots (1)$$

where, P is loading force and d is diameter of diagonal of the indentations.

1.1.2. Rockwell hardness test

Rockwell hardness test (HR) is another widely used method for determining the hardness of steel. In the Rockwell test, indentation is affected by means of a conical or spherical indenter, whereby hardness is expressed in terms of depth of penetration for a given load. This is a fairly quick and simple test, and there are different Rockwell scales—the Rockwell scales A, B, and C, which are used on materials of different hardness[13]. Due to the simplicity and quickness of this technique, Rockwell hardness testing is preferred in many industrial applications. The apparatus of Rockwell hardness test is shown in Figure 2[14].

Figure 2: Illustration of Rockwell hardness tester

1.1.3. Brinell hardness test

The Brinell hardness test, HB, is important for larger materials with coarse or heterogeneous structures. In this test method, a hardened steel or carbide ball is pressed into the surface of the material, and the Brinell hardness number, BHN, is obtained by the formula of the applied load over the surface area of the indentation [13] [15]. Although, it is much slower than the Rockwell test, the Brinell test is more versatile and permits testing of a broad range of hardness items. This is especially suitable for castings, forgings, and other shaft-like steel components. The Brinell hardness number (HB) is calculated by using the equation (2)[13], given below:

$$HB = \frac{P}{\pi D\ (D - (\sqrt{D^2} - \sqrt{d^2}))} \ldots\ldots\ldots\ldots\ldots..(2)$$

1.1.4. Leeb hardness test

A Leeb (or HLD — Hardness, Leebsky devices) test is a dynamic method of testing the hardness without requiring much space for most inspections with large products to be performed on-site. In this test, the hardness is determined by measuring respectively the rebound velocity and impact velocity of a dropped MIRS body on surface material. The Leeb test offers higher advantages and is best performed for on-site testing of steel structures and large machinery, even though it is less used under laboratory settings, as you can still access the data in real-time. In the Leeb hardness testing method, a hardness value is calculated from the energy loss of an impact body that strikes a metal surface. This loss of energy is known as the Leeb quotient and gives information on how much deformation was experienced by the material. The impact body rebounds more rapidly from harder materials than from softer ones, resulting in a greater value of 1000 * (vr / vi), where "vr" denotes the rebound velocity and "vi" signifies the impact velocity. This value is expressed as the Leeb rebound hardness unit, HL. The Leeb hardness tester is shown in Figure 3[16].

Figure 3:Depiction of the Leeb hardness tester.

1.2. Charpy Impact Test

In addition to hardness, toughness is a crucial property that indicates a material's ability to absorb energy during fracture. The Charpy impact test is a standardized method used to assess a material's toughness under high strain rate conditions. This test involves striking a notched specimen with a pendulum hammer. The specimen used in the Charpy impact test can feature either a V-shaped or U-shaped notch, with the notch oriented away from the pendulum during testing. The testing apparatus can vary in size, ranging from a compact, bench-top model to a larger, floor-mounted version, depending on the specific requirements of the test and the size of the specimens being evaluated. The absorbed energy reflects the material's toughness and its resistance to sudden brittle fracture[17]. For steel grades in the range of 300 to 400, the Charpy impact test is particularly important for evaluating their performance in environments requiring high toughness, such as low-temperature settings or situations involving dynamic loading conditions. The schematic diagram of Charpy impact test is shown in Figure 4 [18]and equation used for evaluating the toughness of materials is given in equation (3)[19].

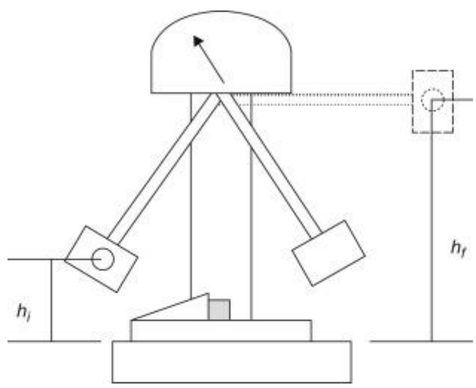

Figure 4: Schematic diagram of Charpy impact test

$$\mu_{total} = \text{mg}\,[h_0 - h_f] \text{ ....(3)}$$

Where, μ_{total} is the total energy stored by the specimen, m is the mass of the specimen, h_0 is the initial height of the pendulum, and h_f is the final height of the pendulum.

1.3. Tensile testing

It is one of the most fundamental methods of mechanical testing of materials wherein measures the resistance of materials against deformation under uniaxial loading. In this testing behaviour of materials are studied under axial load until they break and estimates the strength, ductility, and elasticity of materials. It is a common way in which the mechanical properties of materials are determined and is extensively used throughout industry with applications ranging from aerospace to automotive and construction. Therefore, this test is vital for material characterisation and where the load-bearing capacity of materials is critical. Furthermore, Tensile testing is based on the principle wherein consists of applying an increasing tensile load on a standardized specimen until rupture. The specimen is typically a long piece with a consistent cross-section shape and size that is clamped into a test machine capable of measuring force applied to the sample and, in some cases, elongation as well. Upon the application of load, stress (force/unit area) and strain (deformation/unit length) data are obtained. There are different points on the stress-strain diagram that denotes various regions or zone (elastic zone, yield point, plastic zone, ultimate tensile strength and fracture point of material under axial loading[20,21]. The same can be inferred from Figure 5[21].

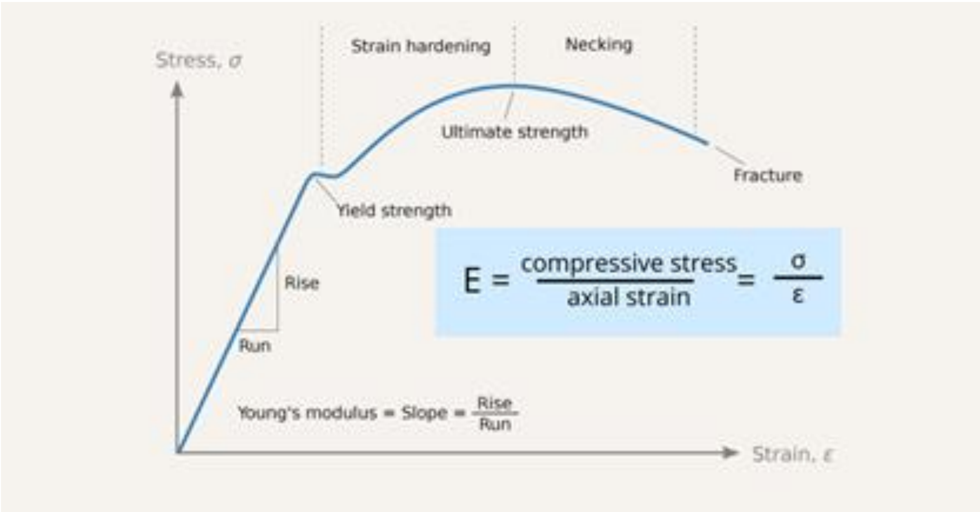

Figure 5: Stress-strain plot of steel materials

Chapter 2: Literature Review

2.1. Significance of Hardness and Charpy Impact Tests in the Expanding Steel Industry

From the last two to three decades, the steel industry has been swiftly growing due to its critical importance in sectors such as building, car manufacturing, and energy production. The steel industry has become pervasive, employed across multiple sectors such as construction, automotive, and energy. In particular, within the building industry [41-40], steel is extensively used, and many engineers are looking for quick assessment methods to evaluate the safety of structures. The increasing demand of steel because of their high-strength and high-performance materials has made this material a central focus of interest. The hardness and impact toughness (assessed with different types of hardness/Charpy tests) properties are important to understand behaviour of steel under several service conditions out of these. Hence, the present literature review, aims to detail these tests as vital tools in ensuring the standards and dependability of numerous steel products within an industry that is still seeing maximum development.

Hardness is a mechanical property that can be characterized by scratch resistance, area to volume ratio and index of plastic deformity (classical meaning). This property is tested using various hardness tests, such as Rockwell and Vickers and Brinell hardness test, etc. The evaluation of hardness plays a vortex in the mechanical characteristics since it offers indirect information about other properties i.e., strength, wear resistance and tensile [41]. The hardness test is frequently used in steel manufacturing to determine the effectiveness of heat treatments, coatings and alloying elements on steel that how can it resist external stresses throughout its service[42].

As per the study presented in [13], it was inferred that the significance of hardness testing lies in its rapid and straightforward non-destructive evaluation of materials, rendering it one of the most prevalent procedures for quality control in high-volume production. The steel industry performs this test to guarantee their steel products meet the requisite performance criteria. For instance, the tool steels and automotive components require an extreme high hardness to withstand against wear as well as fatigue [43]. Hardness tests are also used to evaluate the influence of alloying element such as carbon, chromium and vanadium that would increase steel hardness [44].

(a) (b)

Figure 6: (a) Image of Rockwell, (b) Charpy impact pendulum tester

The Charpy impact test is a measure of material toughness, or the ability to be absorbing energy during breakage. This is very important especially in the steel industry where steel may experience operational dynamic loading conditions like impacts and shocks during its service life[17,26] . The test consists of striking a bar of steel, (standard size 10 x l0mm) by pendulum hammer and observe the energy absorbed in cracking it. The test results, which are usually reported in joules, reflect how much energy it took to break the material at the different temperatures.

Over the years, the importance of Charpy impact test in steel industry has increased as demand for materials which can perform under least or below working conditions like low temperature service and high-pressure requirement community. Charpy impact testing is extremely necessary for shipbuilding industry, in which steel materials was suffered from hostile sea conditions and with the growth of automotive industrial sector worldwide, crashworthiness become a critical point[46]. The test is also important to evaluate the performance of materials in steels used for bridges, pipelines and nuclear reactors were brittle fracture criterion together with dynamic loads on them [47] The image of Rockwell hardness tester and Charpy impact pendulum tester is shown in Figure 6 [48] [18].

2.2. Correlation between Hardness and Mechanical Properties

A major part of any industrial application is determining the mechanical properties of materials, with a focus on metals such as steel. Hardness is one of the most frequently used properties that can serve as a simple and impartially accurate way to examine the material behaviour under stress or wear, for dealing with bending. There are a huge number of studies connecting hardness with important other mechanical properties like tensile strength, yield stress, and fracture toughness. This framework explains the relationship between hardness and mechanical properties, it really gives us a great picture of predicting how materials behave by simply performing some test to know their hardness.

Hardness testing is one of the most established approaches to evaluating mechanical performance on a steel material without breaking it. The resistance of steel to indentation is an important indicator as it helps determine surface hardness, which can be directly evaluated by various type of hardness tests like Vickers test, Schneider scale Brinell test etc[43]. The hardness of steel is mostly determined by various factors, including alloying elements, microstructural composition, and heat treatment methods. For example, higher carbon allows more martensite to form which is hard and homogeneous This causes a phase transformation on quenching which increases hardness and tensile strength also do reduces ductility and toughness [47]. Thus, as a selection criteria hardness it is acceptable, if it aligns with the requisite balance of mechanical qualities (hardness) for each application.

The relationship between **hardness and tensile strength** indicates the maximum stress that materials can endure while being elongated prior to failure. There is a long-accepted correlation that hardness and tensile properties of steel materials [49]. Thus, the concept of utilising hardness measurements as straightforward non-destructive testing methods for determining tensile strength. It was shown in the presented study that hardness is linearly related tensile strength of the materials. The empirical correlation between hardness (H) and tensile strength (σ) can be articulated through many different are given in equation (4).

$$\sigma = kH \ldots\ldots\ldots\ldots\ldots\ldots\ldots\ldots. (4)$$

Where, k is a material dependent constant. In different available studies, it was shown that the tensile strength of steel increases with increasing hardness because this affect mainly by carbon content, heat treatment and alloying elements [50]. Carbon steels with higher carbon content (e.g. 0,6%) increase their hardness and tensile strength after quenching & tempering processes[50,32].

Further, hardness is also directly linked with **yield strength** of the materials. Yield strength is the resistance of the materials that resist to deform plastically. For steels, higher hardness usually corresponds to greater yield strength, especially in high-strength low alloys in which hardness can be an important criterion of the material's resistance against deformation under a load[52] . This relationship has individually been looked at in different grades of steel, and the following general relation was established in equation (4).

$$H = 3\sigma_y \ldots\ldots\ldots\ldots\ldots\ldots (4)$$

Where, σ_y is the yield strength of material. This relation holds good for hardened steel, where hardness is directly related to heat treatment or alloying that can used to predict the variations of yield strength.

A linear relationship of yield strength or tensile and hardness was discovered for steels with a minimum yield strength from 325 to greater than 1700 MPa, other also found when the ultimate tensile strengths ranged within approximately 450 and 2350 MPa. The correlations also predict a lower strength for a given hardness in steels which are capable of significant strain hardening. However, the results show that strength is linearly affected within the range of hardness encountered in a typical steel such as non-austenitic hypoeutectoid steels. The strength is non-linearly related to hardness under low degree of hardness or strength[53]. The same can be observed from Figure **7** [54]**.**

(a) **(b)**

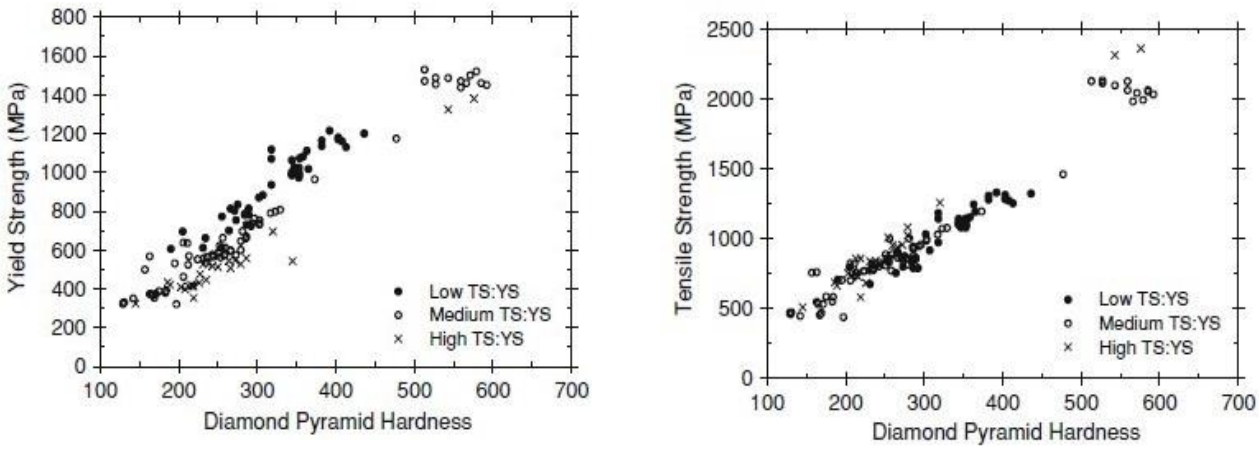

Figure 7: Diagram of (a) yield strength, (b) tensile strength vs hardness

Furthermore, **ductility of a material** is the measure the ability to deform plastically before rupture. It does not have a direct correlation with hardness, similar to yield strength and tensile strength[53]. The content of carbon in the steel in another factor that basically decided the hardness of the material. The same can be observed form Figure 8[55]. Particularly in steel, when hardened through heat treatments such as quenching, a rise in hardness correlates with an enhancement in strength, but at the expense of reduced ductility [43]. The increase in dislocation density and decrease of mobility atoms in a hardened matrix [55] caused reduced ductility. The martensitic steels, which are characterised by their high hardness, generally exhibit reduced toughness and ductility compared to their austenitized ferrite or pearlite counterparts [56].

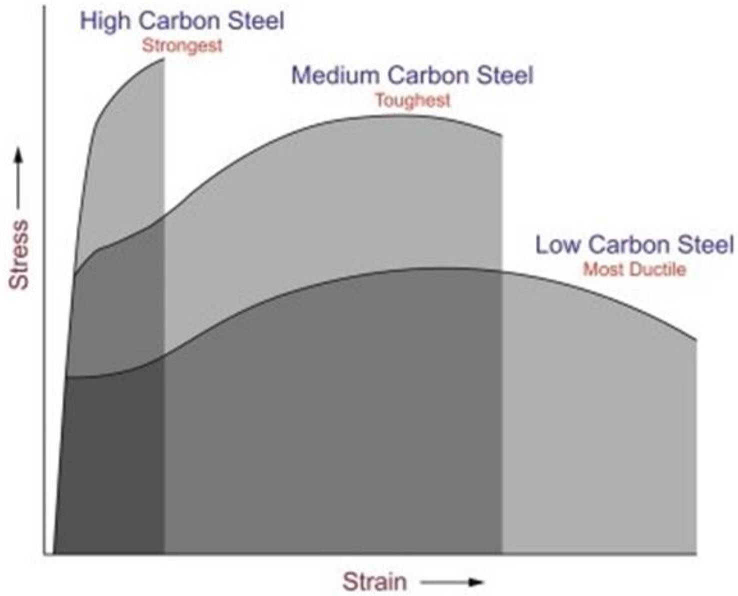

Figure 8: Plot depicted stress-strain plot of different carbon steel

This inverse correlation between hardness and ductility is the key consideration when it comes to alloys used in applications where both strengths followed by some degree of deformation are expected. In structural applications, such as in bridge construction, where internal stresses are concentrated during impact or shock loading for an extended period of time. Consequently, it cannot be neutralised by altering the material to diminish hardness and enhance ductility[57]. The balance is crucial for selecting a steel grade that possesses the requisite toughness and strength for particular purposes.

In parallel, **wear resistance** also means the ability of a material surface to resist wear by friction or abrasion / Erosion. The resistance of wear for the steel materials mainly depends on its hardness [58]. The harder materials are typically more wear-resistant, because they have greater resistance to surface deformation from abrasive or erosive forces [59]. The hardness testing is therefore often employed to predict wear resistance in applications like cutting tools, gears or bearings where material damage at the surface could lead to a failure of performance. Further, Steel microstructure has a significant impact on its abrasive wear behaviour. Austenite exhibits more abrasion resistance than the ferritic, pearlitic, or martensitic phases of the same hardness because, compared to others, austenite has a greater ability for strain hardening and higher ductility. For steels with lower carbon content (less than 1.0% C), when the hardness is around HRc60, similar wear resistance is observed in the order: bainite > water quenching > annealing > spheroidizing microstructure. The effects of steel hardness and microstructures on wear resistance are summarized in Figure 9 [60].

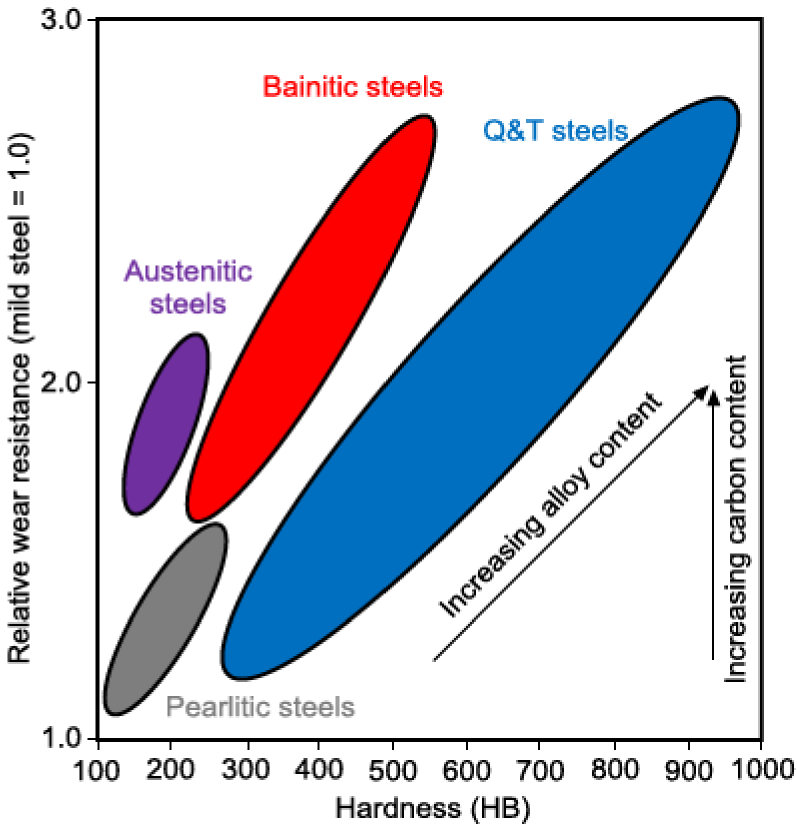

Figure 9: Effect of microstructure on the wear resistance and hardness

2.3. Correlation between Toughness and Mechanical Properties

Toughness, is the measures the amount of energy a material will absorb up to the point of fracture when subjected to sudden impact or dynamic loads. The interrelation among these properties—toughness with strength and ductility—is important for ideal selection of materials in manufacturing, especially for construction, automotive, and aerospace industries. This frame details the correlation between toughness and other mechanical properties and particularly the Charpy impact test, which is one of the most common methods for measuring this property[61].

The Charpy test has been around for many years and is one of the simplest tests for determining material toughness, especially in metals. This test consists of the impact by a pendulum hammer on an extruded specimen and measuring the energy absorbed in fracturing [62]. The energy absorbed is in joules, which indicates the material will not readily break.

One of the most important tests in assessing how a material performs is its ductile-to-brittle transition temperature (DBTT), which can be approximately determined by performing Charpy testing [63]. At high temperatures, materials behave in a ductile fashion and will absorb more energy before fracture occurs[64]. However, materials can be brittle at low temperatures, absorbing minimal energy before failing instantly with little or no deformation[65]. This is especially vital in the case of Arctic pipelines, where materials must retain toughness at low temperatures to avoid brittle fracture during service [66].

The Charpy impact test is a commonly used quality control method for materials and has direct bearing on the qualification of steels in many industrial applications, including construction, pipelines, and heavy machinery. Manufacturers can verify that the material meets toughness levels for use in specific applications by identifying where the DBTT is, as well as overall upper and lower shelf energy requirements[63].

Toughness is determined by numerous mechanical properties like strength, ductility, and hardness primarily. This is crucial for optimizing material selection and design in engineering applications.

Toughness and Strength: The relationship between hardness and strength in steel is non-linear, as it depends on the microstructural features of an alloy and processing. High toughness is usually accompanied by fine microstructures, and the latter improves crack resistance delaying unstable cleavage propagation. In other words, ultra-high toughness (UHT) steel has a yield strength of 1048 MPa with an acceptable Charpy impact energy of lower temperature-40°C at 250 J after controlled rolling and quenching [67]. In addition, the quenching and partitioning (Q&P) treatment can increase strength as well toughness but probably limited formability for room temperature uses.[68] As such, a 39.2% improvement in impact energy was also achieved for the nano precipitates and fine-grained structures[68,50]. The Ashby plot shows the relation between toughness and yield strength of steel materials which can see from Figure 10 [70].

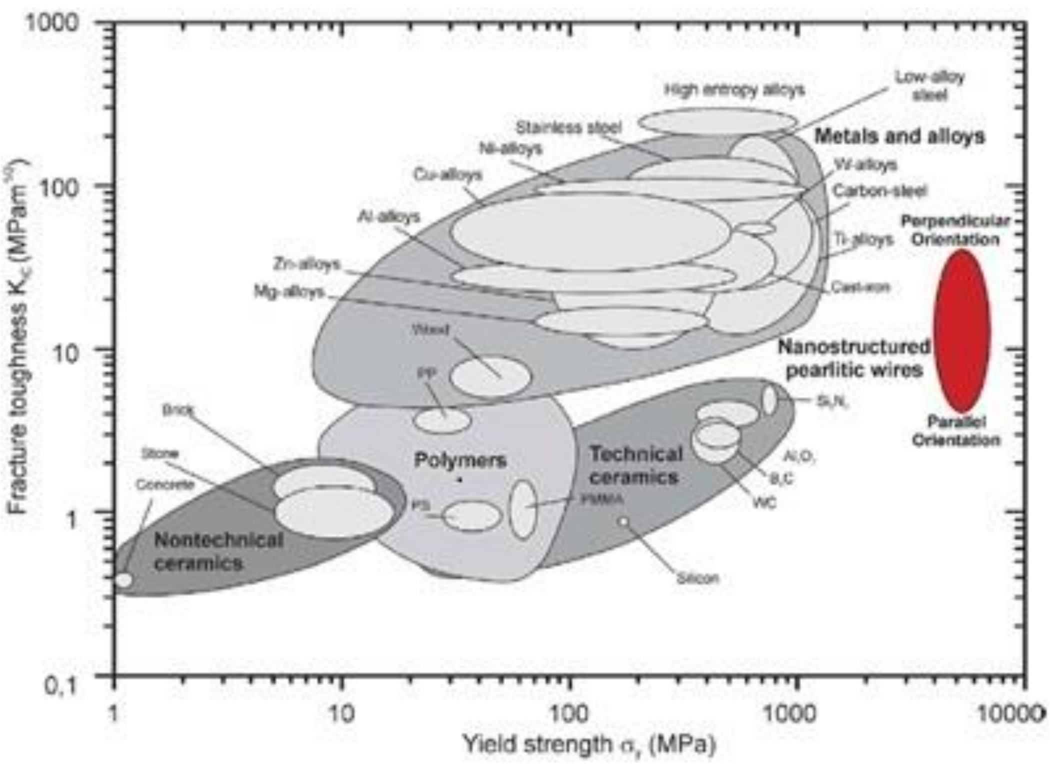

Figure 10: Asbhy plots shows the relation between toughness and strength of the steel materials

Toughness and Ductility: Ductile materials can absorb energy by plastically deforming, which increases their toughness. This is why materials such as copper, aluminium, and low-carbon steels are so tough—they have a large ability to plastically deform[71]. In available literature study, it was observed that the higher ductility can enhance toughness as seen low carbon medium manganese alloyed steel, which shows increased in low temperatures toughness due to refining in microstructure[72]. In contrast, brittle materials like ceramics have low ductility and fail abruptly under impact. Optimizing toughness often involves balancing strength with sufficient ductility[73].

Toughness and Microstructure: The toughness correlates well with other mechanical properties, and is mainly affected by the material microstructure. The toughness of a material often depends on its micro-structural characteristics, like grain size, phase composition and precipitations. In example; fine grained microstructures of steel enhance toughness by retarding the movement of cracks and requiring a greater amount of energy to be consumed during fracture [74]. On the other hand, materials with large grains or those containing more brittle phases generally exhibit lower toughness.

The low carbon steel is frequently subjected to heat-treatment processes such as quenching and tempering. This helps in the fine-adjustment of (specific) steel mechanical properties for specific applications. The manipulation of the microstructure enabled by these processes, leads to materials with a high modern academy strength and adequate toughness properties for assignments as demanding as pressure vessels and pipeline construction [75]. These methods are frequently accompanied by the Charpy impact test to evaluate whether heat treatments were successful in increasing toughness.

In more practical terms, the relationship between toughness and other mechanical properties is crucial to designing materials used in industries like construction, oil and gas production, and transportation. For instance, steel used in pipeline manufacturing must not only be sufficiently strong to bear internal pressure but also tough enough to resist fractures from external impacts [67]. Similarly, in the automotive industry, components like chassis and crash barriers, where energy absorption is crucial during collisions, require high-toughness materials [76].

2.4. Comparison of Hardness Test with Charpy Impact Test

Hardness and toughness are critical mechanical qualities that ascertain a material's suitability for various industrial applications. The hardness test and Charpy impact test are two essential evaluations that assist in the assessment of the aforementioned qualities. While both provide valuable insights into material performance, they do so through distinct methodologies; hardness measures resistance to deformation, whereas Charpy tests quantify energy absorbed prior to fracture. This study presents an analytical framework to compare the two tests based on their operational principles, parameter methods, and experimental data, rendering it suitable in industrial contexts[77].

Hardness test are tests which identify the resistance of a material against indentation or scratching. The Brinell, Vickers and Rockwell tests are three of the most common types of hardness test. In both cases, a hard object such as steel ball or diamond pyramid is pushed into the surface of material under known load and after the application measuring size of indentation. Resistance to localized plastic deformation —often assessed by indentation hardness—is directly related to mechanical properties. Tougher materials are usually more wear and permanent deformation-resistant, so they apply to demanding stress conditions[78].

In contrast, Charpy impact test helps to determine the toughness of a material i.e., ability of the material to absorb energy before fracture. In this test, it hits a piece of the sample with its pendulum hammer, and then measures how much energy was needed to break that part. It is one of the important tests to assess materials under high-velocity or dynamic loading, and hence a need for all automotive engineering & structural mechanics. The Charpy test is to study materials property at different temperatures and hence can be used for Brittle-ductile transition temperature[79].

Table 1: Comparison of different testing methods

Test	Key Advantages	Key Limitations	Relevance
Brinell	Accurate for coarse-grain materials, well-established method.	Sensitive to surface conditions, less portable.	Suitable for static testing in controlled environments.
Rockwell	Quick, automated, and less operator-dependent, good for quality control	Less suitable for thin materials or surface-impaired samples	Ideal for production environments where fast, consistent results are needed.
Vickers	High precision, works well for both micro and macro hardness measurements.	Time-consuming, sensitive to surface conditions.	Useful for predicting both yield and tensile strength in controlled lab settings.
Leeb	Portable, non-destructive, ideal for in-situ testing.	Sensitive to mass and support conditions, less accurate than Vickers for tensile prediction.	Useful for rapid field assessments, especially where portability is key.
Charpy	Excellent for assessing toughness and dynamic properties, evaluates ductile-brittle transition.	Destructive, requires specialized equipment, weaker correlation with static properties.	Best suited for environments with dynamic loads, such as seismic regions.

Chapter- 3: Motivation

3.1 Motivation of the present Study

This study is motivated by the growing significance of mechanical properties, particularly hardness and toughness, in guaranteeing the dependable performance of structural steels. Given steel's fundamental role in key sectors such as construction, automotive manufacturing, and energy, it becomes crucial to understand how different grades of steel behave under varying conditions. The comparative examination of these qualities, which are directly linked to the material's resistance to deformation, wear, and fracture, is essential through various testing procedures. The aim of this work is to cover this lack by assessing the capacity that a variety of hardness tests (Vickers, Rockwell, Brinell and Leeb) as well toughness test (Charpy impact) has for predicting properties characterizing general behaviour under dynamic loads in steel grades around 300-400.

3.2 Research Gaps

1. The different hardness methods, such as Brinell, Vickers, Leeb, and Rockwell, are widely used in both industrial as well as research applications. However, limited studies have shown or discussed these methodologies of their combined prediction skills on various steel grades. Therefore, this research gap is linked to the need for comprehensive comparative studies based on a unifying model of all these hardness tests.

2. Examine the correlation between hardness values derived from different testing methodologies and other essential mechanical qualities, including tensile strength, wear resistance, and toughness. This will offer a more thorough understanding of the mechanical properties of steel.

3. Despite the widespread acceptance of the Charpy impact test, there is an insufficient understanding of its performance under many environmental situations. Furthermore, the

relationship between toughness and other material properties such as hardness and strength has not been adequately explored.

3.3. Research Objectives

- To perform a comparative study of the Vickers, Rockwell, Brinell, and Leeb hardness testing methods for evaluating the mechanical properties of steel grades like 300 to 400.
- To examine the efficacy of the Charpy impact test in finding the toughness of steel grades.
- To establish the relation between hardness and toughness of material.

4. Experimental Methods

4.1. Procuring of Specimens

This section will provide an overview of the research conducted on methods for tensile and hardness testing of metallic materials. All categories of hardness tests, including tensile and Charpy impact tests. The samples were supplied by Grayson Engineering in Auckland [80] and consisted of scrap metals which are extruded from existing structures; thus, a meticulous level of surface treatment is necessary to commence the testing methods. The samples obtained from Grayson Engineering in Auckland are shown below. There are three different grades of scrap steel such as Grade 300, Grade 350, and Grade 400. These samples are received, and they have four different cross-sections: plate, angle, rectangular section, and I section (can be seen in Figure 11).

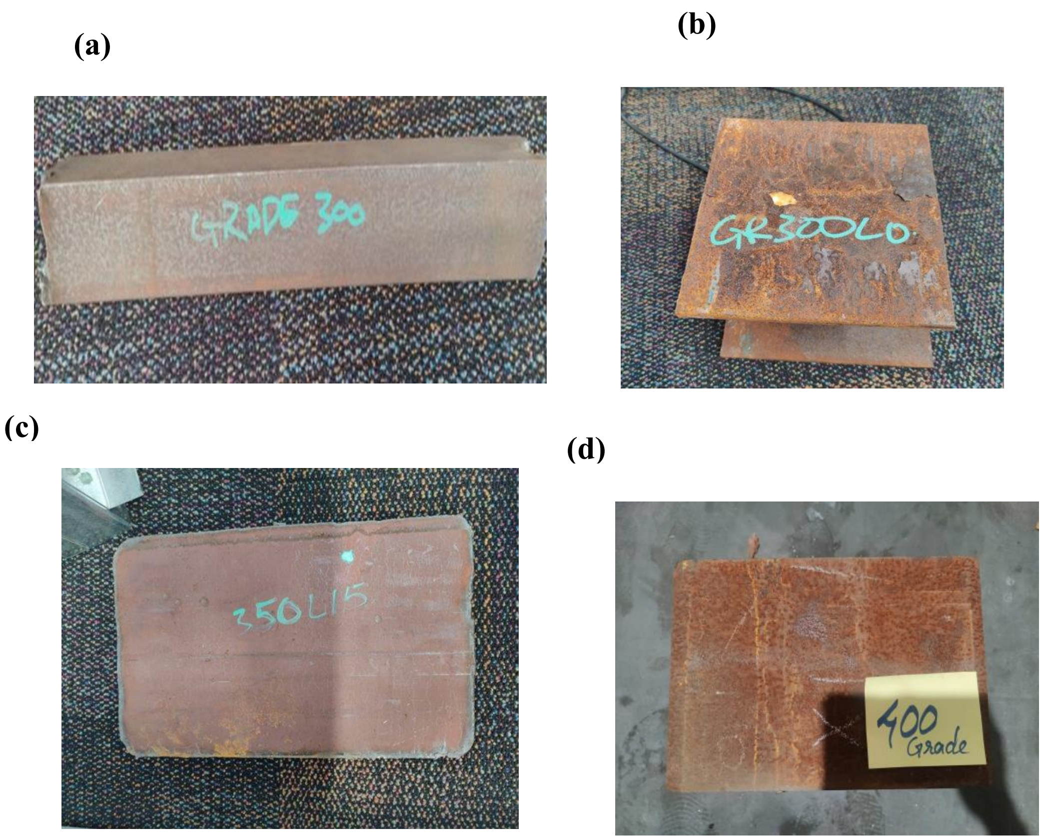

Figure 11: Different grades of received steel specimens (a) 300 grade angle, (b) 300 I section, (c) 350 plate sections, (d) 400 Rectangular Section

The 300, 350, and 400-grade steels have considerable differences in yield strength and ultimate strength depending on the grade as a result of chemical composition differences and mechanical property variations. In general, lower-grade steels like 300 are more ductile and have low yield strength compared to higher grades. The high-grade steels improvement is especially evident due to their higher constraints on endurance, such as in SD700 (Steel deformed 700) grade steel fatigue strength, which can attain 1.68 times that of SD300 and 1.47 times that for the factor SD400, respectively[81] . In a similar way, cold-rolled high strength steel sheets in 300–500 N/mm^2 yield strength were improved by some alloying elements such as manganese while deteriorating formability at very high strength steels [82]. Under dynamic stresses comparisons with standard grades show that high-strength steels (e.g., 350) are less ductile and fail sooner under cyclic loading than is a standard grade [83].

At high temperatures all grades show reductions in strength, but 300°C is highlighted as a temperature range where the reduction in strength becomes greater. Although higher-grade steels like 400 may provide higher yield strength for high-strength applications, they also can have lower levels of impact performance in a highly stressed service. This means that higher-grade steels (350, 400) do have higher yield and ultimate strengths than lower-grade steels, but they are usually only good for load-bearing applications under static stress conditions because they lose their ability to be shaped and curved[84].

4.2. Specimen Preparation

As the samples were big in size, they should be trimmed and cleaned, so to remove heat due to cutting, a vertical band saw cutter is used as it pumps coolant in order to overcome the heat due to friction. Vertical Band saw cutter machine of the model (MOD 370) used to trim down the samples according to ASTM (A370) [85] standard 60mm x 20mm x 10mm. This equipment was found reliable in cutting down the sample to the required size without changing the chemical structure of the steel sample due to heating, which may alter the hardness values. The specimen mark and preparation of different number of samples can be inferred from Figures from 12 to 16. The trimmed samples can be seen from Figure 17. The number of samples across different steel grades used for further experimentation are presented in Table 2.

Table 2: Details of different grades of steel samples and its quantity

Sample Description	No of Samples
Grade 300 Steel Angle	12
Grade 300 Steel I Section	17
Grade 350 Steel Plate I	7
Grade 350 Steel Plate II	20
Grade 400 Square	16

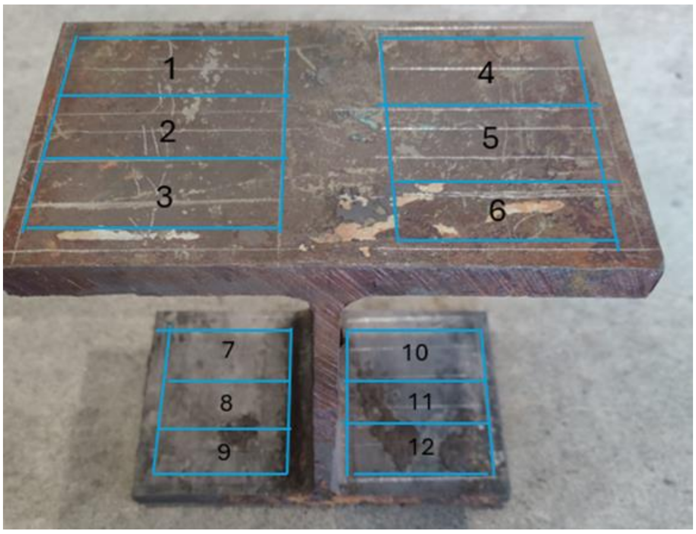

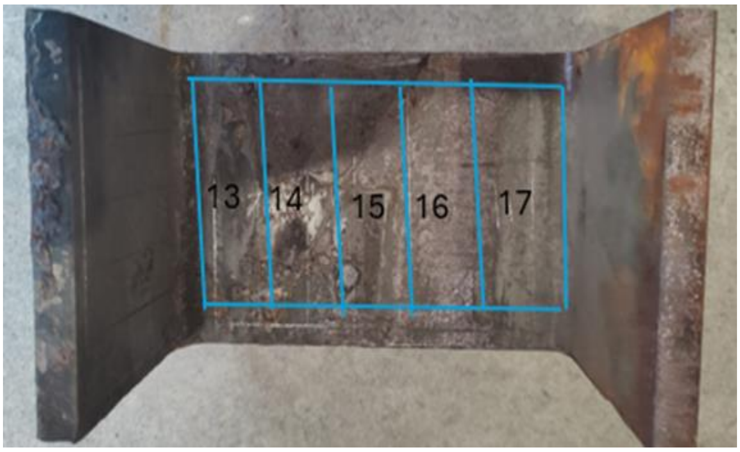

(b)

(a)

(c)

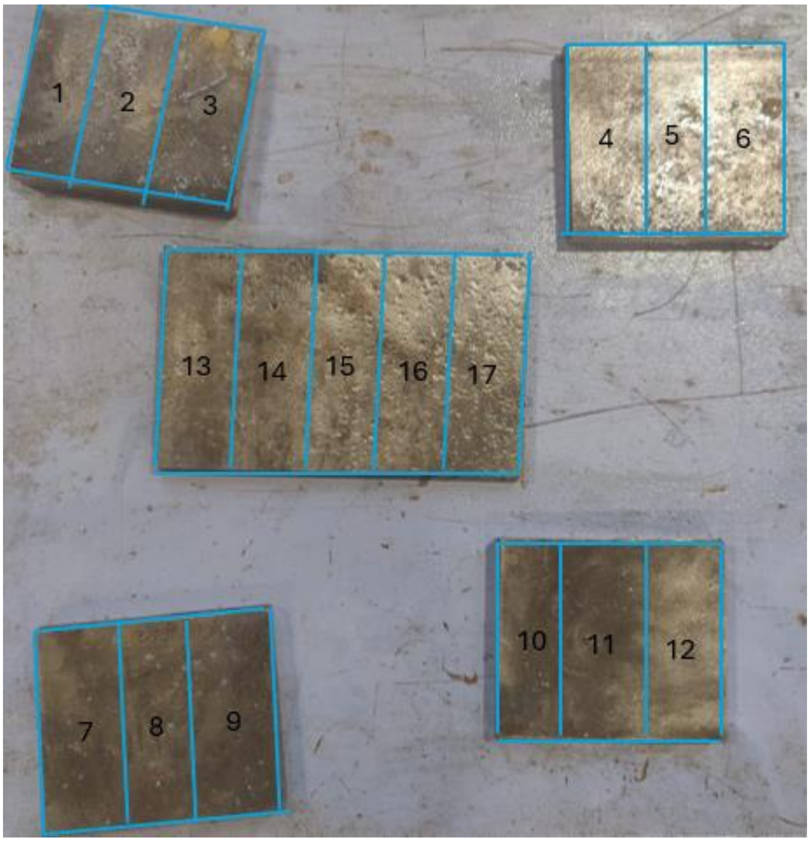

Figure 12: (a), (b), and (c) 300 grade I section specimen location

(a)

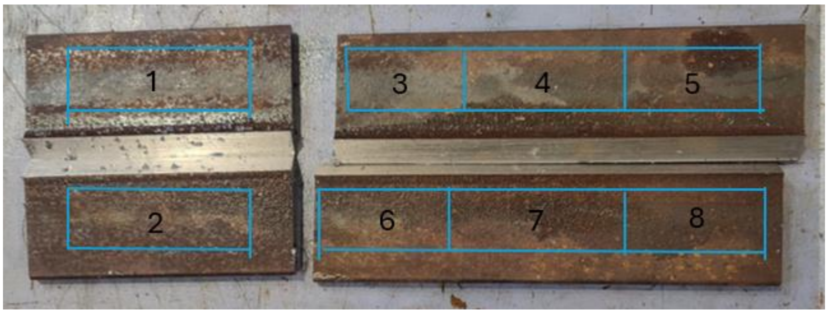

(b)

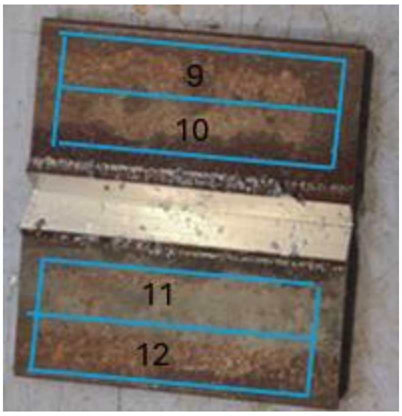

Figure 13 : (a), and (b) 300 grade Angle section specimen location

(a)

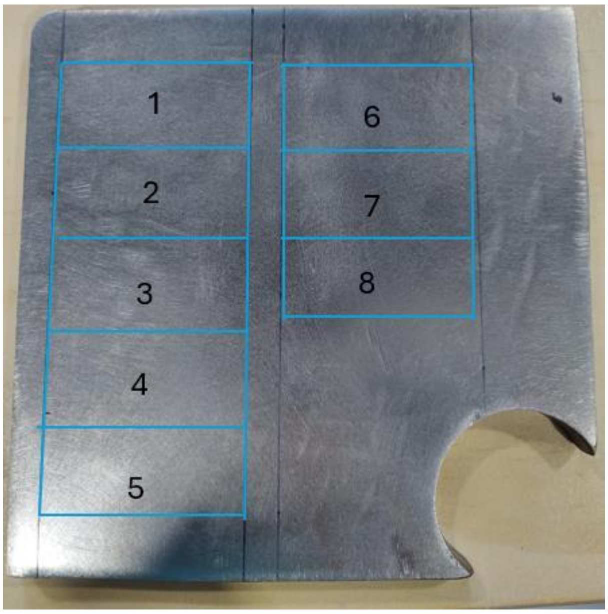

(b)

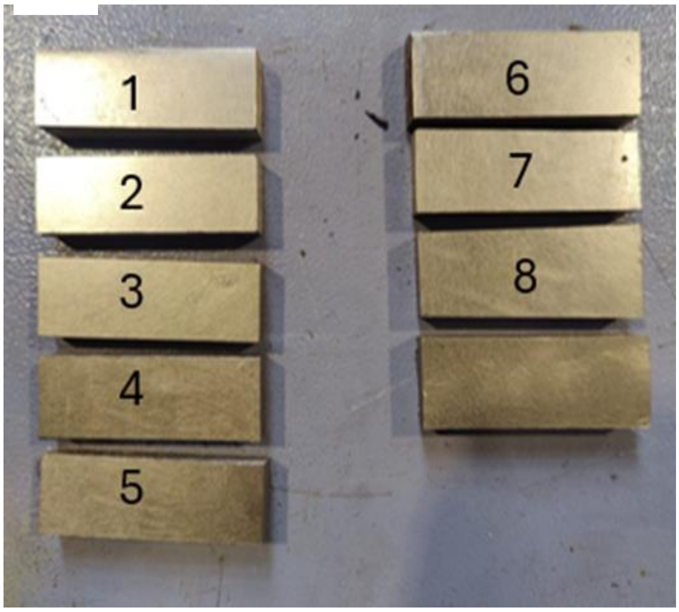

Figure 14: (a) and (b) 350 grade plate section I specimen location

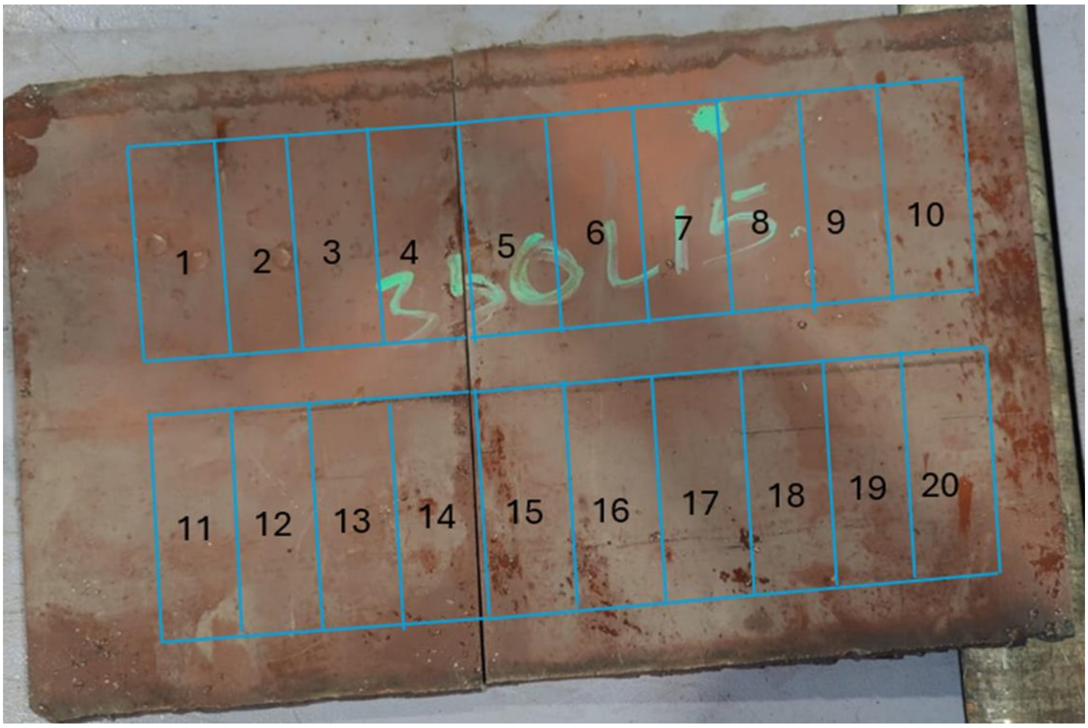

Figure 15: 350 grade plate section II specimen location

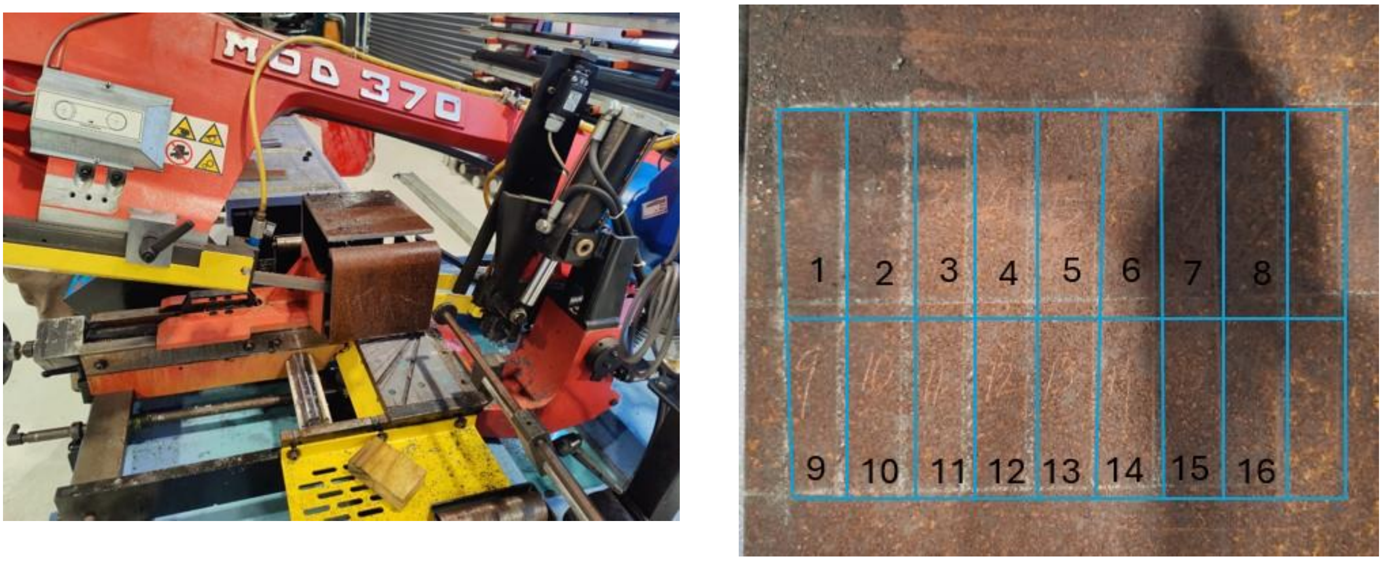

Figure 16: (a) Vertical saw cutter machine and (b) 400-grade rectangular section specimen location

Further samples were cleaned and finished using grinding machine. The emery paper used for cleaning the surface of samples used between from P80, then P120 and finally P320 [86]The grades of emery paper, from coarse to fine, are followed from lower to higher. After using the different grades of emery paper for polishing the specimen surface, rust-free, fine, and even ground surfaces were obtained, which are shown in Figure 18.

(a) **(b)**

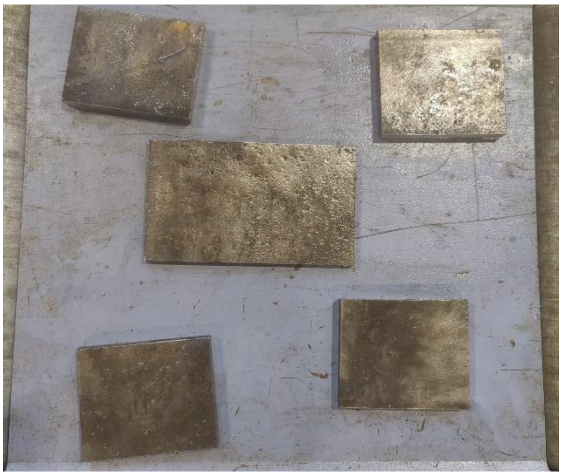

Figure 17: (a) and (b)Trimmed piece of steel samples as per ASTM (A370)

During grinding the surface of samples, a continuous supply of water was provided in the context to reduce the heat which may be produced due to abrasion and scratches that generally occur due to the presence of abrasive particles that may further reduce the evenness of the surface.

(a)

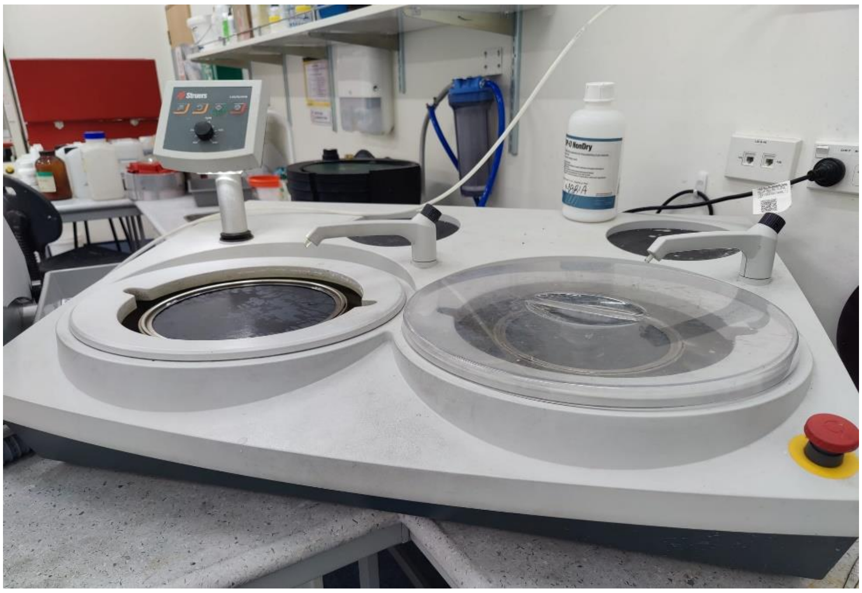

(b)

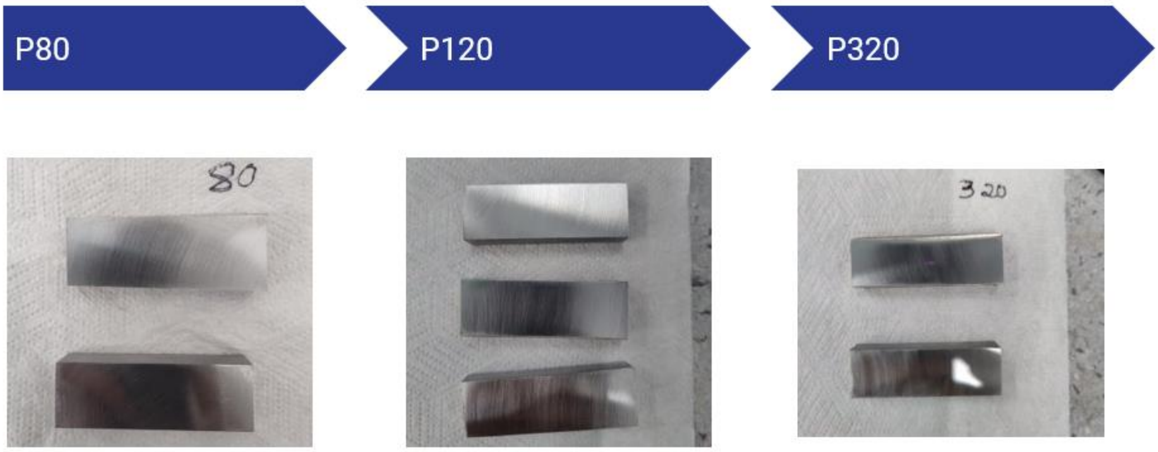

Figure 18: (a) Grinding machine, (b) polished samples after each grade of emery papers used to polish the surface of sample progressively.

4.3. Surface Finish and Microscopic Analysis

Figure 19 shows micrographs at 1000µm were captured during the grinding stages to provide a visual record of surface refinement. These pictures represent the decrease of roughness and texture refinement from one processing step to another. Surface preparation can lead to hardness measurement errors [87]. The essential result is that surfaces affect hardness, the rough surface with a 20 nm fair loss created wide range provide up to 19% [87] are the major utilizes. Samples were polished from P80 to P320 grit level (fine surface and marks have been reduced). The LaboPol-60 also maintains a constant water flow to cool down others for avoiding thermal damage during grinding.

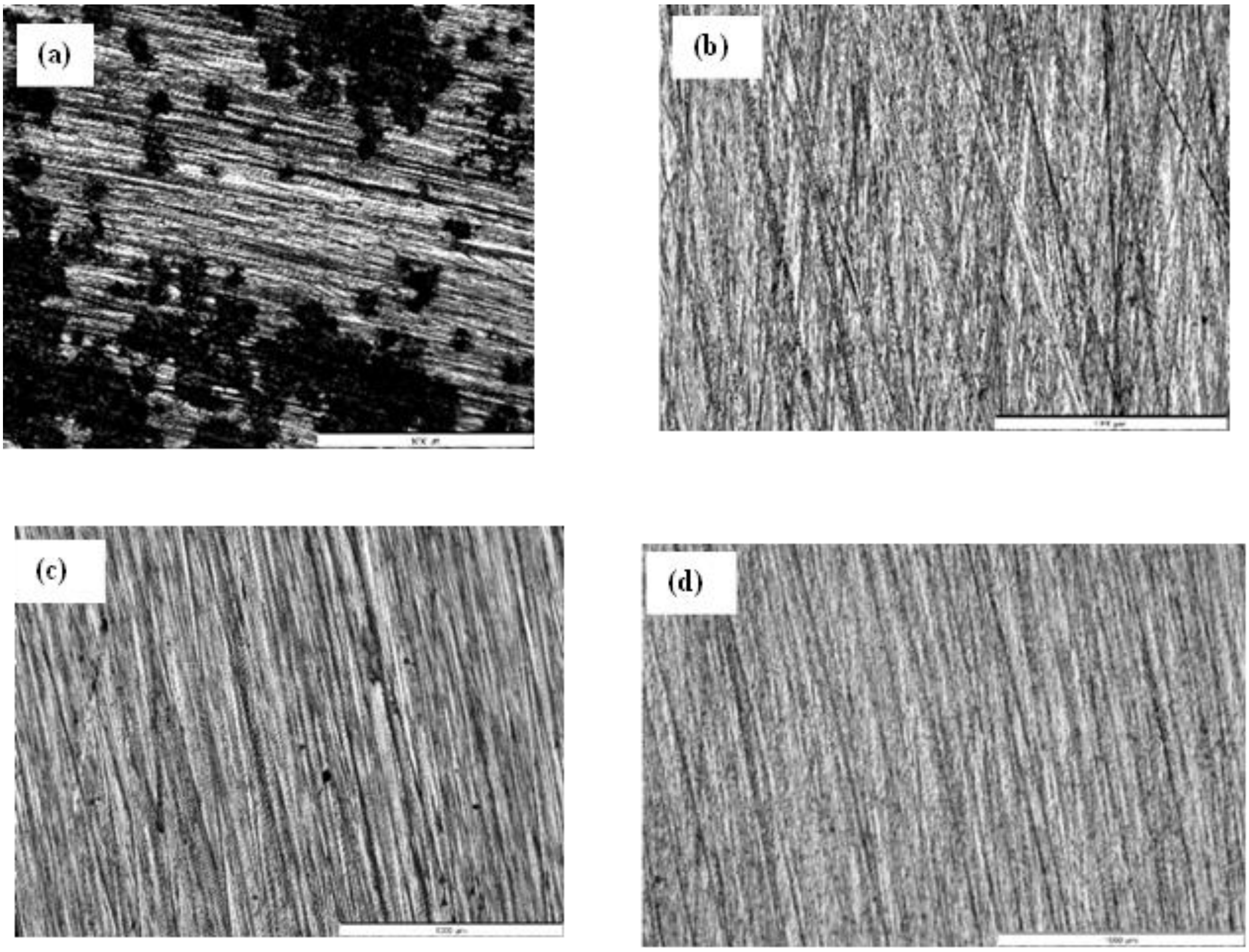

Figure 19: Image of surface captured at 1000 µm after grinding using different emery papers (a) Initial surface, (b) P80, (c) P 120 and (d) P320.

4.4. Methods for measuring hardness

Hardness testing measures the resistance of a material to permanent deformation such as indentation, wear, abrasion, and scratch, while tensile testing measures the elongation that a force causes on certain materials. Both hardness test and tensile tests measure the resistance of a metal to plastic flow, and there is a direct correlation between hardness and tensile strength. It is one of the most widely used mechanical tests and is used to ensure that the material meets minimum strength and ductility requirements.

4.4.1. Hardness testing

A crucial technique for evaluating the mechanical characteristics of structural steel is hardness testing, which offers vital information on the material`s strength and the suitability for various applications. The popular method for determining the hardness of structural steel is Rockwell hardness testing, Brinell hardness testing, Vickers hardness testing and Leeb hardness testing, among these tests Leeb hardness is unique as it is portable tester which even can be used to test pre-existing buildings and very useful due to its portability.

The test is classified as destructive and non-destructive hardness testing. NDT (non-destructive test) this type of testing method which is carried out to evaluate the physical properties of a material or component without causing any damage. The other one is destructive tests (DT): This is about examining the properties and behaviour of materials or products by exposing them to extreme conditions until they fail. This form of testing also plays an integral role in establishing the mechanical aspects, such as stability and robustness, of products & materials. Several types of destructive tests can be used depending on the materials, most common tests are bending test, tensile test, and impact testing.

4.4.2. Leeb hardness testing

A Leeb (or HLD — Hardness, Leebsky devices) test is a dynamic method of testing the hardness without requiring much space for most inspections with large products to be performed on-site. In this test, the hardness is determined by measuring respectively the rebound velocity and impact velocity of a dropped MIRS body on surface material. The Leeb test offers higher advantages and is best performed for on-site testing of steel structures and large machinery, even though it is less used under laboratory settings, as you can still access the data in real-time. In the Leeb hardness testing method, a hardness value is calculated from the energy loss of an impact body that strikes a metal surface. This loss of energy is known as the Leeb quotient and gives information on how much deformation was experienced by the material. The impact body rebounds more rapidly from harder materials than from softer ones, resulting in a greater value of 1000 * (vr / vi), where "vr" denotes the rebound velocity and "vi" signifies the impact velocity. The approach used for measuring the hardness of the specimen using Leeb test is based on ISO 16859 [88]whose schematic diagram is shown in Figure 20 (a).

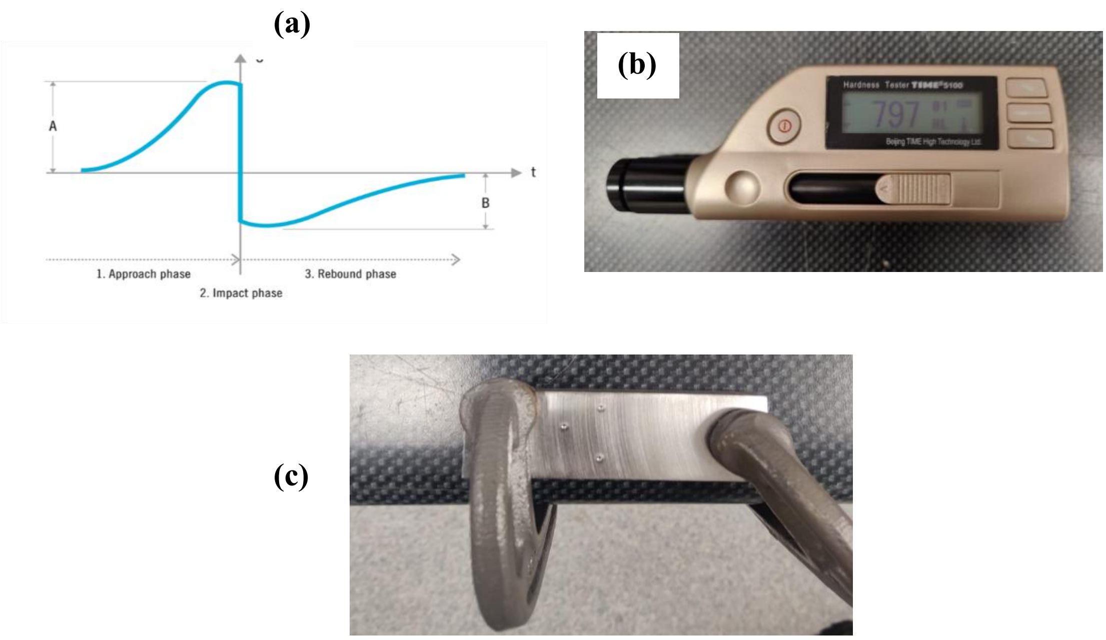

Figure 20: (a) Leeb hardness test method (ISO 16859), (b) TH-170 Leeb hardness tester, and (c) Clamping the sample for Leeb testing for overcoming 5kg requirement for the sample

Further, Figure 18 (b and c) shows the Leeb tester and clamper used to hold the specimen. This was done because the portable tester manual mentioned that the device provides accurate readings when the sample weight is more than 5kg, so attaching the small samples to a big object will help achieve a more precise result. The steps used to perform the Leeb test are discussed below.

- Approach stage where the spring force drives the impactor towards the test surface.
- Contact, such that the impactor and specimen are always touching each. The specimen deforms both elastically and plastically, but the impactor stops entirely. The rebound of the impactor takes place due to elasticity recovery of the impactor as well as specimen.
- Rebound phase – the impactor is re-accelerated by whatever energy remains in it after a portion of this energy has been spent during absorption.

4.4.3. Rockwell Hardness Test

This test involves the use of a cone or a steel ball indenter. The hardness value is determined based on the depth of penetration. LCR-500 is used and by selecting Rockwell type B, which is used in the hardness testing, and it uses a 1/16-inch tungsten carbide indenter. A 100kgs load is applied to the specimen and it takes about 20-30 seconds for the upper arm with indenter moves down with the load making an indent the hardness value is recorded in the machine. The image of hardness tester is shown in Figure 21.

Figure 21: LCR 500- Used for both Rockwell and Brinell hardness test

4.4.4. Vickers Hardness Test

This method uses a diamond-shaped indenter and measures the diagonals of the resulting indentation. LM-700 is used and by selecting Vicker, which is used in the hardness testing, and it uses a diamond indenter. A 1kg load is applied to the specimen and it takes about 20 seconds (dwell time) for the upper arm with indenter moves down with the load making an indent the hardness value is recorded in the machine. The illustration of Vicker hardness tester and its diamond indentation mark is shown in Figure 22**.**

(a) **(b)**

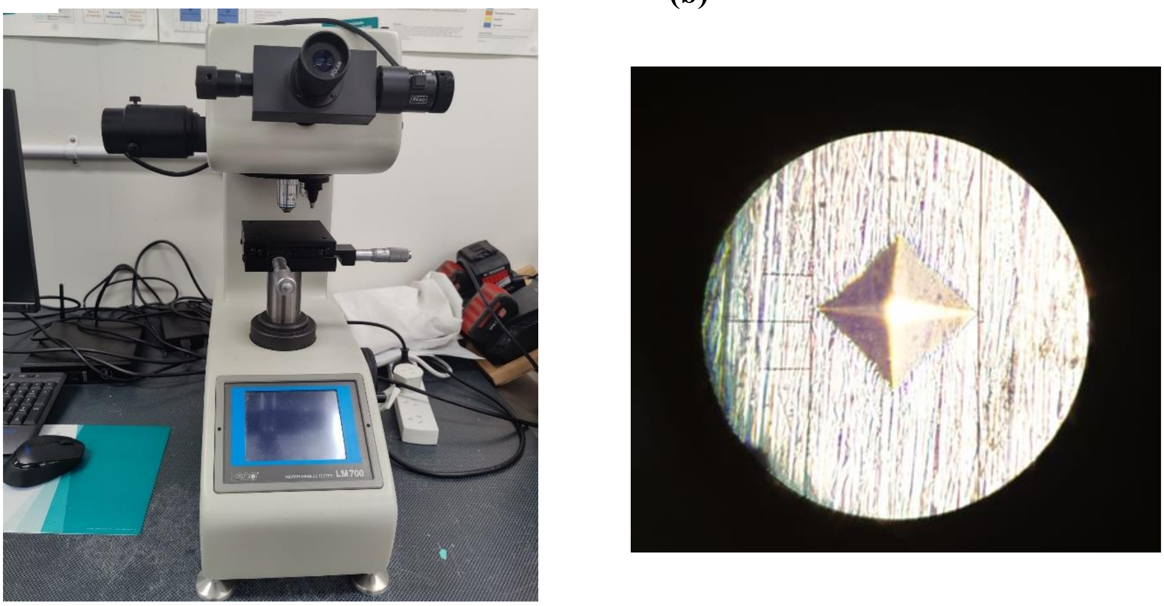

Figure 22: (a) Vicker hardness tester of model LM700, (b) indentation on the surface of sample during testing.

4.4.5. Brinell Hardness Test

In this test, a hardened steel ball is pressed into the material surface, and the diameter of the resulting indentation is measured. LCR-500 is used and by selecting Brinell, which is used in the hardness testing, and it uses a 2mm indenter. A 40kgs load is applied to the specimen and it takes about 20-30 seconds for the upper arm with indenter moves down with the load making an indent the hardness value is recorded in the machine.

Figure 23 (a) shows the schematic indicating the indentation pattern. The distance between two indents is then maintained (specimen edge justification), one indent diameter apart 3t ensuring no interaction between adjacent indents. The distance of the material is at 2.5d, this avoids that edge affects are influencing in the test results. The spacing is important to provide the necessary accuracy in hardness measurements by preventing an overlap of stress fields.

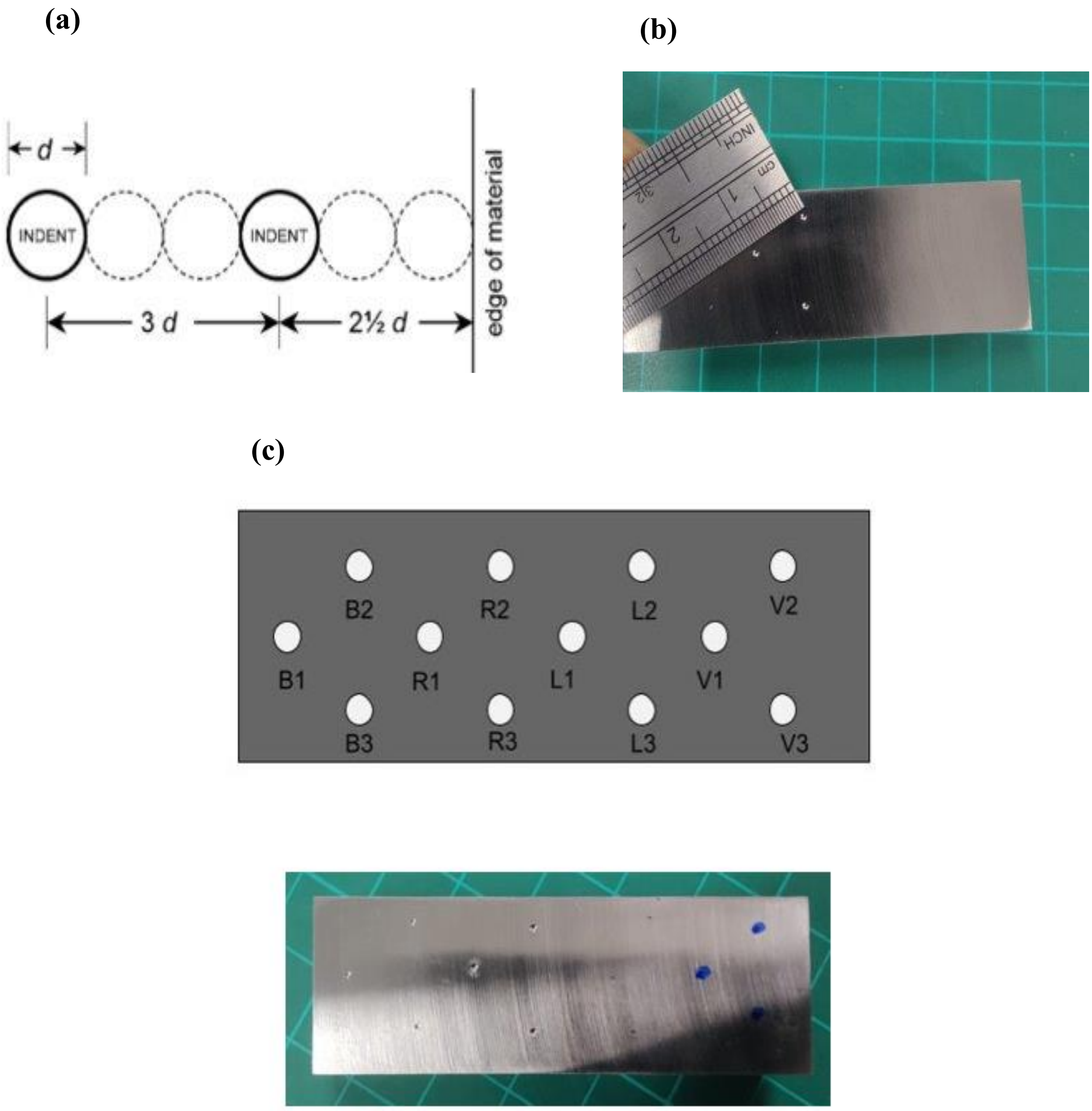

Figure 23: (a) Procedure indent on sample as per ASTM E18-11, (b) 10mm (about 0.39 in) gap between each indent, (c) Indented samples

Additionally, Figure 23 (b) illustrates a metallic specimen with indentations, accompanied by a ruler for visual scale, demonstrating the precise alignment and spacing of the surface indents. This configuration facilitates numerous hardness assessments on a singular specimen. In the third image (Figure 23 (c)) depicted the layout specifying the indent position marked as (B1 B2 R1 R2) etc is shown which is the positions where systematic hardness testing is required on the sample. This presented arrangement is quite useful in that it ensures that data is captured uniformly over various sections of the sample which enables a wide grasp of the hardness pattern of the material. The collection of all tested samples using Brinell hardness test is shown in Figure 24.

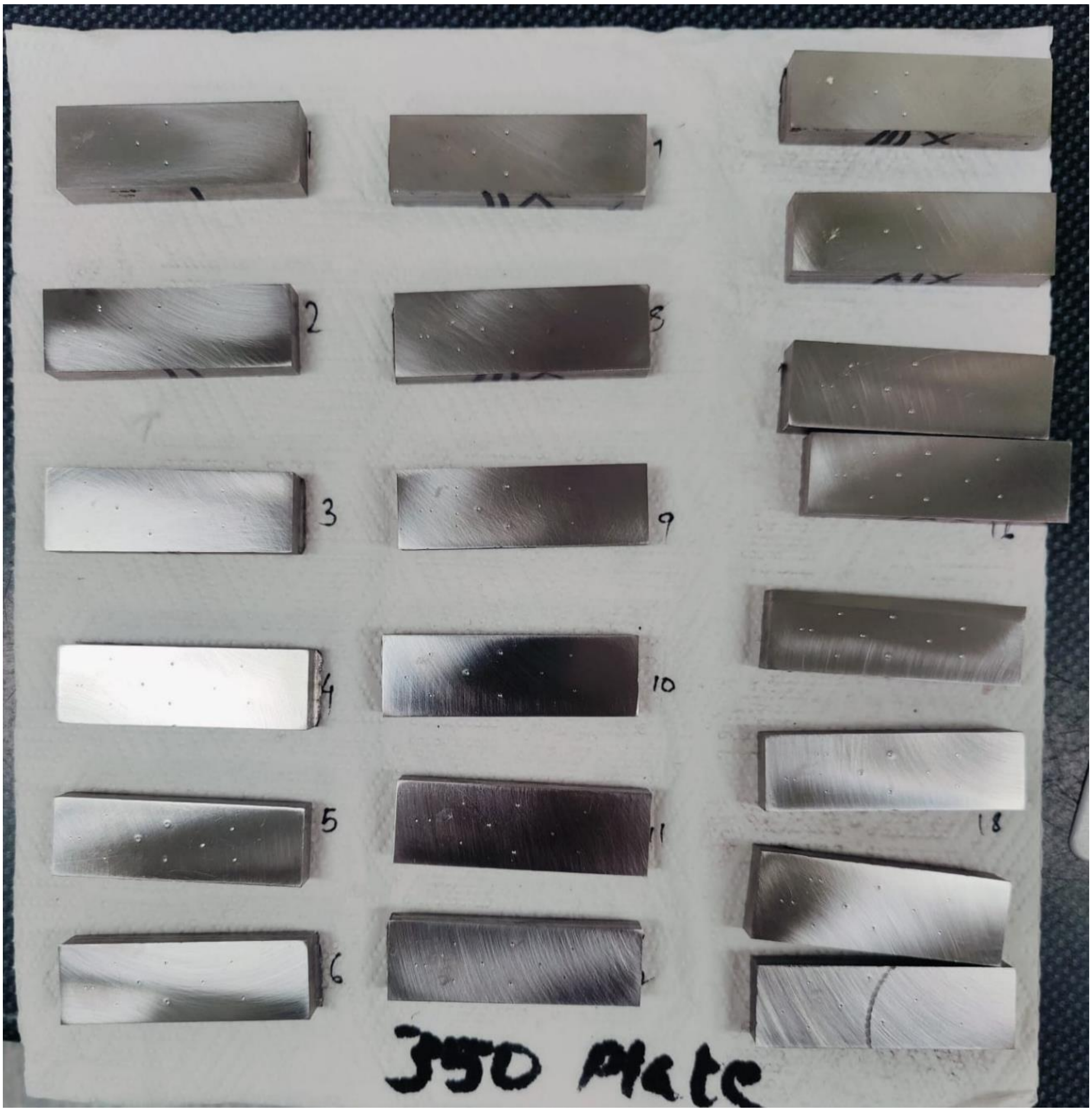

Figure 24: Collection of indented samples

4.5 Charpy impact testing

The Charpy impact test, also known as the Charpy V-notch test is a standardized high strain-rate method used for this purpose. It is commonly used in industries due to its simplicity of both preparation and conduct, easy observation process providing results fast and accurate. The test includes a pendulum of known mass and length that is dropped from a predetermined height to strike the notched material sample. The illustration of Charpy impact tester is shown in Figure 25.

Figure 25: Illustration of Charpy impact test available in the lab.

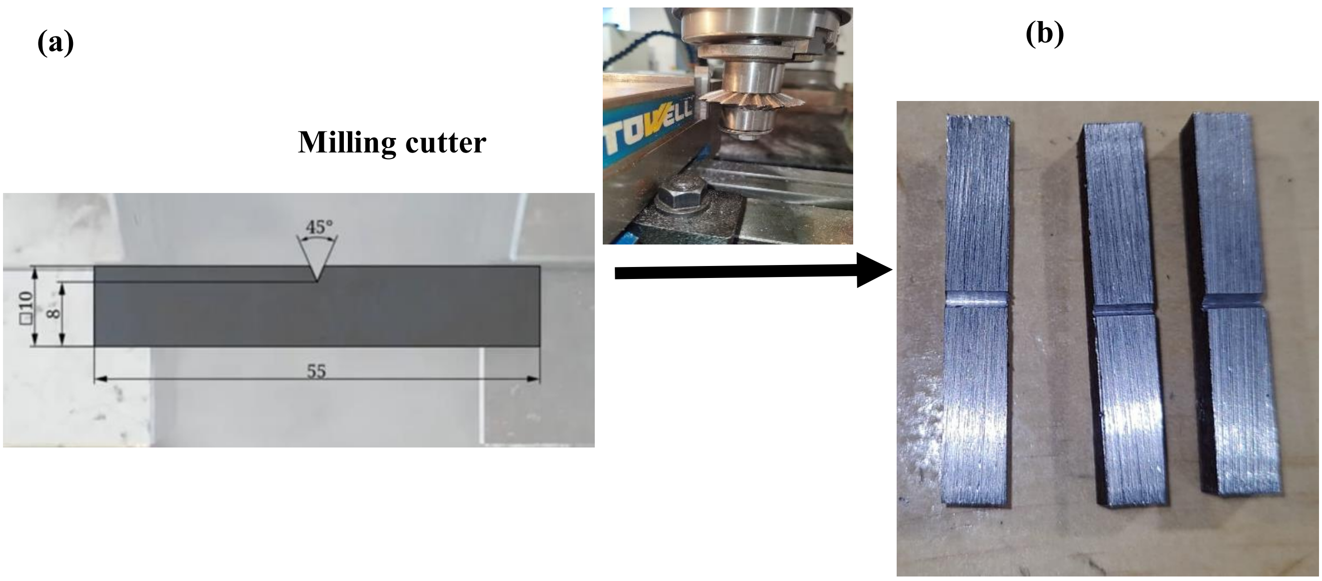

Figure 26: (a) Schematic diagram of Charpy test specimen, and (b) prepared samples for testing.

The test specimens of the original steel samples were procured from Grayson Engineering Ltd. The steel samples were machined into Charpy V-notch (CVN) specimens of 10mm × 10 mm × 55 mm, containing a 2 mm deep V notch with a 45-degree angle using milling cutter according to ASTM E23 [89] (the same can be inferred from Figure 26). A notch is located in the middle of one side of the specimen, enabling impact stress concentration to mimic fracturing behaviour. Further, the energy transferred to the material can be calculated by measuring how much lower in height is the hammer after fracture than before (the amount of energy absorbed during a catastrophic event - fracture). As the notch in the sample influences to a greater or lesser extent on the results of impact test, it has been recognized that for an adequate quantification and detection of semi-micro components present inside testing samples like retained austenite, pearlite. The testing was performed using a PIT-D Dual Beam Charpy-Pendulum Impact Tester (as shown in Figure 25). This machine strikes the specimen with a pendulum and measures the energy required to fracture it. As per ASTM E23-24, the following parameters were used during the testing (Table 3).

Table 3: Details of compliance for Charpy impact test as per ASTM standards

Parameter	**Value Used**	**ASTM E23 Clause**	**Compliance**
Notch Depth	2mm	Clause A3.1	Complies (Standard depth: 2.0 mm ± 0.025 mm)
Notch Type	V-notch	Clause A3.1	Complies (V-notch with 45° angle and 0.25 mm tip radius)
Angle of Striking	-150 degrees	Clause 9.3.3	Complies (No direct specification, but standard procedure for releasing the pendulum is followed)
Energy	300 J	Clause A2.4.4.2	Complies (Energy within the machine's capacity, ensuring accurate readings)
Test Machine	PIT-D Dual Beam Charpy-Pendulum Impact Tester	Annex A1 and A2	Complies (Meets machine design and verification standards)

4.6. Tensile Testing

The hardness-tested samples were machined into "Tensile Testing-dog bone" specimens for tensile testing using the EW3 VC Electric Discharge Machining (EDM) cutter. EDM was chosen over conventional milling due to its superior precision and surface finish. A study by Kanlayasiri and Boonmung [90] highlighted the effectiveness of EDM, showing that controlling machining variables like pulse-on time and pulse-peak current significantly improved surface quality. This precision makes EDM ideal for applications requiring acceptable tolerances, such as tensile test specimens. The dog bone specimen dimensions followed by standard available in [91] (can be seen from Figure 27).

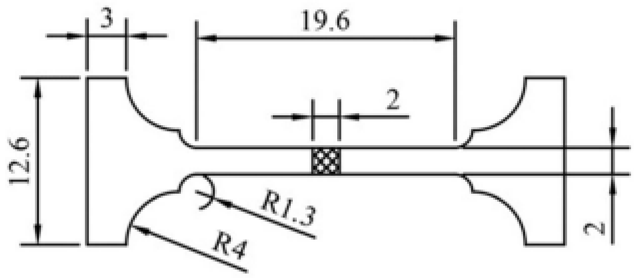

Figure 27: Schematic diagram of tensile testing dog bone.

The ISO-6892-1 [92] standard was chosen to ensure consistent and reliable tensile testing by providing precise guidelines for specimen preparation and testing. This standard is widely used to assess mechanical properties such as yield strength, tensile strength, and elongation. Its specified geometry minimizes stress concentrations, allowing uniform deformation in the gauge length. This promotes accuracy and comparability with other studies, aiding in the validation and standardization of test results across various industries. The progression from hardness testing samples to tensile test specimens is shown in Figure 28. The hardness samples were first cut to the specified dimensions and then precisely sliced into tensile specimens as per ASTM E8/E8M-22 standard.

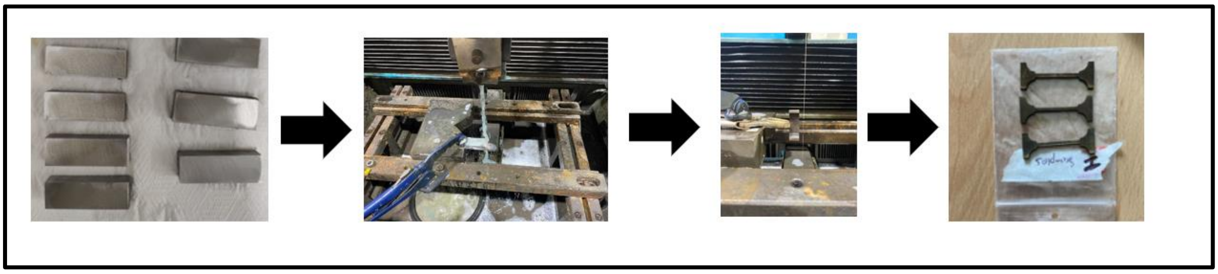

Figure 28: Illustration of steps involved for preparation of tensile testing specimen

Following the preparation of the tensile test specimens, tensile testing was conducted using the Instron 33R 4204 tensile testing machine, as shown in Figure 29. The test was performed with an extension rate of 0.05 mm/min, as per ASTM E8/E8M-22 standard [93].

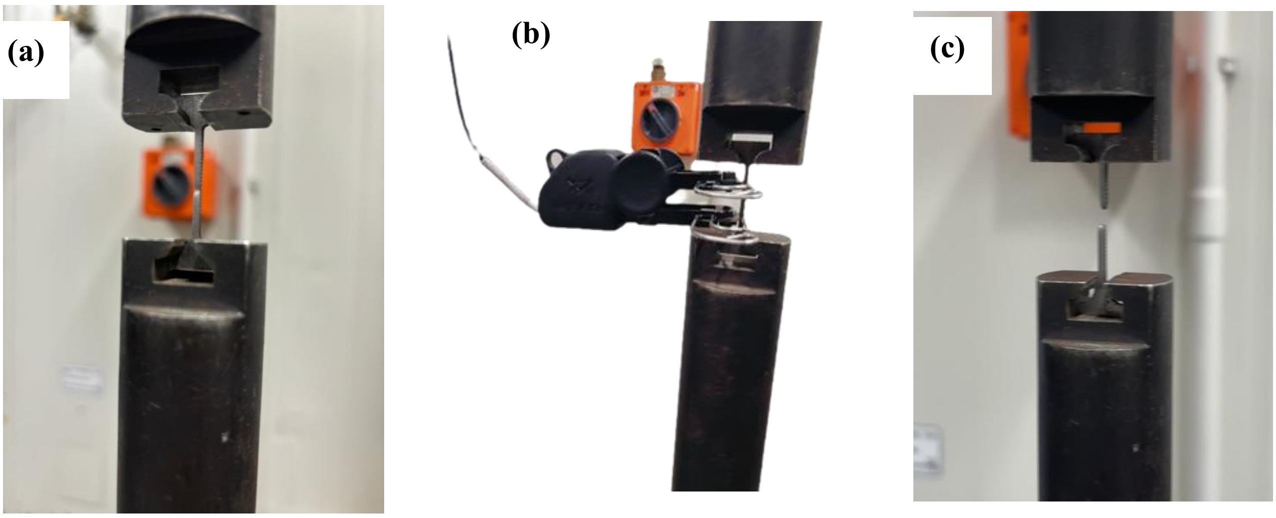

Figure 29: (a) Universal testing machine (Instron 33R 4204), (b) extensometers coupled specimen, (c) fractured TT dog-bone specimen during testing.

The TT-dog bone specimen was employed for the monotonic tensile test to ascertain the material's mechanical characteristics. Upon establishing the mechanical properties of the steel through tensile testing, all data will be compared and analysed to elucidate the correlation between hardness and tensile testing.

5. Results and Discussions

5.1 Evaluation of hardness test results

Hardness testing is a fundamental tool to assess the mechanical properties of structural steels. In this section, four different hardness tests (BHN, HRB, HV and HL) were performed to evaluate the performance of various steel samples. These tests have respective pros and cons, and sensibilities regarding surface condition, material inhomogeneity, and operator variability. The subsequent subsections describe the methodologies, the outcomes, and an assessment of the respective advantages and disadvantages of each testing phase.

5.1.1. Brinell Hardness Test (BHN)

Brinell hardness testing was performed using LCR 500 testing equipment (Figure 21) following the procedure in ASTM E10-18[94]. From Table 1 (available in appendix section), it was depicted that the standard mean deviation (STDEV) of the Brinell test was 8.02, and the error percentages were 5.3% overall. As presented in Figures 30 and 31, the error percentages reached values as high as 16% for some samples. This discrepancy was mainly caused by the material homogeneity and surface defects remaining after polishing.

The results discussed by Katok et al. have shown the study in combination with these deviations only strengthen this conclusion. The brinelling method used for estimating the hardness in high strength steels [95]. In addition, surface imperfections remain a significant factor to consider after polishing as noted in the current experimental work, which is also in agreement with the findings of Katok et al. [95]. Despite its informative nature, Brinell has poor surface sensitivity, which is prone to errors if appropriate special devices are not used, and direct measurement of hardness requires more labour, relative to easier methods. This gives variability as it is susceptible to microstructural variations, making the large indenter useful for coarse-grained materials. Besides, the improvements in the surface preparation and setting up of Brinell measurement systems in automated forms, it can lead to a better accuracy at lower costs.

5.1.2. Vickers Hardness Test (HV)

Figures 32 and 33 shows the Vickers hardness determination with LM-700 (as per ASTM E84-22[96]. With the Vickers test, macro and micro hardness measurements are taken in the same test to produce a more thorough assessment of material properties, which is part of its precision. Due to the small size of the indentation, the test is less sensitive to material inhomogeneity than Brinell, as it can detect smaller variations in localized hardness. The Vickers test relies on the smoothness and polished nature of measured surface since rough surface can directly affect size of indentation, surface preparation is major significant point. More specifically, while compositions were unambiguously homogeneous and the properties of the bulk materials were extremely consistent, minute differences in microstructure (e.g. carbide precipitates and grain boundaries) contributed to some measurable deviations between some samples.

In line with this, the study by Dai et al.[97], the Vickers hardness test is highly accurate in materials with complex microstructures. While, its accuracy and versatility are why it is one of the valuable instruments for hardness testing, but it is essential to prepare a specimen and calibrate the indenter correctly to result error-free.

5.1.3. Rockwell B Hardness Test (HRB)

The Rockwell hardness testing was carried out by using the LCR 500 and results are shown in Figures 30 to 33. This LCR 500 meets requirements of ASTM E-18[98]. When it comes to structural steel, the Rockwell B test is the most dependable hardness testing method, showing low variance and minimal operator error or surface condition dependence. Due to its automated nature, it is ideal for quality control and non-destructive testing, especially in this study reproducibility is critical.

5.1.4. Leeb Hardness Test (HL)

The Leeb hardness test was performed using TH170 Leeb hardness tester as shown in Figure 3 and in accordance with ASTM A956-06[86]. The calculated results are shown in Figures 34 and 35. One major challenge encountered when conducting the Leeb hardness testing was the weight of the samples; the TH170 Leeb hardness tester is used in accordance with ASTM A956-06 [86]. As a result, these findings are in accordance with the discovers by Vaško et al. [99]. The leeb hardness test is not as accurate as the other hardness testing methods especially when the obtained results must be accurate and repetitive. Due to its variability with sample mass, support conditions, and surface roughness, it is less useful for precise hardness measurements. It is useful for rapid field assessments but is not appropriate for applications requiring high precision. Further, comparison of different types of hardness in terms of advantages and disadvantages are tabulated in Table 4.

Table 4: Comparison of different types of hardness testing method

Hardness testing Method	Advantages	Disadvantages
Brinell Hardness Test	Effortless to execute and appropriate for evaluating substantial components and coarse substances.	Creates a significant indentation, potentially rendering it unsuitable for final components.
Vickers Hardness Test	Highly accurate and applicable to various materials and thicknesses.	Indentation is very small, making it difficult to use on rough or coarse surfaces
Rockwell Hardness Test	Effortless and expedient to do with minimal surface preparation required.	Restricted applicability for extremely thin or fragile materials.
Leeb Hardness Test	Portable and suitable for large parts and field testing	Inferior accuracy relative to laboratory-based hardness assessments like as Vickers or Rockwell.

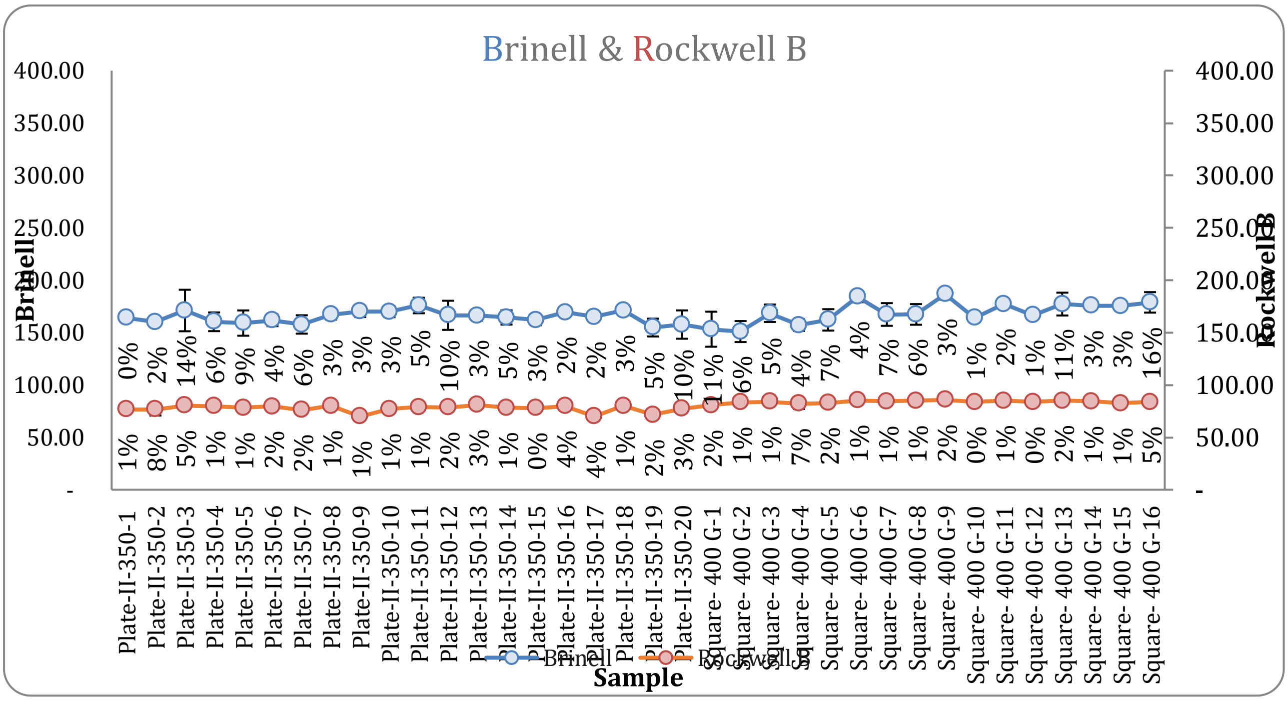

Figure 30: Comparison plot between Brinell and Rockwell hardness of 350 plate and square 400 grade steel

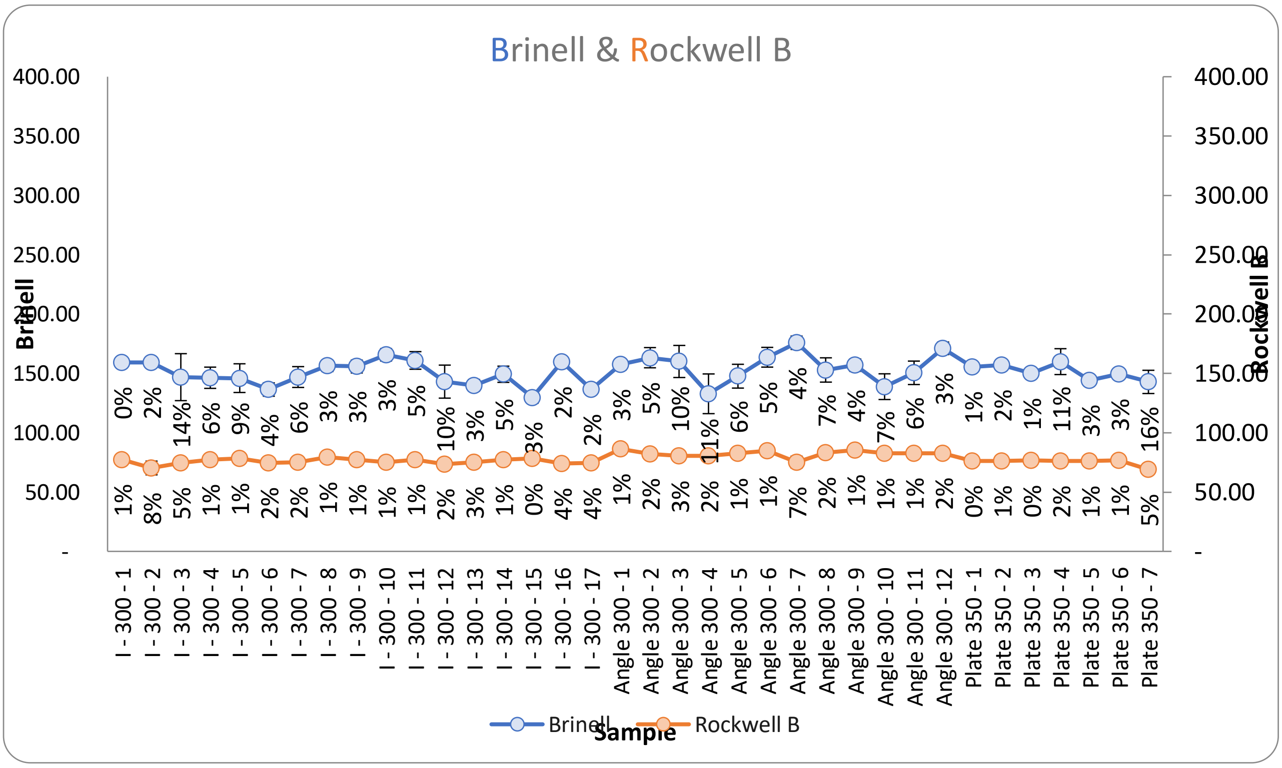

Figure 31: Comparison plot between Brinell and Rockwell hardness of 300 grade of I and angle section steel

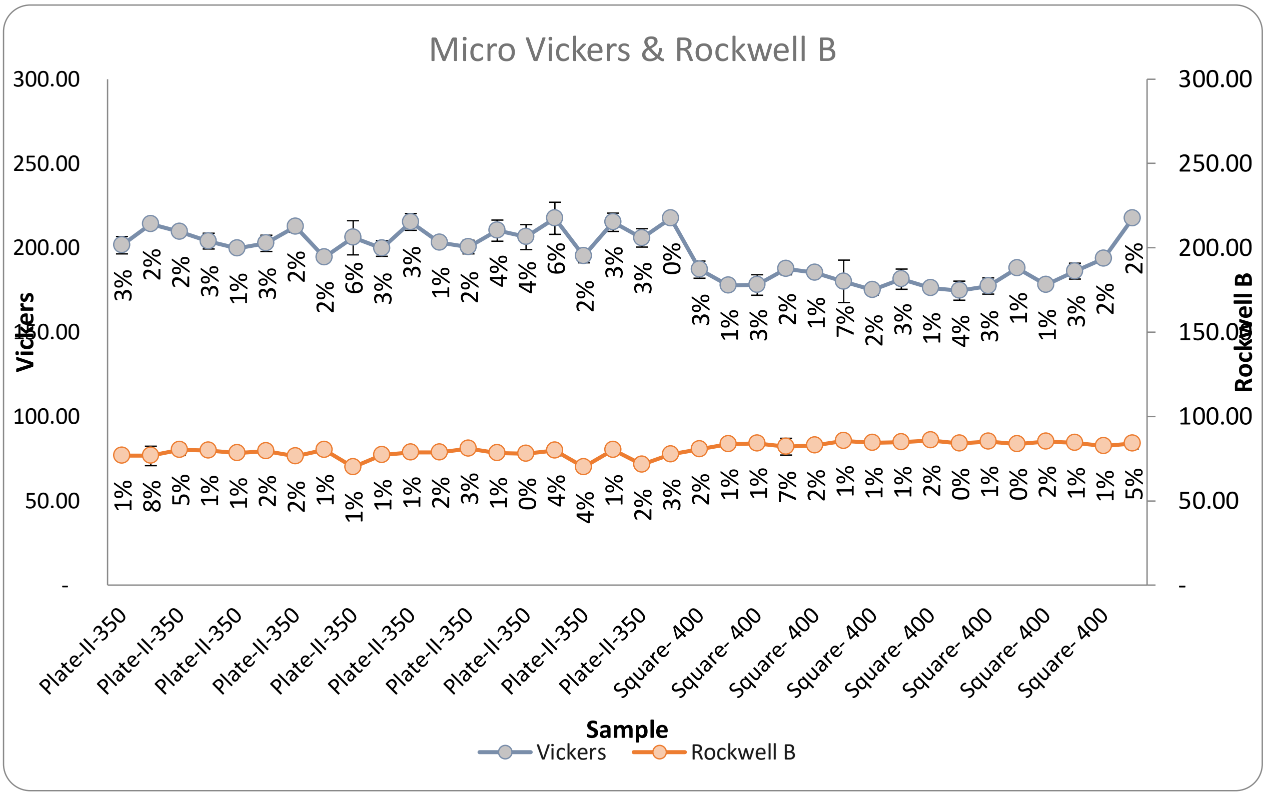

Figure 32: Comparison plot between Vickers and Rockwell hardness of 350 plate and square 400 grade steel

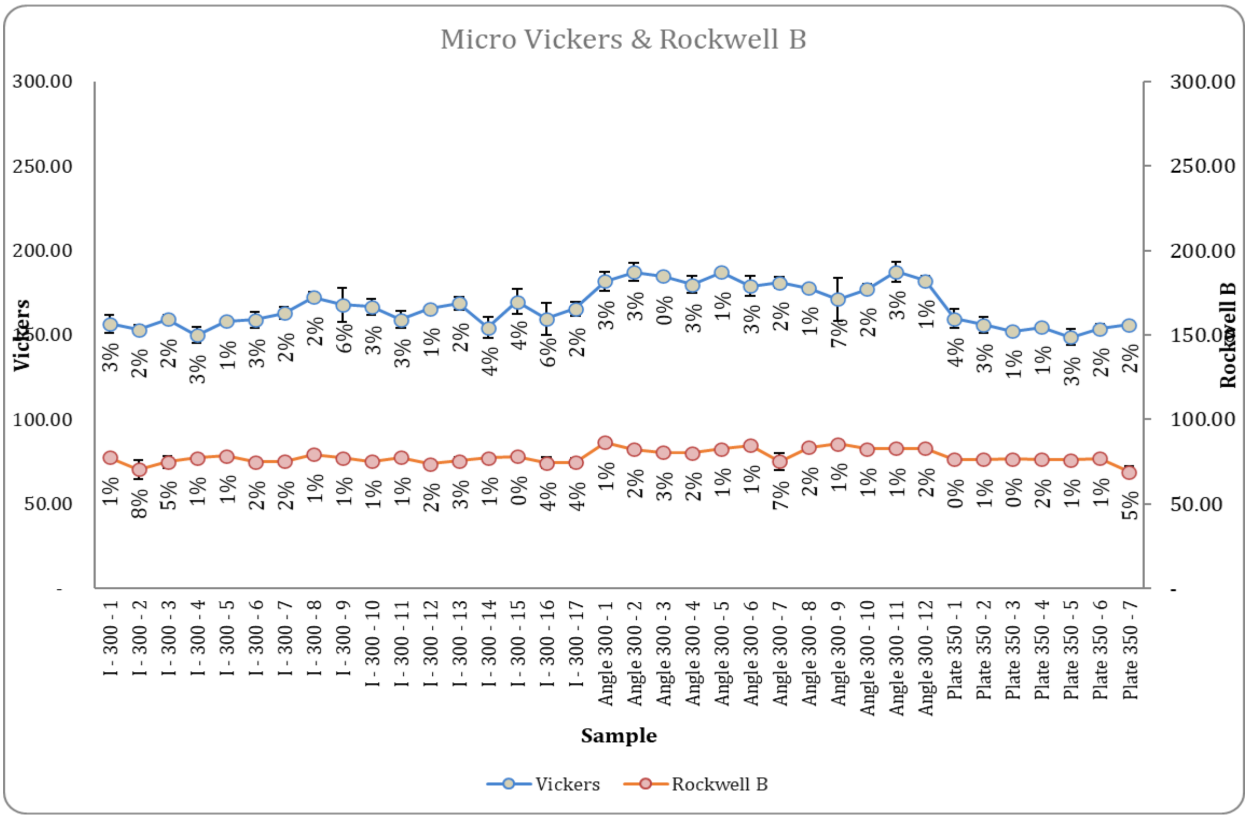

Figure 33: Comparison plot between Vickers and Rockwell hardness of 300 grade of I and angle section steel

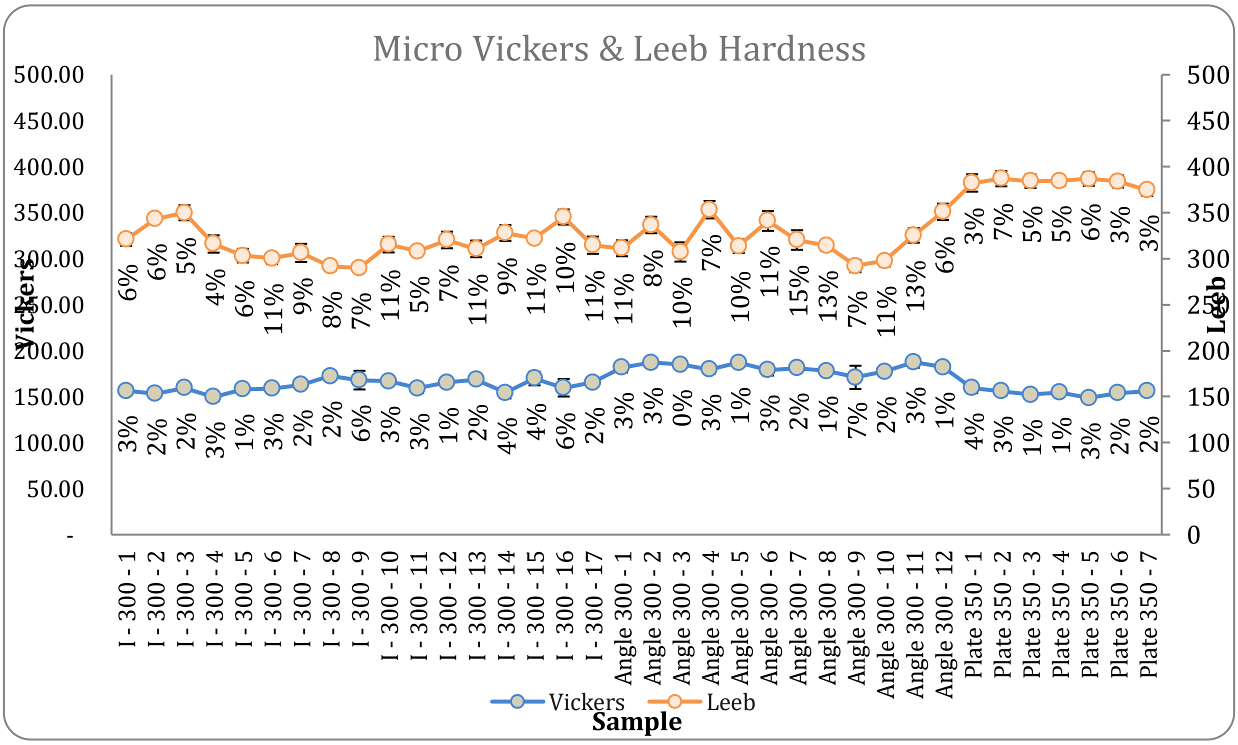

Figure 34: Comparison plot between Vickers and Leeb hardness of 300 grade of I and angle section steel

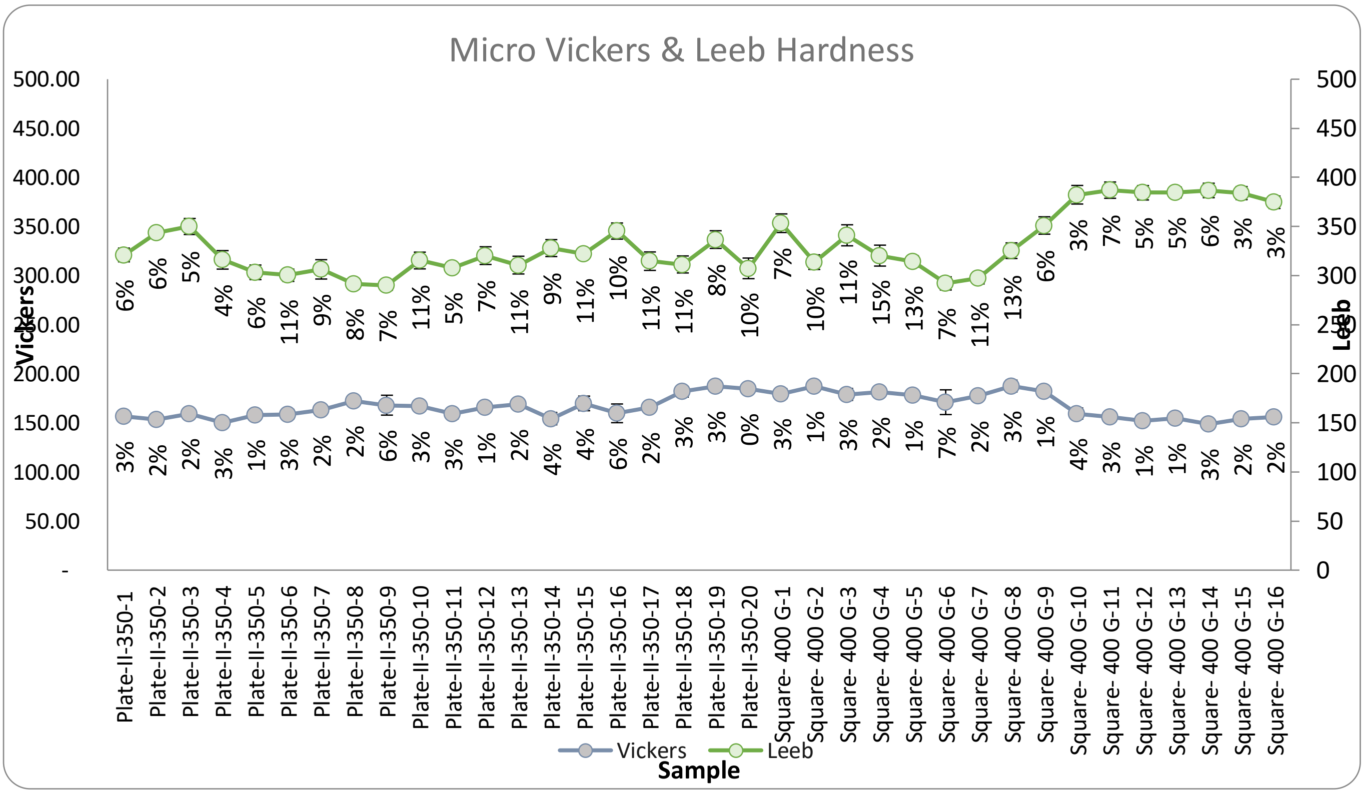

Figure 35: Comparison plot between Vickers and Leeb hardness of of 350 plate and square 400 grade steel

5.1.5. Reliability of Methods

Based on the standard deviations and percentage of error, the most consistent and reliable methods for hardness testing are the Rockwell B and the Vickers. Though Rockwell B is popular for testing structural steel due to automated, low operator dependence and reduced susceptibility to surface roughness or material inhomogeneity, likewise from the above, the Vickers test gives maximum accuracy, in evaluation of the microhardness, especially for relatively smaller areas of the material, where there is stress localization.

Conversely, variability was higher for both Brinell and Leeb test, with higher standard deviations and error percentages. While the Brinell test is prone to surface finish and human interpretation errors due to the fact that it is performed on the basis of indentation diameter measurement, the Leeb test is tricky again due to its dynamic rebound measurement that depends heavily on external testing parameters including but not limited to the mass and support of the sample. For the accurate and consistent applications, the Rockwell B and Vickers methods are most often used, especially for the non-destructive testing in buildings and civil engineering application.

Leeb hardness testing, based on the principle of rebound, became notable as a practical and non-destructive examination method. The accuracy of navigation with this method as compared to the conventional static procedures has already been called into question by researchers. Further study indicates that Leeb hardness testing may produce considerably less reliable results in some situations [100].

From **Table 2** (available in appendix section), shows the summary of Hardness tests results. After calculating the standard deviation and the error percentage for each test to compare the accuracy. According to the results the Rockwell and Vickers provide more reliable readings between the four hardness tests. The average error percentage of each test is shown in Table 1.

Rockwell B: HRB ± 5.29%, Vickers: HV ± 1.56%, Leeb: HL ± 1.69% and Brinell: HBS ± 6.87%.

Similar is in the case of Leeb hardness, where an average percentage observed from experiment was well matched with the portable tester manual. The manual claimed that error should be about 3.9%, and the results confirmed with experiment result.

Nevertheless, properties of the material and needs from its applications should be considered in the choice of hardness testing methods for steel materials. Leeb, Brinell, Micro Vickers and Rockwell all have certain pros (and cons) with regards to accuracy of hardness testing techniques. The present analysis underscores the importance of properly selecting and controlling testing conditions in order to provide reliable hardness estimates for steel samples.

5.2. Tensile Testing Results and Analysis

Tensile test of structural steel is an essential technique used to accurately measure values that includes yield strength as well as tensile strength. This paper presented tensile tests on steel grades 300, 350 and 400. In order to perform the experimentation, test was performed on the Universal Testing Machine (UTM, Instron) as shown in Figure 29 (a). The compression testing of the fabricated samples were performed at a Universal Testing Machine (Instron) with a constant crosshead speed of 0.005 *mm/sec.* It was observed from the Figure 29 (b) that the cross-section of the dog bone sample is square, and the clippers of the extensometer in the Instron machine are circular shape. At the same time, the load is applied at a strain rate of *0.005mm/sec*. Due to the round and square cross-section of both the extensometer and dog-bone sample, the graph plotted while the load is applied will be highly fluctuating lines as the extensometer gets slipped on the sample. So accurate measurement of yield strength cannot be taken from the instrument results directly. And from plastic region the graph plotted while loading be stable. Thereafter, the stress-strain curves were generated using the computed values of the applied load and the corresponding displacements of the produced samples. Further, tensile yield strength, Young's modulus and ultimate strength of the materials were calculated. Figure 36 (a) shows the yield strength at approximately 300 MPa after which the material starts to deform plastically. The ultimate load is also known as ultimate tensile strength that is the maximum stress a material can bear and it equals close to 400 MPa. After this, the stress reduces slightly until fracture and there is high level of ductility was inferred[101]. The low yield and ultimate tensile strengths along with the high ductility indicate that this material is appropriate for applications that need a degree of flexibility or energy absorbance due to being able to handle increased amounts of strain before failure. The tensile yield strength of the specimen was determined by employing the 0.2% offset approach and utilising the slope of the elastic segment of the stress-strain curve. Further, tensile yield strength, Young's modulus and ultimate strength of the materials were calculated. It can see from Figure 36 (b) that the yield strength for 350 grade steel is high (around 350 MPa), as seen from the curve where more stress is required to irreversibly deform this material. The ultimate tensile strength here is significantly greater than the 300-grade steel material, about 500 MPa. The reduction and ductility of the material is lower[102,84]. This lower strength but greater ductility means that this material could be targeted for applications under less load, in which large deformation could be possible without fracture. The yield strength of the 400-grade steel (as shown in Figure 36 (c)) is approximately 350 MPa, which is similar to that of the 350-grade steel curve, and its ultimate tensile strength is about 500 MPa. However, the ductility of the material is somewhat larger (i.e., it can sustain slightly more disturbance than the 300-grade steel until fracture). It was observed that 400 grade steel was exhibited greater ultimate tensile strength as compared to other 350 and 300 grade steel of materials[103].

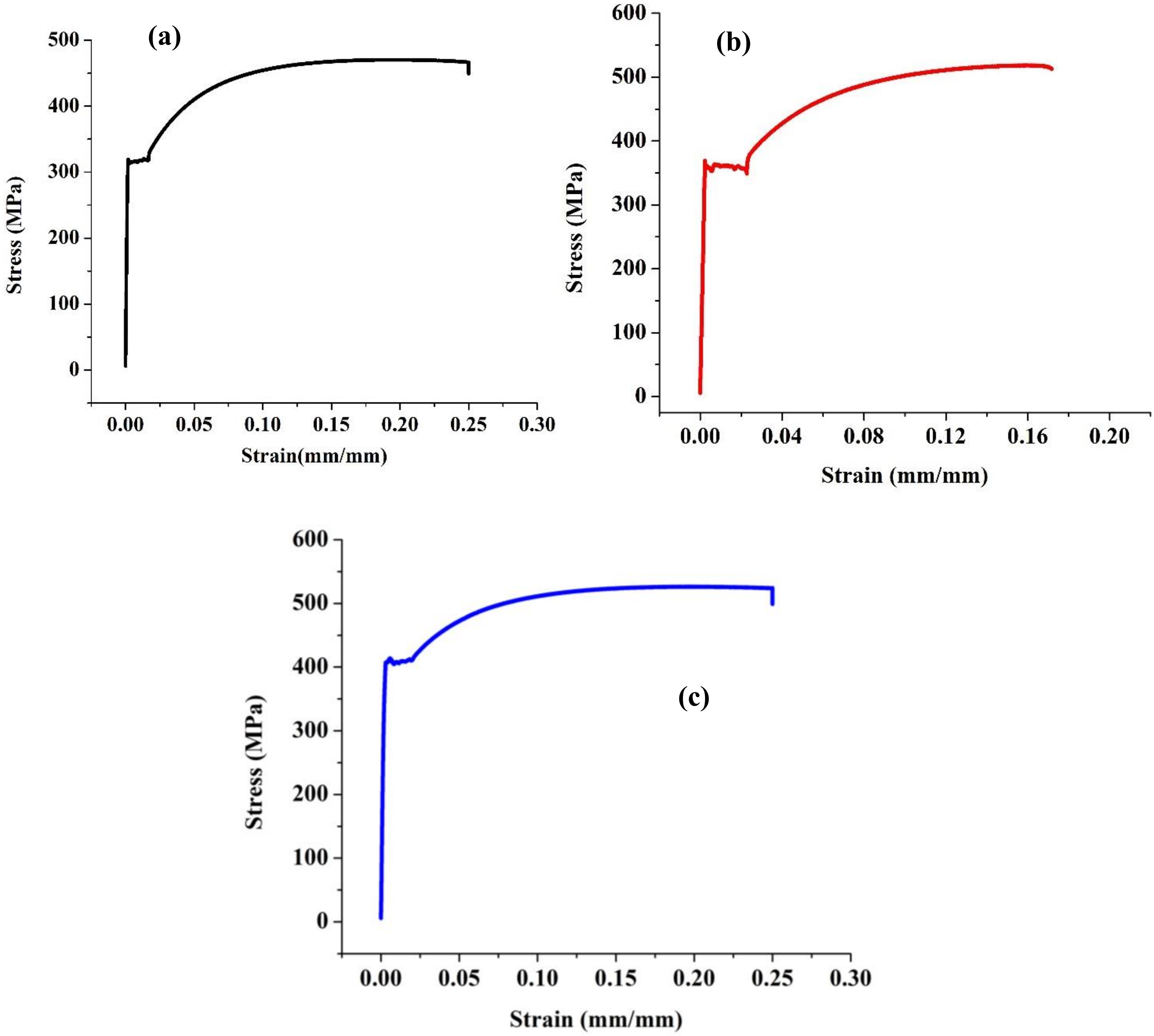

Figure 36: Stress-strain plot of (a) 300 grade, (b) 350 grade and (c) 400 grade steel under tensile testing.

It was observed from Tables (5 to 7) and Figure 32, 400 grade steel samples were exhibited maximum yield strength, Young's modulus and ultimate tensile strength. The reason was attributed to higher carbon content and/or additional alloying elements (such as manganese, chromium, or molybdenum)[104]

Table 5: Details of Mechanical properties extracted from stress-strain plot of 300 grade steel

Specimen label	Width [mm]	Thickness [mm]	Length [mm]
	1.72000	1.92000	21.32000

Maximum Load [N]	Tensile stress at Maximum Load [MPa]	Strain 2 at Maximum Load [mm/mm]	Load at Break (Standard) [N]
1911.49463	578.81982	0.16169	1011.27289

Tensile stress at Break (Standard) [MPa]	Strain 2 at Break (Standard) [mm/mm]	Tensile extension at Break (Standard) [mm]	Modulus (Automatic) [MPa]
306.22360	0.18838	1.88376	10516.78169

Load at Yield (Offset 0.2 %) [N]	Tensile stress at Yield (Offset 0.2 %) [MPa]	Tensile strain (Strain 2) at Yield (Offset 0.2 %) [mm/mm]	Load at Yield (Zero slope) [N]
-----	-----	-----	1911.49463

Tensile stress at Yield (Zero slope) [MPa]	Tensile strain (Strain 2) at Yield (Zero slope) [mm/mm]	Maximum Tensile strain (Strain 2) [mm/mm]	Maximum Tensile extension [mm]
578.81982	0.16169	0.20882	2.08822

Table 6: Details of Mechanical properties extracted from stress-strain plot of 350 grade steel.

	Specimen label	Width [mm]	Thickness [mm]	Length [mm]
1		1.72000	1.92000	21.32000

	Maximum Load [N]	Tensile stress at Maximum Load [MPa]	Strain 2 at Maximum Load [mm/mm]	Load at Break (Standard) [N]
1	1712.51196	518.56586	0.15895	938.66357

	Tensile stress at Break (Standard) [MPa]	Strain 2 at Break (Standard) [mm/mm]	Tensile extension at Break (Standard) [mm]	Modulus (Automatic) [MPa]
1	284.23679	0.17150	1.71501	161179.62859

	Load at Yield (Offset 0.2 %) [N]	Tensile stress at Yield (Offset 0.2 %) [MPa]	Tensile strain (Strain 2) at Yield (Offset 0.2 %) [mm/mm]	Load at Yield (Zero slope) [N]
1	1181.27373	357.70158	0.00424	1712.51196

	Tensile stress at Yield (Zero slope) [MPa]	Tensile strain (Strain 2) at Yield (Zero slope) [mm/mm]	Maximum Tensile strain (Strain 2) [mm/mm]	Maximum Tensile extension [mm]
1	518.56586	0.15895	0.17268	1.72678

Table 7: Details of Mechanical properties extracted from stress-strain plot of 400 grade steel.

	Specimen label	Width [mm]	Thickness [mm]	Length [mm]
1		1.72000	1.92000	21.32000

	Maximum Load [N]	Tensile stress at Maximum Load [MPa]	Strain 2 at Maximum Load [mm/mm]	Load at Break (Standard) [N]
1	1743.42822	527.92761	0.16809	967.95728

	Tensile stress at Break (Standard) [MPa]	Strain 2 at Break (Standard) [mm/mm]	Tensile extension at Break (Standard) [mm]	Modulus (Automatic) [MPa]
1	293.10721	0.25000	2.50000	191888.19674

	Load at Yield (Offset 0.2 %) [N]	Tensile stress at Yield (Offset 0.2 %) [MPa]	Tensile strain (Strain 2) at Yield (Offset 0.2 %) [mm/mm]	Load at Yield (Zero slope) [N]
1	1357.39233	411.03205	0.00408	1743.42822

	Tensile stress at Yield (Zero slope) [MPa]	Tensile strain (Strain 2) at Yield (Zero slope) [mm/mm]	Maximum Tensile strain (Strain 2) [mm/mm]	Maximum Tensile extension [mm]
1	527.92761	0.16809	0.25000	2.50000

5.3. Relationship between Hardness and Tensile testing results

From Table 3 and Table 4 (available in the appendix section), the correlation between the hardness testing results and the tensile testing results achieved in this study is evaluated, specifically the accuracy of the hardness values in predicting the yield strength (fy) and ultimate tensile strength (fu) of the structural steel samples. The main objective was to see if a stable relationship between hardness and mechanical properties could be derived.

The following empirical equations used to correlate the hardness values and mechanical properties were obtained from ISO 18265:2013[105] and used in this research. These equations were incorporated from ISO 18265:2013 section C.2.2 [105]in the present study.

$$fy = 2.70H_v - 71 \quad (5)$$

$$fu = 2.70H_v + 100 \quad (6)$$

Where:

- H_v represents the Vickers Hardness value for each sample
- fy is the yield strength
- fu is the ultimate tensile strength

These equations are derived from empirical correlations found in ISO 18265:2013[105], and provides guidance for converting hardness data to steel mechanical properties. Among the hardness tests, the Vickers hardness value (H_v) was selected as the main method in the study because the formulas in the standard are filled for the Vickers hardness value. This allowed the hardening–tensile property correlations to follow an internationally accepted framework, enabling more reliable predictions of mechanical performance. Besides from Figure 37 explains the relations between tensile strength and Vickers hardness, to respective groups of material types (I-300, Angle 300, Plate 350. Plate-II -350 …. Square.400). For the Vickers hardness, an increase in this parameter is usually due to increasing yield strength. Hence it confirmed that with a higher material quality (higher hardness), the stronger will be. According to the obtained results a higher hardness indicated better yield strength, also Plate-II 350 and Square 400 performed with that manner consequence of their levels of hardness. Such correlation is very essential for the materials selection and further optimization of their performance in engineering applications where both hardness as well as yield strength have importance.

Figure 38, shows the Vickers hardness (H_v) versus ultimate tensile strength. The positive correlation indicates that materials with a higher hardness generally have a higher tensile strength, but the relationship is not as linear. However, materials show increase in tensile strength with hardness based on linear trendlines, but I-300 does not follow the similar tendency at higher hardness level. This result underlines the dependence of tensile strength on hardness is intricate and that it varies between different material types as well as treatments.

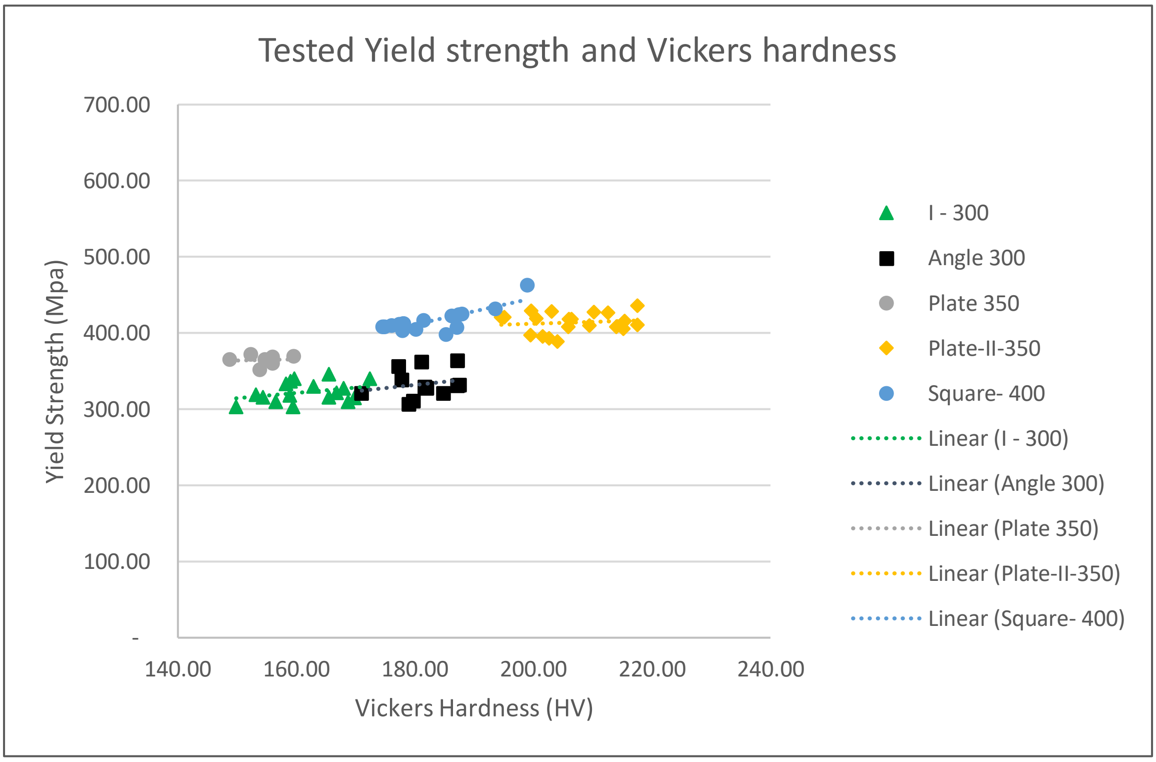

Figure 37. Plot shows the comparison between tested yield strength and Vickers hardness

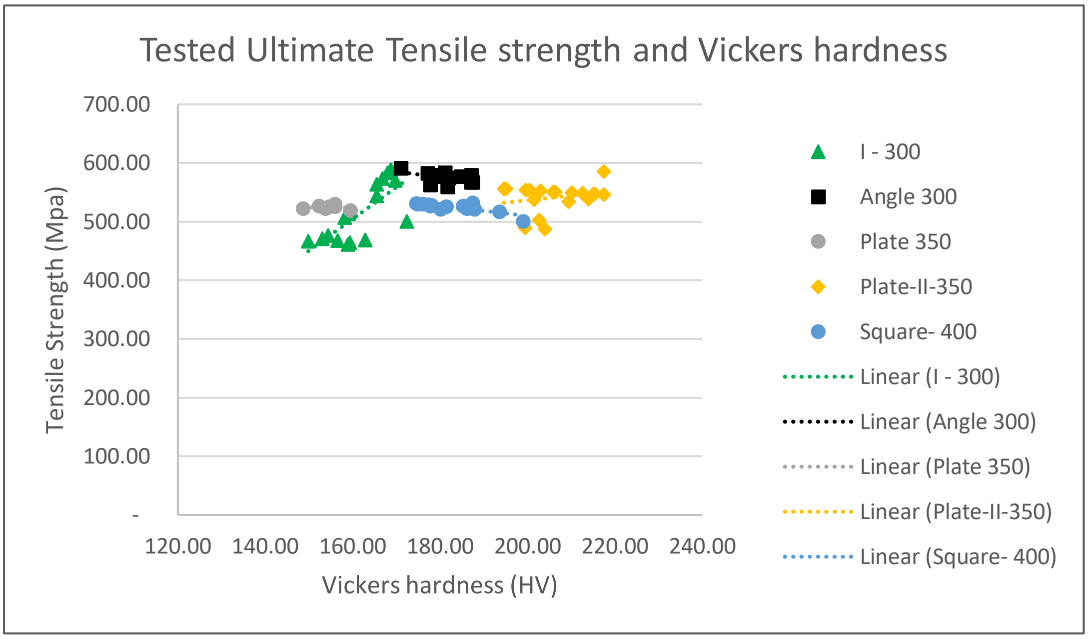

Figure 38. Plot shows the comparison between ultimate tensile strength and Vickers hardness

Figure 39**,** shows the calculated ultimate tensile strength vs Vickers hardness test for I-300, Angle-300, Plate-350, Plate-II-350 and Square–400. The linear trend for each material group is represented by using regression analysis $\boldsymbol{y = 2.7x - 71}$, suggest consistent relationship between two variables such as y is yield strength (fy) and x is Vickers hardness (H_v). The correlation equation suggests that Vickers hardness may be an effective method to predict yield strength for different material grades because of the consistency in materials.

The graph (Figure 40) shows the estimated ultimate tensile strength (UTS, MPa) vs Vickers hardness (HV) for different materials. The linear relationship of tensile strength with hardness is the same for material groups, and represented by $\boldsymbol{y = 2.5x + 100}$**,** suggest consistent relationship between two variables such as y is ultimate tensile strength (fu) and x is Vickers hardness (H_v)**.** This linear passivity between hardness and tensile strength implies that increasing Vickers Hardness leads to better the material tensile properties. In such cases, the relationship is vital for material choice and performance optimization based on hardness as well as tensile strength. This shows that hardness can be a good predictor of mechanical strength.

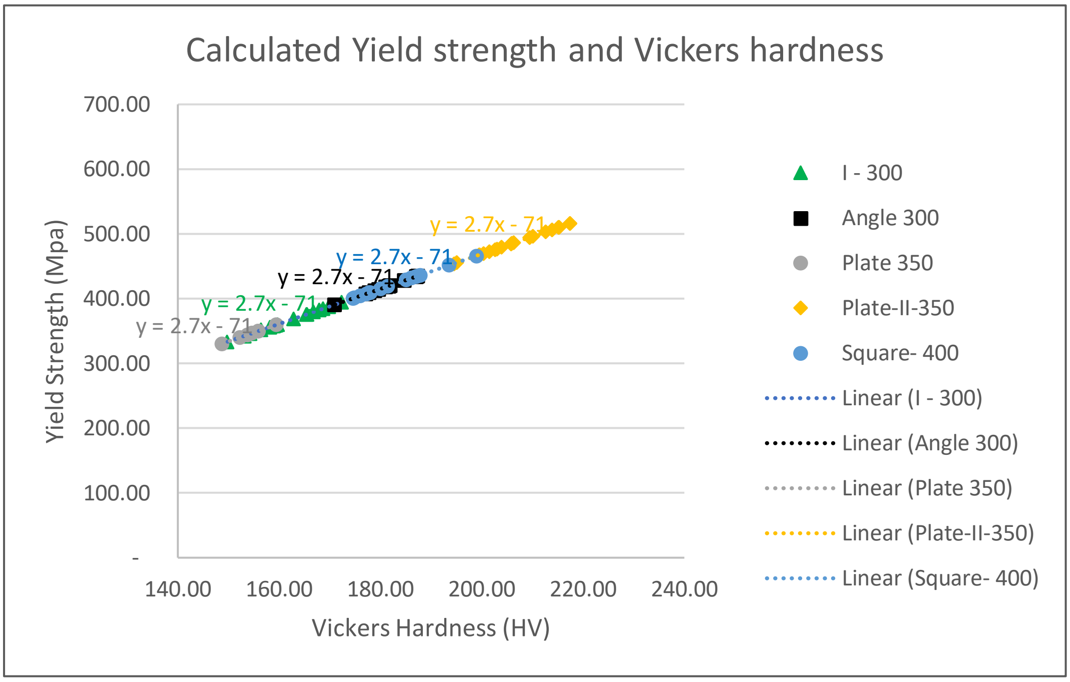

Figure 39. Comparison plot between calculated yield strength and Vickers hardness

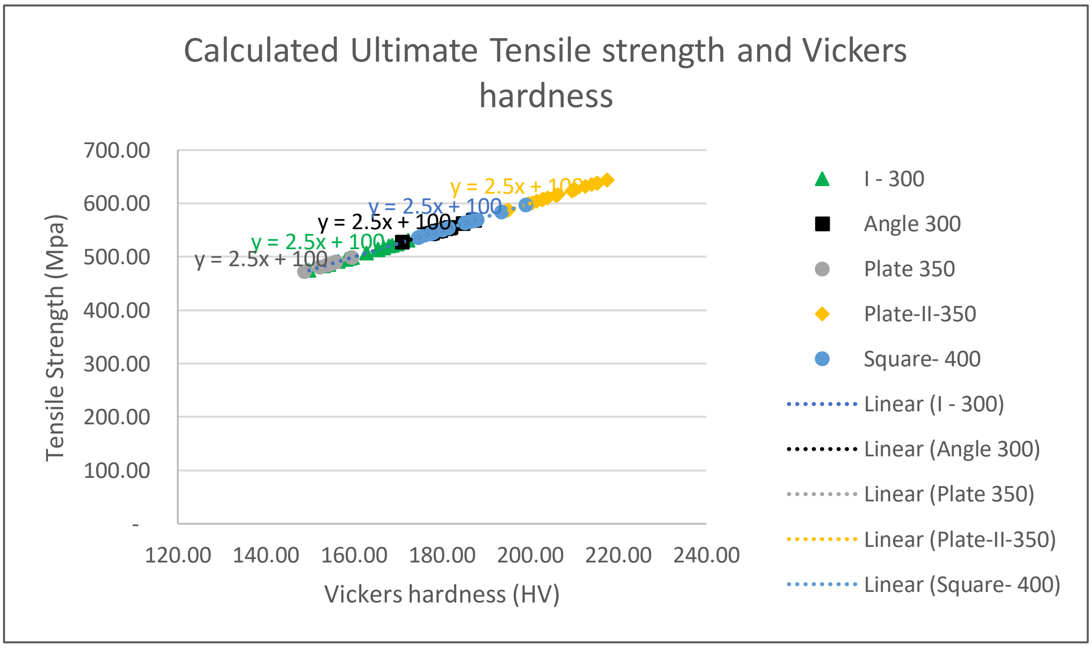

Figure 40. Comparison plot between calculated yield strength and Vickers hardness

Figure 41, shows the relationship of Yield Strength (MPa) with Rockwell Hardness (Rockwell B scale), between different materials categories: I-300, Angle-300, Plate -350, Plate-II-350 and Square – 400. The equation 6 utilized for the estimation of yield strength. Further, the lines represent a linear trendline for each material type and further suggesting very little correlation between Rockwell hardness and yield strength. This shows that prediction of yield strength compared to using Vickers hardness correlation resulted weak observable changing behaviour of the yield strength while evaluating harder range.

Figure 42, depicts the ultimate tensile strength (MPa) vs. hardness (Rockwell B scale) relationship for various materials. The tensile strength as a function of Rockwell hardness provides data points with little scatter. The linear trendlines for each material predicts a weak relation between tensile strength and Rockwell hardness. Moreover, it was observed that Rockwell hardness is not a good index of tensile strength for the materials tested since there are little variations in tensile strength over the range concerning about Rockwell hardness.

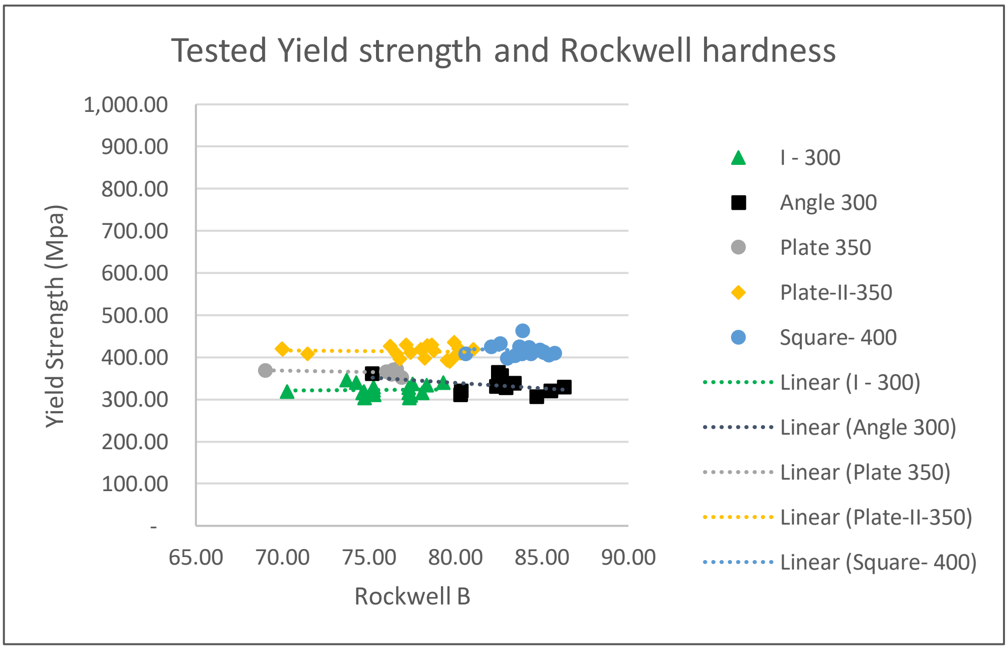

Figure 41: Plot shows the comparison between yield strength and Rockwell hardness.

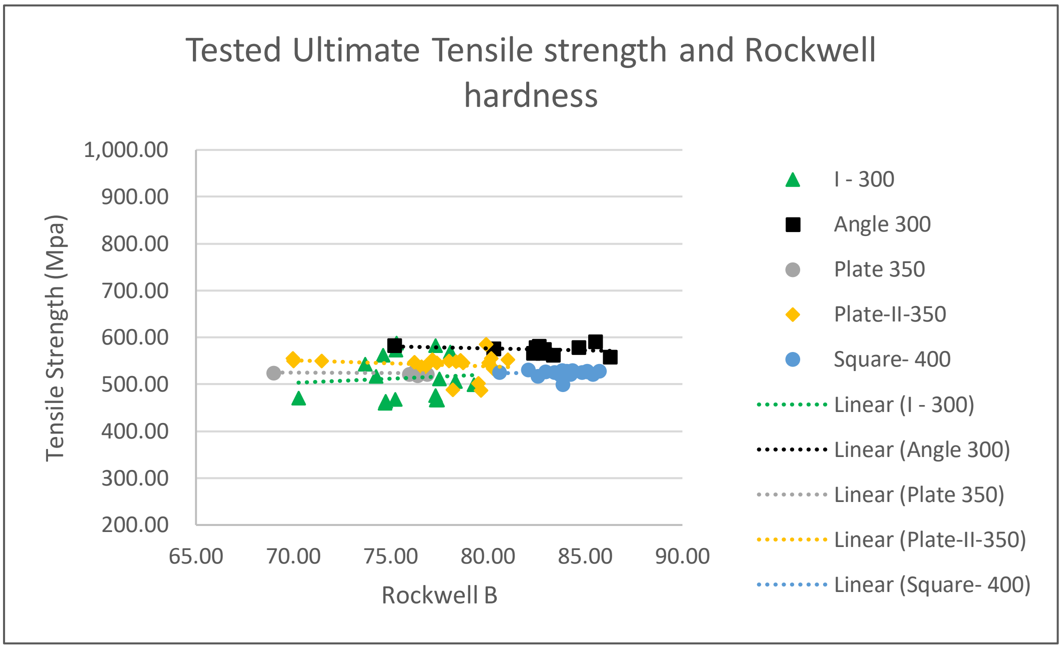

Figure 42: Plot shows the comparison between ultimate tensile strength and Rockwell hardness.

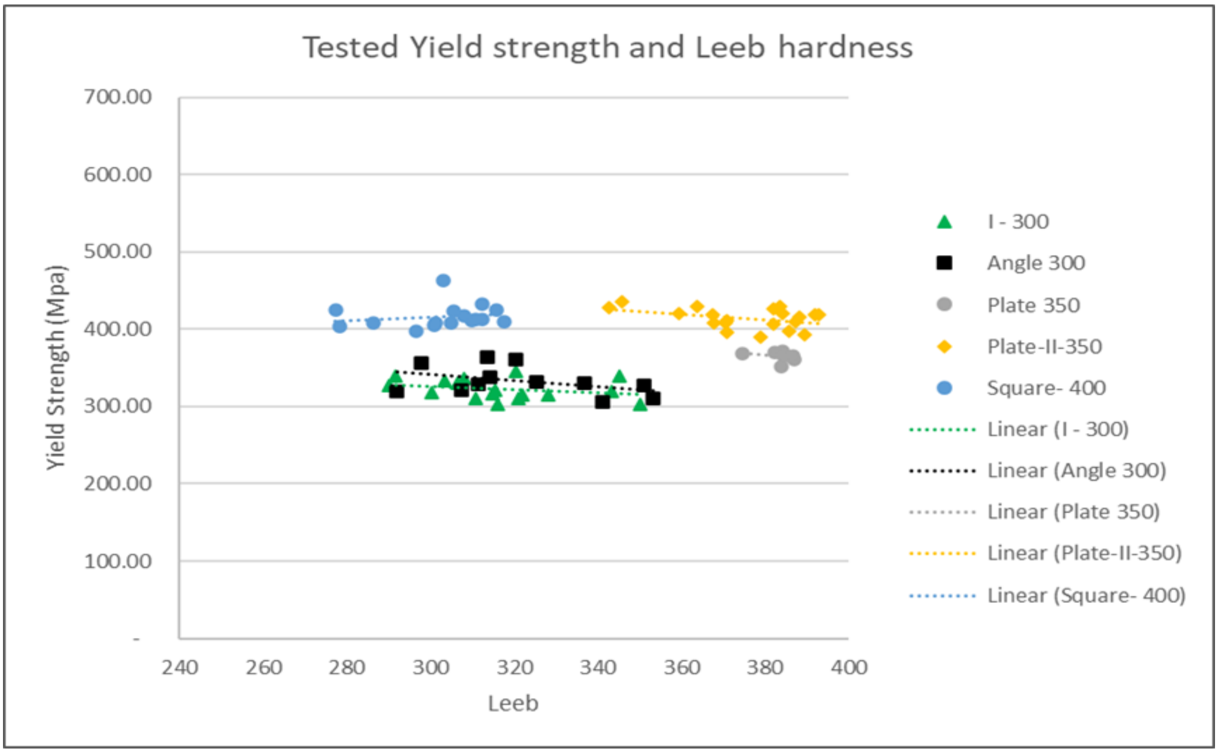

Figure 43. Plot shows the comparison between yield strength and Leeb hardness.

The Leeb hardness test is based on a different principle, measuring rebound velocity, rather than direct indentation, but there are conversion tables for Leeb HSD [106]to Vickers hardness that have been standardized. For this study, conversion formula was used as follows.

$$HV10 = 2.9085E + 02 - 2.4113E + 00(HLD) + 8.2399E - 03(HLD)^2 - 1.0056E - 05(HLD)^3 + 5.3754E - 09(HLD)^4$$

Whereas Vickers hardness was used directly, Leeb hardness values were converted and Vickers and Leeb were integrated within the same analytical model ensuring that tensile property predictions based on Vickers or Leeb values could be compared directly to values obtained experimentally. From Figure 43, shows the relationship between yield strength(intensity) in (MPa), and Leeb hardness corresponding to distinct types of materials. The x-axis represents the Leeb hardness values, and y-axis shows the yield strength. I-300 and Angle-300 materials have lower yield strengths (~ 300 MPa) over a Leeb hardness range of 260 to 320. These materials defined the linear trends as slightly sloped flat lines, which revealed weak relation between Leeb hardness and yield strength. Plate-350 and Plate-II-350 materials have yield strengths of 400 to 500 MPa matching Leeb hardness values from 320 to about 380.

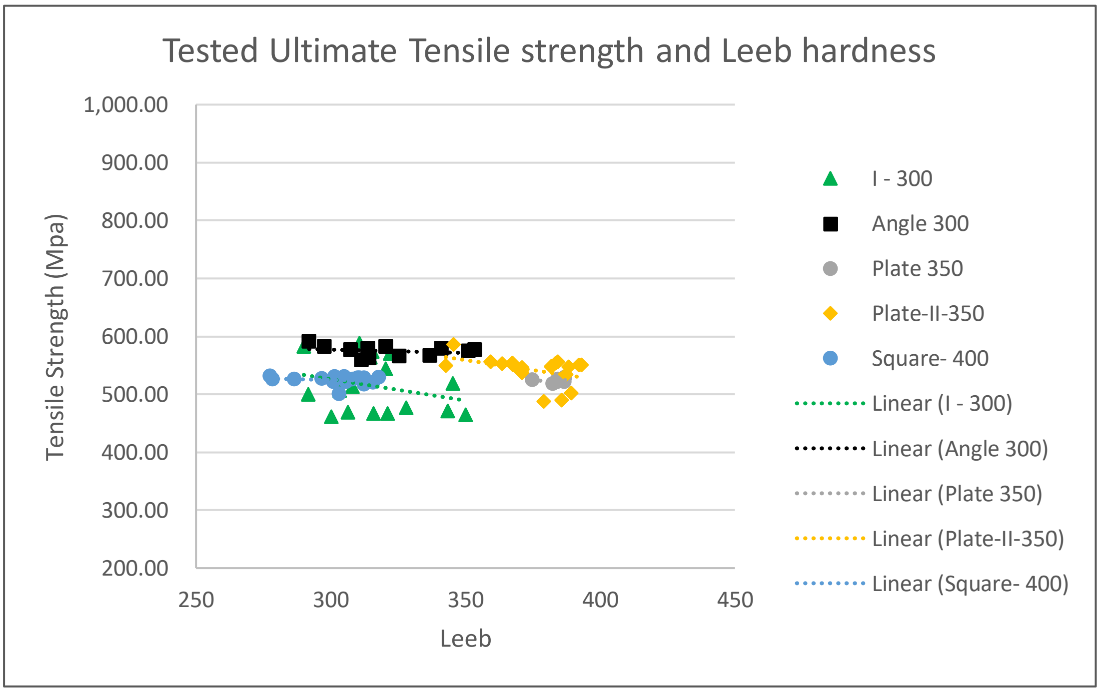

Figure 44. Plot shows the comparison between ultimate tensile strength and Leeb hardness.

Square-400 materials exhibit yield strength of about 450 MPa, with Leeb hardness based on a range between 280 to 340. The trendlines for these materials show very slight increase of yield strength with Leeb hardness going up, in some case (e.g. Plate-II-350) and other remains nearly constant. The correlation between yield strength and Leeb hardness is generally weak and cannot be determined for all grades, hence restricting its utility as a predictor of yield strength in these materials.

Figure 44, shows the ultimate tensile strength (MPa) Vs Leeb hardness for various materials. The x-axis corresponds to different Leeb hardness values and the y-axis illustrate ultimate tensile strength. I-300 materials (green triangles) tend to be of relatively lower tensile strength, with strengths that overall fall between 450 and 550 MPa across a Leeb hardness range. Further tensile strength: 550–600 MPa, Leeb hardness:290-340 for Angle-300 material (black squares) shows a more stable linear relationship. Its tensile strength is about 500～600 MPa, and the Leeb hardness ranges from 290 to 380. The linear trendlines demonstrate that Leeb hardness and tensile strength are positively correlated individually for some of the materials (Plate-II-350. In general, the Leeb hardness does not appear to be a strong predictive factor in ultimate tensile strength for these materials.

The graph shows the Yield strength (MPa) Vs. Brinell hardness for different types of material such as I-300, Angle-300, Plate-350, Plate-II-350 and Square -400 is shown below in Figure 45. It was observed from the plot that **I-300** and also **Angle 300** material demonstrate a small yield strength. In addition, slight increase in yield strength with an increasing Brinell hardness as shown by the linear trendlines for these materials. Further, Plate-350, Plate-II-350 and Square-400 materials exhibiting yield strengths of 350 MPa to 500 MPa combined with Brinell hardness in the range from around values between140 HB to around about maximum up.150 or max.and185 approx. In the case of these materials, the linear trendlines between Brinell hardness and yield strength tend to be more positively connected suggesting that harder material tends to have higher yield strengths.

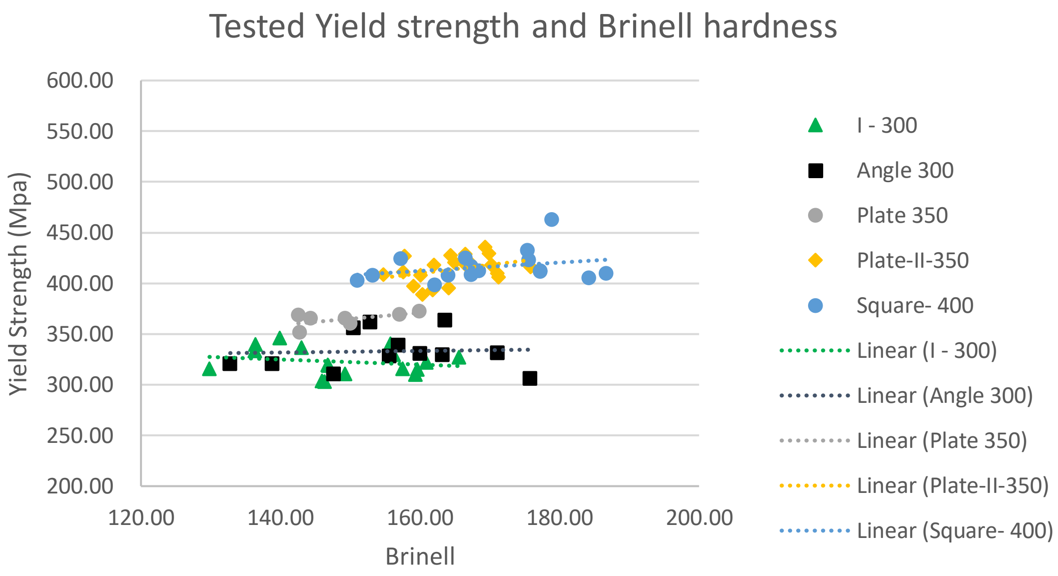

Figure 45. Plot shows the comparison between yield strength and Brinell hardness.

Figure 46, represents the relationship between UTS (MPa) and Brinell hardness for a variety of materials. The linear trend in plot explains, tensile strength as a function of Brinell hardness slightly increases. The tensile strengths of Angle-300 (black squares) materials are higher, 550 to 600 MPa with Brinell hardness values between 150 and180 vs. the lower consistent relationship. The tensile strength of Plate-350, Square300 materials is lies within 500–600 MPa with Brinell hardness values neither less than 140 nor greater than 190. Further, it can be concluded that Brinell hardness is closely related to tensile strength but in angle-300 material (which has wide range of HP), there is significant inconsistency between Brinell hardness with tensile strength.

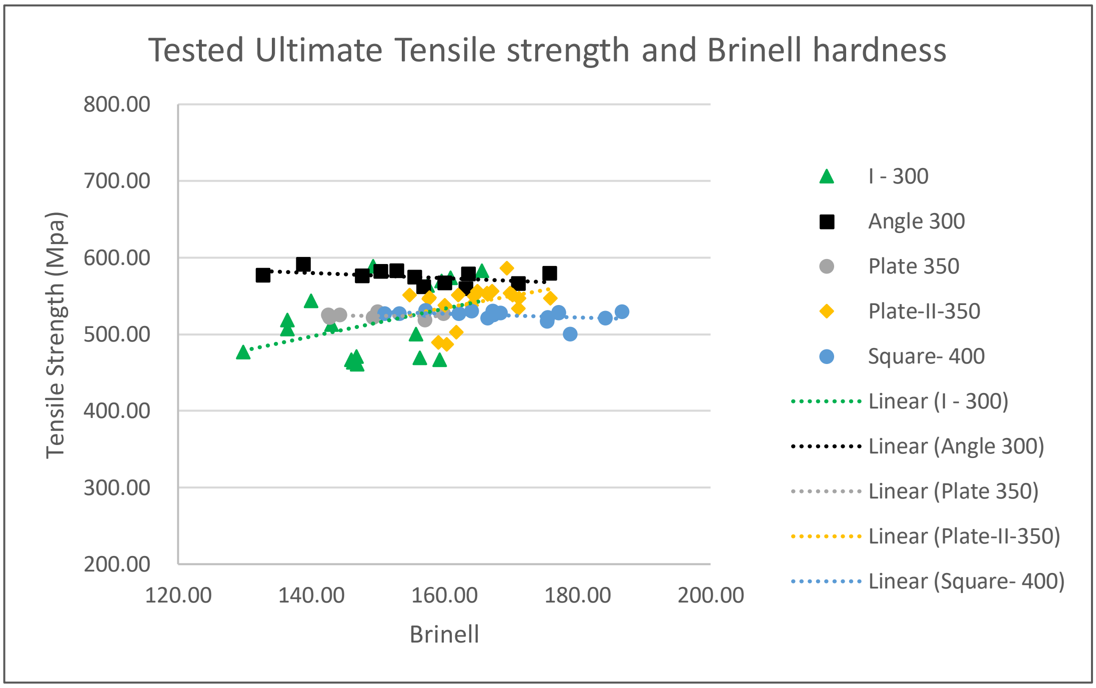

Figure 46. Plot shows the comparison between ultimate strength and Brinell hardness.

5.4. Analysis of Charpy impact testing results

The results of Charpy impact testing for grades 300, 350 and 400 were compared with the results obtained from AS/NZS 3678 [50] to evaluate the validity and reliability of the standards. As shown in Table 4 below, the minimum and average values of impact energy are shown for recorded test values at about room temperature (~20°C).

Table 8: Details of Charpy Impact test analysis

Grade	**Average Impact Energy [J]**	**Minimum Impact Energy [J]**	**AS/NZS 3678 Standard Requirement [J]**
300	81.85	60.81	27 at - 20°C
350	94.50	84.46	27 at -40°C
400	74.91	66.79	47 at -20°C

As shown in Table 8, all grades considerably exceed the minimum energy absorption provisions set out in the AS/NZS 3678 standard. It can be inferred from Figure 42, the impacts for Grade 300 (minimum of 65.38 J and average of 85.65 J) are much higher than the 27 J minimum requirement at -20°C, and Grade 350 also shows high impact energy, with a minimum of 89.13 J and average of 96.23 J, exceeding the 27 J requirement at -40°C, and for Grade 400, the minimum impact energy was 69.11 J, which exceeds the 40 J minimum requirement at -20°C (which coincidentally is much lower than the room temperature impact energy data would be) shown in Table 5 (available in appendix section). The results at room temperature should generally result in larger impact energy values as compared to results with steel subjected to testing at sub-zero temperatures, as steel tends to be more brittle at lower temperatures [17,18]

A study by Tanguy et al. the temperature dependence of Charpy impact values were discussed- in [107] on the ductile-to-brittle transition behaviour of A508 steel. Charpy impact values were found to be lower at lower temperatures, but the material maintains sufficient toughness to meet the necessary energy absorption levels at temperatures even below what is typically called for. The impact energy values are many times higher than the minimum requirements at -20°C and -40°C, even when testing at room temperature (~20°C). This means that the tested steel grades are very flexible and only become brittle at much lower temperatures. These results indicate that the impact energy levels required by the standards would still be satisfied with the materials tested, even for lower temperatures, which corroborates the validity of the test results. The same can be observed from Figure 47.

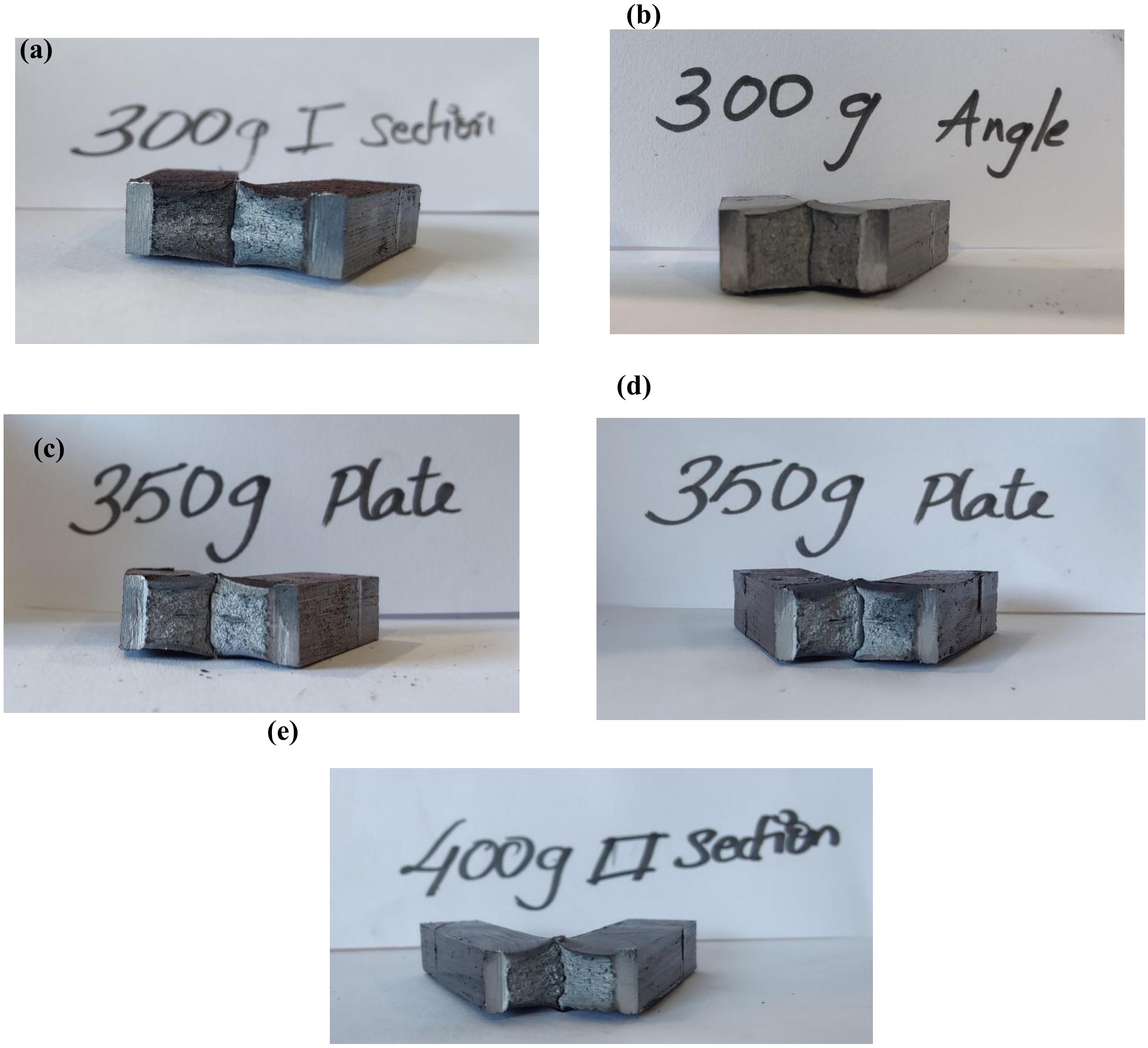

Figure 47: (a) 300G -I section sample after Charpy Test, (b) 300G -angle section sample after Charpy Test (c) 350G -Plate 1 section sample after Charpy Test , (d) 350G -Plate 2 section sample after Charpy Test and € 400G section sample after Charpy Test.

5.5. Comparison between Charpy and Hardness test

From the dataset available in Table 5 (available in the appendix section), it can observe that the impact energy values (such as 98.48 J, 69.14 J, and 70.6 J) reveal that different samples exhibit varying degrees of toughness when subjected to dynamic loading. On the other hand, hardness values (for example, Brinell: 159.33, 146.81; Rockwell: 77.43, 70.27) show that the same material consistently maintains surface resistance across these samples.

Besides, Brinell hardness values tend to correlate inversely with Charpy toughness. A lower of Brinell value, which suggests a softer material, is often linked to higher toughness, whereas higher Brinell hardness values are associated with lower energy absorption in the Charpy test. This observation aligns with the common understanding that tougher materials are generally softer and more ductile, while harder materials tend to exhibit greater brittleness. The hardness and Charpy impact tests are counterparts for material delineation. The hard-ness tests provide a surface resistance of the material and serve as an eligibility criterion for wear-resistant applications, meanwhile Charpy test inferred that the material can absorb energy when loaded suddenly to prevent breakage. The comparison charts are shown in Figure 48**.**

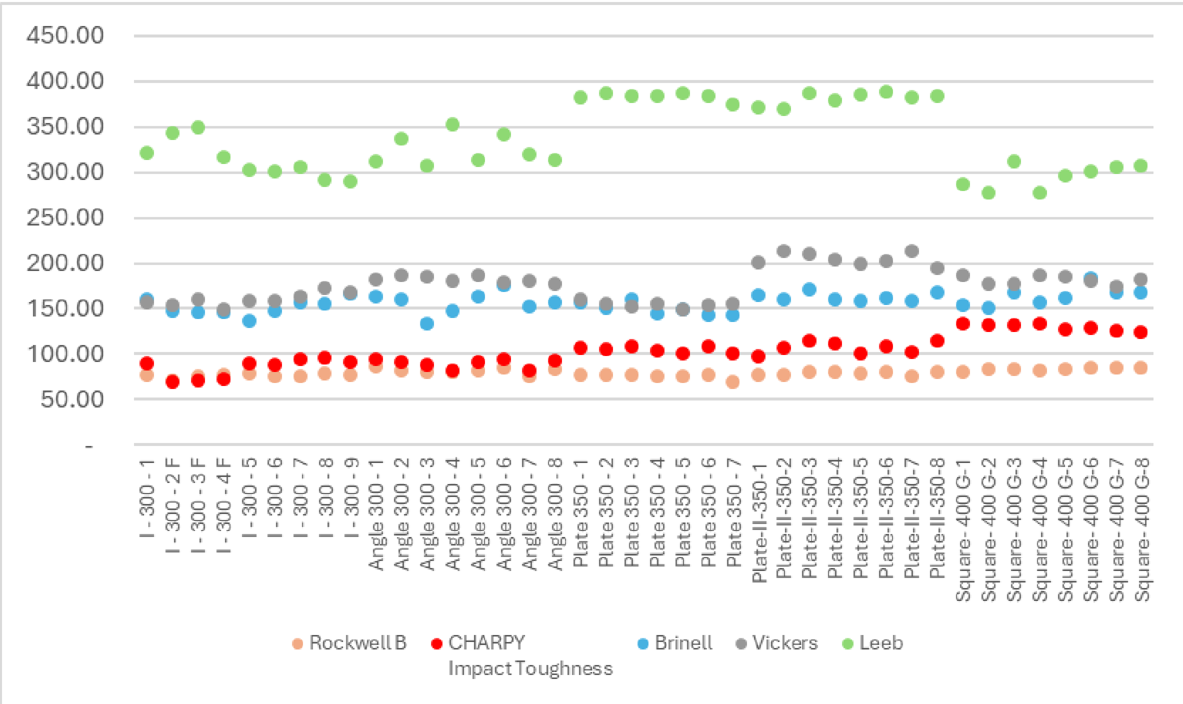

Figure 48: Comparison plot between Charpy Impact Toughness and Hardness test

6. Conclusion

6.1. Introduction

This section describes the main results obtained from the research, including microhardness tests, Charpy impact tests and the relation of those to mechanical behaviour, primarily tensile strength. It also provides information about the testing methods that have been recommended for predicting mechanical characteristics and suggests future research trajectories and applications, particularly for infrastructure and materials testing in construction applications.

6.2. Research Findings

According to the result of this investigation, Vickers hardness testing is a powerful tool for predicting the yield strength (fy) with moderate accuracy and reliability (low bias accord with standards) in concrete testing. The Vickers method also shows fairly high correlation with yield strength, so while not viable for direct tensile testing it is useful for non-destructive methods where direct tensile testing may be impractical. For instance, the correlation between the Vickers method to predict the fu is very weak. Thus, although fu is correlated with Vickers hardness, fu cannot be estimated solely from Vickers hardness.

Conversion to Vickers hardness from the Leeb hardness test provides a relatively high accuracy in estimating yield strength (fy), with moderate to high correlation, making it practical for field testing or cases where invasive testing cannot be performed. Meanwhile, its portability and in situ testing capability ensure that it can be used effectively in structural evaluations in particular environments that have limited access to conventional testing devices. Conversely, ultimate tensile strength (fu) shows a very weak correlation with the Leeb test, and thus the Leeb test is not appropriate to accurately predict (fu). As a result, the Leeb test is better suited for general yield strength evaluations as opposed to ultimate tensile strength evaluations.

The Leeb hardness test still displays a good accuracy to estimate yield strength (fy) making it an alternative for field experiments or those testing conditions which do not allow a non-destructive approach. This makes it a valuable tool for rapid in situ assessments of structures under conditions when more traditional testing approaches are not feasible. When the Leeb test correlation with fu is shown a very low correlation can be observed, which means it is not suitable for predicting fu. This puts the Leeb test in a proper situation to evaluate yield strength generally as opposed to ultimate tensile strength specifically.

6.3. Accuracy of Charpy Impact Test

All grades of structural steels performed very well in the Charpy impact test, exceeding the AS/NZS 3678 minimum energy absorption requirements and could be seen as a well-defined trend. The average impact energies for the three grades at room temperature (~20°C) are 81.85 J (Grade 300), 94.50 J (Grade 350), and 74.91 J (Grade 400), respectively. These results are consistent with the study by Tanguy et al [107]

6.4. Recommended Method

In controlled conditions, where exact prediction of yield strength is required, sample extraction is feasible, and possible methods are conducted on the same sample on which mechanical properties are required, Vickers hardness testing is proposed as the best approach due to its best accuracy and high reliability for predicting of yield strength. The error percentage was very low for yield and ultimate tensile strength using Vickers, indicating its application in engineering due to near-impossible of direct tensile testing.

While the Leeb hardness test itself is less accurate, it is the least sophisticated answer possible in a field testing or non-destructive testing scenario. It is portable, and tests the material in situ, hence it can be used for structural assessments when access to conventional testing apparatuses is restricted.

Hardness testing, especially Vickers hardness testing, provides an acceptable, non-destructive alternative to the more direct experimental estimation of mechanical properties of structural steel.

7. Future Scopes

The future scopes based on the work performed in the present study:

- Progress in non-destructive testing techniques for real-time surveillance of steel materials in essential industrial applications.
- Enhancement of reliability in Leeb hardness testing for fine-grained materials and structures.
- Creation of hybrid techniques that integrate hardness and toughness testing for steel employed in dynamic load conditions.
- Integration of artificial intelligence and machine learning with testing methodologies in Charpy and hardness test.

References

[1] J.T. Busby, M.C. Hash, G.S. Was, The relationship between hardness and yield stress in irradiated austenitic and ferritic steels, Journal of Nuclear Materials 336 (2005) 267–278. https://doi.org/https://doi.org/10.1016/j.jnucmat.2004.09.024.

[2] J.T. Busby, M.C. Hash, G.S. Was, The relationship between hardness and yield stress in irradiated austenitic and ferritic steels, Journal of Nuclear Materials 336 (2005) 267–278. https://doi.org/https://doi.org/10.1016/j.jnucmat.2004.09.024.

[3] M.O. Lai, K.B. Lim, On the prediction of tensile properties from hardness tests, J Mater Sci 26 (1991) 2031–2036. https://doi.org/10.1007/BF00549163.

[4] W. Zhang, Technical Problem Identification for the Failures of the Liberty Ships, Challenges 7 (2016). https://doi.org/10.3390/challe7020020.

[5] E. Broitman, Indentation Hardness Measurements at Macro-, Micro-, and Nanoscale: A Critical Overview, Tribol Lett 65 (2017). https://doi.org/10.1007/s11249-016-0805-5.

[6] A.Z. Gušin, B. Žužk, B. Podgornik, V. Kevorkijan, The uncertainty of hardness measurements related to the measurement method, surface preparation and range of the measurements, Materiali in Tehnologije 53 (2019) 897–904. https://doi.org/10.17222/mit.2019.098.

[7] S. Caprili, F. Mattei, I. Mazzatura, F. Ferrari, M. Gammino, M. Mariscotti, M. Mori, A. Piscini, Evaluation of mechanical characteristics of steel bars by nondestructive Vickers micro-hardness tests, in: Procedia Structural Integrity, Elsevier B.V., 2022: pp. 886–893. https://doi.org/10.1016/j.prostr.2023.01.115.

[8] K. G, Challenge of Industrial High-load One-point Hardness and of Depth Sensing Modulus, Journal of Material Science & Engineering 06 (2017). https://doi.org/10.4172/2169-0022.1000348.

[9] S.K. Kang, J.Y. Kim, C.P. Park, H.U. Kim, D. Kwon, Conventional Vickers and true instrumented indentation hardness determined by instrumented indentation tests, in: J Mater Res, 2010: pp. 337–343. https://doi.org/10.1557/jmr.2010.0045.

[10] W.-C. Kwon, M.-G. Park, Evaluation of mechanical properties of dental zirconia in different milling conditions and sintering temperatures, J Prosthet Dent 130 (2023) 909–916. https://doi.org/https://doi.org/10.1016/j.prosdent.2021.12.006.

[11] W.-C. Kwon, M.-G. Park, Evaluation of mechanical properties of dental zirconia in different milling conditions and sintering temperatures, J Prosthet Dent 130 (2023) 909–916. https://doi.org/https://doi.org/10.1016/j.prosdent.2021.12.006.

[12] D. Adamovic, F. Zivic, Hardness and Non-Destructive Testing (NDT) of Ceramic Matrix Composites (CMCs), in: D. Brabazon (Ed.), Encyclopedia of Materials: Composites, Elsevier, Oxford, 2021: pp. 183–201. https://doi.org/https://doi.org/10.1016/B978-0-12-819724-0.00074-4.

[13] G. Sundararajan, M. Roy, Hardness Testing, in: K.H.J. Buschow, R.W. Cahn, M.C. Flemings, B. Ilschner, E.J. Kramer, S. Mahajan, P. Veyssière (Eds.), Encyclopedia

of Materials: Science and Technology, Elsevier, Oxford, 2001: pp. 3728–3736. https://doi.org/https://doi.org/10.1016/B0-08-043152-6/00665-3.

[14] E.A. Campo, 5 - Physical Properties of Polymeric Materials, in: E.A. Campo (Ed.), Selection of Polymeric Materials, William Andrew Publishing, Norwich, NY, 2008: pp. 175–203. https://doi.org/https://doi.org/10.1016/B978-081551551-7.50007-3.

[15] A. Razaq, Y. Yin, J. Zhou, X. Shen, X. Ji, I. Ullah, Influence of alloying elements Sn and Ti on the microstructure and mechanical properties of gray cast iron, in: Procedia Manuf, Elsevier B.V., 2019: pp. 353–359. https://doi.org/10.1016/j.promfg.2019.12.059.

[16] N. GÜNEŞ YILMAZ, R.M. GÖKTAN, Analysis of the Leeb Hardness Test Data Obtained by Using Two Different Rock Core Holders, Süleyman Demirel Üniversitesi Fen Bilimleri Enstitüsü Dergisi 0 (2018) 10. https://doi.org/10.19113/sdufbed.28343.

[17] A. Rossoll, C. Berdin, P. Forget, C. Prioul, B. Marini, Mechanical aspects of the Charpy impact test, Nuclear Engineering and Design 188 (1999) 217–229. https://doi.org/https://doi.org/10.1016/S0029-5493(99)00017-5.

[18] Charpy Impact Test-Metallurgical Processes, 2013. https://www.azom.com/article.aspx?ArticleID=9604.

[19] M. Chandrasekar, M.R. Ishak, M. Jawaid, S.M. Sapuan, Z. Leman, 14 - Low velocity impact properties of natural fiber-reinforced composite materials for aeronautical applications, in: M. Jawaid, M. Thariq (Eds.), Sustainable Composites for Aerospace Applications, Woodhead Publishing, 2018: pp. 293–313. https://doi.org/https://doi.org/10.1016/B978-0-08-102131-6.00014-1.

[20] R. Singh, Chapter 11 - Mechanical Properties and Testing of Metals, in: R. Singh (Ed.), Applied Welding Engineering, Butterworth-Heinemann, Boston, 2012: pp. 87–94. https://doi.org/https://doi.org/10.1016/B978-0-12-391916-8.00011-X.

[21] K.K. Chawla, Mechanical Properties: Tensile Properties, in: F. Bassani, G.L. Liedl, P. Wyder (Eds.), Encyclopedia of Condensed Matter Physics, Elsevier, Oxford, 2005: pp. 312–318. https://doi.org/https://doi.org/10.1016/B0-12-369401-9/00570-2.

[22] Z. Fang, K. Roy, S. Padiyara, B. Chen, G.M. Raftery, J.B. Lim, Web crippling design of cold-formed stainless steel channels under interior-two-flange loading condition using deep belief network, in: Structures, Vol. 47, Elsevier, January 2023, pp. 1967-1990.

[23] A.L.Y. Ng, H.H. Lau, Z. Fang, K. Roy, G.M. Raftery, J.B. Lim, Experimental studies of timber to cold-formed steel connections with self-drilling screws, in: Structures, Vol. 49, Elsevier, March 2023, pp. 492-507.

[24] Z. Fang, K. Roy, J. Mares, C.W. Sham, B. Chen, J.B. Lim, Deep learning-based axial capacity prediction for cold-formed steel channel sections using Deep Belief Network, in: Structures, Vol. 33, Elsevier, October 2021, pp. 2792-2802.

[25] Z. Fang, K. Roy, Q. Ma, A. Uzzaman, J.B. Lim, Application of deep learning method in web crippling strength prediction of cold-formed stainless steel channel

sections under end-two-flange loading, in: Structures, Vol. 33, Elsevier, October 2021, pp. 2903-2942.

[26] Z. Fang, K. Roy, Y. Chi, B. Chen, J.B. Lim, Finite element analysis and proposed design rules for cold-formed stainless steel channels with web holes under end-one-flange loading, in: Structures, Vol. 34, Elsevier, December 2021, pp. 2876-2899.

[27] Z. Fang, K. Roy, A. Uzzaman, J.B. Lim, Numerical simulation and proposed design rules of cold-formed stainless steel channels with web holes under interior-one-flange loading, Engineering Structures, 252 (2022), 113566.

[28] Z. Fang, K. Roy, D. Lakshmanan, P. Pranomrum, F. Li, H.H. Lau, J.B. Lim, Structural behaviour of back-to-back cold-formed steel channel sections with web openings under axial compression at elevated temperatures, Journal of Building Engineering, 54 (2022), 104512.

[29] K. Liu, W. Chen, J. Ye, J. Jiang, Z. Fang, J.B. Lim, Heat transfer mechanism of superabsorbent polymers phase change energy storage cold-formed steel wall under fire, Journal of Building Engineering, 97 (2024), 110826.

[30] K. Liu, W. Chen, J. Ye, J. Jiang, Z. Fang, J.B. Lim, Fire performance of superabsorbent polymers protected full-scale cold-formed steel wall lined with plasterboards, Thin-Walled Structures, 204 (2024), 112353.

[31] K. Liu, M. Yu, Y. Liu, W. Chen, Z. Fang, J.B. Lim, Fire resistance time prediction and optimization of cold-formed steel walls based on machine learning, Thin-Walled Structures, 203 (2024), 112207.

[32] K. Liu, W. Chen, J. Ye, J. Jiang, Z. Fang, J.B. Lim, Fire performance enhancement of cold-formed steel walls: experimental and numerical study, Engineering Structures, 314 (2024), 118419.

[33] M.S. Maali, M. Maali, Z. Fang, K. Roy, Assessment of cold-formed steel screwed beam-column connections: Experimental tests and numerical simulations, Steel and Composite Structures, 50(5) (2024), 515-529.

[34] D.L. Chandramohan, K. Roy, Z. Fang, J.B. Lim, Moment capacity of cold-formed steel channel beams with edge-stiffened and unstiffened elongated web holes, Thin-Walled Structures, 206 (2025), 112605.

[35] Y. Chi, K. Roy, B. Chen, Z. Fang, A. Uzzaman, G.B.G. Ananthi, J.B. Lim, Effect of web hole spacing on axial capacity of back-to-back cold-formed steel channels with edge-stiffened holes, Steel and Composite Structures, 40(2) (2021), 287-305.

[36] Z. Fang, K. Roy, B. Chen, C.W. Sham, I. Hajirasouliha, J.B. Lim, Deep learning-based procedure for structural design of cold-formed steel channel sections with edge-stiffened and un-stiffened holes under axial compression, Thin-Walled Structures, 166 (2021), 108076.

[37] S. Tiwari, K. Roy, Z. Fang, J.B. Lim, Metal roof cladding system under wind loading: State-of-the-art, Journal of Wind Engineering and Industrial Aerodynamics, 257 (2025), 105939.

[38] B. Paul, Z. Fang, K. Roy, H. Tehari, M. Karpenko, J.B. Lim, Effect of axial misalignments in fillet welded cruciform joint under static loading, International Journal of Steel Structures, 24(2) (2024), 231-245.

[39] D.L. Chandramohan, K. Roy, G.B.G. Ananthi, Z. Fang, J.B. Lim, Structural behaviour and capacity of cold-formed steel channel sections with elongated edge-stiffened and unstiffened web holes under compression, Journal of Constructional Steel Research, 218 (2024), 108681.

[40] K. Ghosh, K. Roy, S. Tiwari, Z. Fang, B. Paul, J.B. Lim, Axial capacity of cold-formed steel channel sections with slits, Engineering Structures, 322 (2025), 119094.

[41] P.K. Jena, B. Mishra, M. RameshBabu, A. Babu, A.K. Singh, K. SivaKumar, T.B. Bhat, Effect of heat treatment on mechanical and ballistic properties of a high strength armour steel, Int J Impact Eng 37 (2010) 242–249. https://doi.org/https://doi.org/10.1016/j.ijimpeng.2009.09.003.

[42] S. Birosca, A. Nadoum, D. Hawezy, F. Robinson, W. Kockelmann, Mechanistic approach of Goss abnormal grain growth in electrical steel: Theory and argument, Acta Mater 185 (2020) 370–381. https://doi.org/https://doi.org/10.1016/j.actamat.2019.12.023.

[43] Z. Ghasemi, T. dos Santos, J.A. Rodríguez-Martínez, A. Srivastava, Inertial effect on dynamic hardness and apparent strain-rate sensitivity of ductile materials, J Mech Phys Solids 180 (2023) 105418. https://doi.org/https://doi.org/10.1016/j.jmps.2023.105418.

[44] Q. Liu, Y. Lin, Z. Zong, G. Sun, Q. Li, Lightweight design of carbon twill weave fabric composite body structure for electric vehicle, Compos Struct 97 (2013) 231–238. https://doi.org/https://doi.org/10.1016/j.compstruct.2012.09.052.

[45] Designation: A 370-07a Standard Test Methods and Definitions for Mechanical Testing of Steel Products 1, n.d. www.astm.org,.

[46] T. Kobayashi, Impact Testing, in: K.H.J. Buschow, R.W. Cahn, M.C. Flemings, B. Ilschner, E.J. Kramer, S. Mahajan, P. Veyssière (Eds.), Encyclopedia of Materials: Science and Technology, Elsevier, Oxford, 2001: pp. 4027–4031. https://doi.org/https://doi.org/10.1016/B0-08-043152-6/00707-5.

[47] H. Dizdar, B. Aydemir, C. Vatan, Impact Test Applications in Steel Industry, Testing and Uncertainty Calculation, 2019.

[48] Why-is-Material-Hardness-Testing-Important (1), (n.d.).

[49] A.M. Samuel, E.M. Elgallad, H.W. Doty, S. Valtierra, F.H. Samuel, Effect of metallurgical parameters on the microstructure, hardness impact properties, and fractography of Al-(6.5–11.5) wt% Si based alloys, Mater Des 107 (2016) 426–439. https://doi.org/https://doi.org/10.1016/j.matdes.2016.06.051.

[50] N.A. Babu, B.B. naik, B. Ravi, Microstructure and Mechanical properties of As-cast Al7075-Tungsten carbide metal matrix composites, Mater Today Proc 18 (2019) 413–419. https://doi.org/https://doi.org/10.1016/j.matpr.2019.06.319.

[51] Y.-L. Shen, N. Chawla, On the correlation between hardness and tensile strength in particle reinforced metal matrix composites, 2001. www.elsevier.com/locate/msea.

[52] D. Cui, Z. Yang, B. Guo, L. Liu, Z. Wang, J. Li, J. Wang, F. He, Microstructures and mechanical properties of a precipitation hardened refractory multi-principal element alloy, Intermetallics (Barking) 151 (2022) 107727. https://doi.org/https://doi.org/10.1016/j.intermet.2022.107727.

[53] E.J. Pavlina, C.J. Van Tyne, Correlation of Yield strength and Tensile strength with hardness for steels, J Mater Eng Perform 17 (2008) 888–893. https://doi.org/10.1007/s11665-008-9225-5.

[54] E.J. Pavlina, C.J. Van Tyne, Correlation of Yield strength and Tensile strength with hardness for steels, J Mater Eng Perform 17 (2008) 888–893. https://doi.org/10.1007/s11665-008-9225-5.

[55] K. Sotoodeh, Chapter Four - Corrosion study and material selection for cryogenic valves in an LNG plant, in: K. Sotoodeh (Ed.), Cryogenic Valves for Liquefied Natural Gas Plants, Gulf Professional Publishing, 2022: pp. 175–211. https://doi.org/https://doi.org/10.1016/B978-0-323-99584-9.00001-X.

[56] L. Zhu, X. Liu, P. Fan, J. Liu, A study of microstructure evolution during creep of 9Cr-1Mo steel using ultrasonic and hardness measurements, J Mater Eng Perform 28 (2019) 2348–2355.

[57] W.D. Callister Jr, D.G. Rethwisch, Materials science and engineering: an introduction, John wiley & sons, 2020.

[58] M.F. Ashby, D.R.H. Jones, Engineering materials 1: an introduction to properties, applications and design, Elsevier, 2012.

[59] G. Stachowiak, A.W. Batchelor, Engineering tribology, Butterworth-heinemann, 2013.

[60] D. Delagostini, J.R. Tinto, Technology Properties and Applications of Niobium Carbide Reinforced Steel and Iron Alloys, 2015. https://www.researchgate.net/publication/333429503.

[61] H. Safari, H. Nahvi, M. Esfahanian, Improving automotive crashworthiness using advanced high strength steels, International Journal of Crashworthiness 23 (2018) 645–659.

[62] V.S. Barbosa, L.A.C. de Godois, K.E. Bianchi, C. Ruggieri, Charpy impact energy correlation with fracture toughness for low alloy structural steel welds, Theoretical and Applied Fracture Mechanics 113 (2021) 102934.

[63] M. Ashby, H. Shercliff, D. Cebon, Chapter 8 - Fracture and fracture toughness, in: M. Ashby, H. Shercliff, D. Cebon (Eds.), Materials (Fourth Edition), Butterworth-Heinemann, 2019: pp. 203–230. https://doi.org/https://doi.org/10.1016/B978-0-08-102376-1.00008-1.

[64] P.R. Sreenivasan, Estimation of ASTM E-1921 reference temperature from Charpy tests: Charpy energy-fracture toughness correlation method, Eng Fract Mech 75 (2008) 5229–5245. https://doi.org/10.1016/j.engfracmech.2008.08.007.

[65] G. Terán, S. Capula-Colindres, D. Angeles-Herrera, J.C. Velázquez, M.J. Fernández-Cueto, Estimation of fracture toughness KIC from Charpy impact test data in T-welded connections repaired by grinding and wet welding, Eng Fract Mech 153 (2016) 351–359. https://doi.org/10.1016/j.engfracmech.2015.12.010.

[66] P. Bai, C. Shang, H.-H. Wu, G. Ma, S. Wang, G. Wu, J. Gao, Y. Chen, J. Zhang, J. Zhu, X. Mao, A review on the advance of low-temperature toughness in pipeline steels, Journal of Materials Research and Technology 25 (2023) 6949–6964. https://doi.org/https://doi.org/10.1016/j.jmrt.2023.07.119.

[67] H. Zhao, C. Ge, H. Teng, J. Fan, L. Guo, H. Dong, Correlation between Microstructure and Fracture Mechanism of 960 MPa Grade Ultra-High Toughness Steel, n.d. https://ssrn.com/abstract=4718240.

[68] X. Wei, X. Cao, J.H. Luan, Z.B. Jiao, C.T. Liu, Z.W. Zhang, Synergy of strengthening and toughening of a Cu-rich precipitate-strengthened steel, Materials Science and Engineering: A 832 (2022) 142487. https://doi.org/https://doi.org/10.1016/j.msea.2021.142487.

[69] H. Liu, P. Fu, H. Liu, C. Sun, N. Du, D. Li, Simultaneously enhancing strength and toughness of medium-carbon martensitic steel via nano precipitates and fine-grained structure, Materials Science and Engineering: A 842 (2022) 143030. https://doi.org/https://doi.org/10.1016/j.msea.2022.143030.

[70] A. Nouri, A. Rohani Shirvan, Y. Li, C. Wen, Biodegradable metallic suture anchors: A review, Smart Materials in Manufacturing 1 (2023). https://doi.org/10.1016/j.smmf.2022.100005.

[71] W.F. Hosford, ed., Ductility and Fracture, in: Mechanical Behavior of Materials, 2nd ed., Cambridge University Press, Cambridge, 2009: pp. 208–224. https://doi.org/DOI: 10.1017/CBO9780511810923.014.

[72] J. Chen, M. Lv, Z. Liu, G. Wang, Combination of ductility and toughness by the design of fine ferrite/tempered martensite–austenite microstructure in a low carbon medium manganese alloyed steel plate, Materials Science and Engineering: A 648 (2015) 51–56. https://doi.org/https://doi.org/10.1016/j.msea.2015.09.032.

[73] S. Chen, J. Hu, X. Zhang, H. Dong, W. Cao, High Ductility and Toughness of a Micro-duplex Medium-Mn Steel in a Large Temperature Range from −196 °C to 200 °C, Journal of Iron and Steel Research International 22 (2015) 1126–1130. https://doi.org/10.1016/S1006-706X(15)30122-9.

[74] C. Suryanarayana, Mechanical behavior of emerging materials, Materials Today 15 (2012) 486–498.

[75] K.M. Rajan, P.U. Deshpande, K. Narasimhan, Effect of heat treatment of preform on the mechanical properties of flow formed AISI 4130 Steel Tubes—a theoretical and experimental assessment, J Mater Process Technol 125–126 (2002) 503–511. https://doi.org/https://doi.org/10.1016/S0924-0136(02)00305-9.

[76] J. Li, D. Zhan, Z. Jiang, H. Zhang, Y. Yang, Y. Zhang, Progress on improving strength-toughness of ultra-high strength martensitic steels for aerospace

applications: a review, Journal of Materials Research and Technology 23 (2023) 172–190.

[77] D.G. Zisopol, N. Ion, A.I. Portoaca, Comparison of the Charpy Resilience of Two 3D Printed Materials: A Study on the Impact Resistance of Plastic Parts, Engineering, Technology and Applied Science Research 13 (2023) 10781–10784. https://doi.org/10.48084/etasr.5876.

[78] P. Rhomadloni, B. Junipitoyo, Y. Suprapto, Effect of Heat Treatment and Anodizing of Aluminum 2024 on Hardness Test and Impact Test, Proceeding of International Conference of Advance Transportation, Engineering, and Applied Social Science 2 (2023) 792–797. https://doi.org/10.46491/icateas.v2i1.1742.

[79] J. Mao, Q. Xu, J. Yang, C. Cao, D. Wang, F. Zhong, M. Chen, Nonlinear Impact Damage Evolution of Charpy Type and Analysis of Its Key Influencing Factors, Chinese Journal of Mechanical Engineering 37 (2024) 3. https://doi.org/10.1186/s10033-023-00986-3.

[80] Grayson Engineering in Auckland , (n.d.).

[81] J. Lee, S.-H. Lee, H. Kim, Fatigue Strength of High Strength Reinforcing Bars Having Yield Strength of 700 MPa, Journal of The Korea Concrete Institute 30 (2018) 269–279. https://api.semanticscholar.org/CorpusID:229776081.

[82] T. Matsuoka, K. Yamamori, Metallurgical aspects in cold rolled high strength steel sheets, Metallurgical Transactions A 6 (1975) 1613. https://doi.org/10.1007/BF02641975.

[83] I.U. Amobi, H.C. Uzoegbo, Structural, economic and material comparison of various steel grades under dynamic/fatigue loading, in: WIT Transactions on Engineering Sciences, 2007: pp. 263–271. https://doi.org/10.2495/MC070261.

[84] M. Ashraf, L. Gardner, D.A. Nethercot, Compression strength of stainless steel cross-sections, J Constr Steel Res 62 (2006) 105–115.

[85] Test Methods and Definitions for Mechanical Testing of Steel Products, (2016). https://doi.org/10.1520/A0370-16.

[86] Test Method for Leeb Hardness Testing of Steel Products, (2006). https://doi.org/10.1520/A0956-06.

[87] S. Yang, W. Li, H.L. Chen, Surface finishing theory and new technology, Springer, 2018.

[88] Metallic materials-Leeb hardness test-Part 1: Test method, 2015. www.iso.org.

[89] ASTM-E23-01, (n.d.).

[90] K. Kanlayasiri, S. Boonmung, An investigation on effects of wire-EDM machining parameters on surface roughness of newly developed DC53 die steel, J Mater Process Technol 187 (2007) 26–29. https://doi.org/10.1016/j.jmatprotec.2006.11.220.

[91] Y. Guo, P. Genelot, A.P. Singh, L. Bolzoni, Y. Qu, H. Kou, J. Lin, F. Yang, High-Strength Near-Beta Titanium Alloy Fabricated by Direct Hot Pressing of the

Machining Swarf, J Mater Eng Perform 31 (2022) 8619–8629. https://doi.org/10.1007/s11665-022-06846-w.

[92] Metallic materials-Tensile testing-Part 1: Method of test at room temperature COPYRIGHT PROTECTED DOCUMENT, 2019. www.iso.org.

[93] Test Methods for Tension Testing of Metallic Materials, (2013). https://doi.org/10.1520/E0008_E0008M-13A.

[94] Designation: E10 − 17 E10 − 18 Standard Test Method for Brinell Hardness of Metallic Materials 1 2. Referenced Documents 2.1 ASTM Standards: 2 A833 Test Method for Indentation Hardness of Metallic Materials by Comparison Hardness Testers A956 Test Method for Leeb Hardness Testing of Steel Products A1038 Test Method for Portable Hardness Testing by the Ultrasonic Contact Impedance Method B647 Test Method for Indentation Hardness of Aluminum Alloys by Means of a Webster Hardness Gage, (n.d.). https://doi.org/10.1520/E0010-1.

[95] V. Kharchenko, O. Katok, A. Sereda, M. Rudnitskyi, R. Kravchuk, S. Bisyk, Determination of strength characteristics of high-strength sheet steels by hardness and instrumented indentation, Procedia Structural Integrity 36 (2022) 277–283. https://doi.org/https://doi.org/10.1016/j.prostr.2022.01.035.

[96] Test Method for Surface Burning Characteristics of Building Materials, (n.d.). https://doi.org/10.1520/E0084.

[97] G. Dai, K. Herrmann, F. Menelao, Two approaches for enhancing the accuracy of the Rockwell hardness test, Meas Sci Technol 20 (2009) 065701.

[98] Test Methods for Rockwell Hardness of Metallic Materials, (2015). https://doi.org/10.1520/E0018-15.

[99] V. Syasko, A. Nikazov, Research and development of metrological assurance elements for leeb hardness measurements, Inventions 6 (2021) 86.

[100] A. Vaško, J. Sovík, Z. Sedliackova, Accuracy of Portable Hardness Testers, Manufacturing Technology 19 (2019) 886–890. https://doi.org/10.21062/ujep/389.2019/a/1213-2489/MT/19/5/886.

[101] W. Zhang, G. Xin, Z. Wenhan, M. Zhitao, D. Xuanming, Review of transparent soil model testing technique for underground construction: Ground visualization and result digitalization, Underground Space 7 (2020). https://doi.org/10.1016/j.undsp.2020.05.003.

[102] S. Zheng, J. Fan, F. Yu, B. Feng, B. Lou, Q. Zou, G. Xie, S. Lin, R. Wang, X. Yang, Viral load dynamics and disease severity in patients infected with SARS-CoV-2 in Zhejiang province, China, January-March 2020: retrospective cohort study, Bmj 369 (2020).

[103] M. Komarasamy, C. Smith, J. Darsell, W. Choi, S. Jana, G. Grant, Microstructure and mechanical properties of friction stir welded Haynes 282, Mater Charact 182 (2021) 111558.

[104] E.J. Pavlina, C.J. Van Tyne, Correlation of Yield strength and Tensile strength with hardness for steels, J Mater Eng Perform 17 (2008) 888–893. https://doi.org/10.1007/s11665-008-9225-5.

[105] INTERNATIONAL STANDARD ISO 18265 : Metallic materials — Conversion of hardness values, 2013.

[106] ASTM Standard: Hardness Conversion Table For Metals Relationship, (n.d.).

[107] B. Tanguy, J. Besson, R. Piques, A. Pineau, Ductile to brittle transition of an A508 steel characterized by Charpy impact test: Part I: experimental results, Eng Fract Mech 72 (2005) 49–72. https://doi.org/https://doi.org/10.1016/j.engfracmech.2004.03.010.

Appendix

Table 1:

		Brinell	STDEV	Error %	Rockwell B	STDEV	Error %	Vickers	STDEV	Error %	Leeb	STDEV	Error %
I - 300	**I - 300 - 1**	159.33	0.67	0%	77.43	0.41	1%	156.53	5.14	3%	321	6.98	6%
I - 300	**I - 300 - 2**	146.81	2.31	2%	70.27	5.77	8%	153.13	2.50	2%	343.33	2.83	6%
I - 300	**I - 300 - 3**	146.31	19.79	14%	74.76	3.49	5%	159.43	2.44	2%	350	8.16	5%
I - 300	**I - 300 - 4**	145.99	8.93	6%	77.34	0.42	1%	149.83	4.68	3%	316	9.42	4%
I - 300	**I - 300 - 5**	136.38	12.09	9%	78.34	0.42	1%	158.20	1.98	1%	303.33	7.41	6%
I - 300	**I - 300 - 6**	146.92	5.61	4%	74.72	1.39	2%	158.90	4.82	3%	300.33	6.24	11%
I - 300	**I - 300 - 7**	156.27	8.76	6%	75.25	1.18	2%	162.90	3.41	2%	306.33	9.84	9%
I - 300	**I - 300 - 8**	155.76	4.73	3%	79.31	0.94	1%	172.37	3.00	2%	291.67	5.25	8%
I - 300	**I - 300 - 9**	165.63	5.40	3%	77.32	1.05	1%	168.00	10.13	6%	290	4.97	7%
I - 300	**I - 300 - 10**	160.89	5.16	3%	75.28	0.86	1%	166.80	4.68	3%	315.33	8.5	11%
I - 300	**I - 300 - 11**	143.04	7.40	5%	77.52	0.44	1%	159.03	4.97	3%	308	2.94	5%
I - 300	**I - 300 - 12**	139.96	13.91	10%	73.71	1.74	2%	165.47	1.72	1%	320.33	8.99	7%
I - 300	**I - 300 - 13**	149.26	4.87	3%	75.32	2.15	3%	168.73	4.03	2%	310.67	9.03	11%
I - 300	**I - 300 - 14**	129.82	6.81	5%	77.31	1.14	1%	154.33	6.27	4%	328	8.6	9%

I - 300	**I - 300 - 15**	159.63	4.94	3%	78.08	0.23	0%	169.80	7.42	4%	322	3.74	11%
I - 300	**I - 300 - 16**	136.43	2.99	2%	74.25	3.23	4%	159.70	9.51	6%	345.33	8.22	10%
I - 300	**I - 300 - 17**	157.49	3.51	2%	74.62	2.71	4%	165.53	4.00	2%	314.67	9.39	11%
Angle 300	**Angle 300 - 1**	163.22	4.51	3%	86.29	1.02	1%	181.73	5.42	3%	311.33	8.65	11%
Angle 300	**Angle 300 - 2**	160.03	8.50	5%	82.37	1.81	2%	187.17	5.45	3%	336.67	8.96	8%
Angle 300	**Angle 300 - 3**	132.79	13.52	10%	80.33	2.23	3%	184.77	0.60	0%	307.33	10.5	10%
Angle 300	**Angle 300 - 4**	147.63	16.73	11%	80.31	1.65	2%	179.73	5.07	3%	353.33	9.46	7%
Angle 300	**Angle 300 - 5**	163.60	10.03	6%	82.48	0.72	1%	187.17	1.99	1%	313.67	7.41	10%
Angle 300	**Angle 300 - 6**	175.82	8.32	5%	84.70	0.63	1%	179.00	6.08	3%	341	10.71	11%
Angle 300	**Angle 300 - 7**	152.87	5.60	4%	75.21	4.97	7%	181.10	3.37	2%	320.33	10.66	15%
Angle 300	**Angle 300 - 8**	156.93	10.24	7%	83.39	1.47	2%	177.83	1.49	1%	314.33	5.79	13%
Angle 300	**Angle 300 - 9**	138.80	5.19	4%	85.53	0.51	1%	171.03	12.59	7%	292	6.68	7%
Angle 300	**Angle 300 - 10**	150.47	10.84	7%	82.65	1.11	1%	177.23	2.85	2%	297.67	6.18	11%
Angle 300	**Angle 300 - 11**	171.12	9.88	6%	82.83	1.08	1%	187.47	5.99	3%	325.33	7.93	13%
Angle 300	**Angle 300 - 12**	155.59	5.26	3%	82.91	1.64	2%	182.00	2.71	1%	351	8.83	6%
Plate 350	**Plate 350 - 1**	157.06	0.92	1%	76.40	0.05	0%	159.50	5.65	4%	382.33	9.46	3%
Plate 350	**Plate 350 - 2**	149.96	2.56	2%	76.32	1.05	1%	155.97	4.80	3%	387	8.29	7%
Plate 350	**Plate 350 - 3**	159.89	1.24	1%	76.60	0.32	0%	152.33	1.27	1%	384.33	7.32	5%
Plate 350	**Plate 350 - 4**	144.31	10.90	11%	76.19	1.28	2%	154.70	0.79	1%	384.67	5.44	5%

Plate 350	**Plate 350 - 5**	149.30	3.21	3%	75.99	0.59	1%	148.73	4.71	3%	386.67	7.36	6%
Plate 350	**Plate 350 - 6**	142.80	2.98	3%	76.89	0.54	1%	153.80	2.50	2%	384	6.68	3%
Plate 350	**Plate 350 - 7**	142.55	9.79	16%	69.01	3.12	5%	155.97	2.43	2%	374.67	6.34	3%
Plate-II-350	**Plate-II-350-1**	164.10	5.58	3%	76.79	0.97	1%	201.57	5.84	3%	371	11.05	12%
Plate-II-350	**Plate-II-350-2**	160.08	13.70	9%	76.59	3.95	5%	213.97	8.72	4%	370.67	8.99	8%
Plate-II-350	**Plate-II-350-3**	171.10	7.21	4%	80.29	0.48	1%	209.47	11.88	6%	387.33	8.65	5%
Plate-II-350	**Plate-II-350-4**	160.33	9.76	6%	79.67	1.74	2%	204.00	4.04	2%	379	9.9	9%
Plate-II-350	**Plate-II-350-5**	159.08	10.65	7%	78.22	1.65	2%	199.53	6.04	3%	385.67	9.46	5%
Plate-II-350	**Plate-II-350-6**	161.80	9.82	6%	79.54	0.88	1%	202.67	4.22	2%	389.33	2.62	7%
Plate-II-350	**Plate-II-350-7**	157.78	15.45	10%	76.23	2.37	3%	212.63	0.95	0%	382	9.93	9%
Plate-II-350	**Plate-II-350-8**	167.18	2.52	2%	80.20	1.04	1%	194.57	6.71	3%	384.33	7.72	5%
Plate-II-350	**Plate-II-350-9**	170.24	4.67	3%	70.01	3.87	6%	205.97	4.29	2%	392	8.64	3%
Plate-II-350	**Plate-II-350-10**	169.90	11.00	6%	77.17	2.36	3%	199.67	3.55	2%	383.67	8.65	7%
Plate-II-350	**Plate-II-350-11**	175.88	6.28	4%	78.75	1.99	3%	215.37	3.94	2%	388.33	5.56	7%
Plate-II-350	**Plate-II-350-12**	166.50	12.06	7%	78.62	1.44	2%	203.03	2.45	1%	363.67	3.77	3%
Plate-II-350	**Plate-II-350-13**	166.39	5.33	3%	81.04	0.37	0%	200.47	3.24	2%	367.33	10.34	6%
Plate-II-350	**Plate-II-350-14**	164.44	10.79	7%	78.36	0.29	0%	210.20	4.95	2%	342.67	6.02	4%
Plate-II-350	**Plate-II-350-15**	162.05	14.90	9%	78.01	1.55	2%	206.37	5.88	3%	393	9.2	6%
Plate-II-350	**Plate-II-350-16**	169.34	11.14	7%	79.93	1.34	2%	217.53	3.14	1%	345.67	6.65	5%

Plate-II-350	**Plate-II-350-17**	164.92	9.12	6%	69.99	1.06	2%	195.13	2.58	1%	359.33	7.41	6%
Plate-II-350	**Plate-II-350-18**	171.26	6.11	4%	80.06	1.48	2%	215.17	6.60	3%	382	8.52	6%
Plate-II-350	**Plate-II-350-19**	154.80	9.33	6%	71.46	5.48	8%	205.90	5.39	3%	367.67	9.46	8%
Plate-II-350	**Plate-II-350-20**	157.66	9.73	6%	77.40	3.10	4%	217.53	5.73	3%	371	11.52	10%
Square- 400	**Square- 400 G-1**	153.23	11.33	7%	80.60	3.41	4%	187.07	3.47	2%	286.33	13.82	5%
Square- 400	**Square- 400 G-2**	151.02	11.93	8%	83.44	0.29	0%	177.87	5.23	3%	278.33	19.60	7%
Square- 400	**Square- 400 G-3**	168.47	19.86	12%	84.08	0.03	0%	177.97	4.74	3%	312.33	15.46	5%
Square- 400	**Square- 400 G-4**	157.21	10.72	7%	82.08	1.29	2%	187.40	2.90	2%	277.33	21.06	8%
Square- 400	**Square- 400 G-5**	162.15	16.57	10%	82.99	0.67	1%	185.20	2.05	3%	296.67	22.81	8%
Square- 400	**Square- 400 G-6**	184.22	8.07	4%	85.42	0.53	1%	180.13	8.43	5%	301.00	16.31	5%
Square- 400	**Square- 400 G-7**	167.31	7.42	4%	84.37	0.22	0%	174.87	2.70	2%	305.00	19.44	6%
Square- 400	**Square- 400 G-8**	167.36	1.09	1%	84.87	0.95	1%	181.43	2.76	2%	308.00	16.87	5%
Square- 400	**Square- 400 G-9**	186.70	6.06	3%	85.75	0.36	0%	176.10	2.87	2%	317.67	14.08	4%
Square- 400	**Square- 400 G-10**	164.08	2.30	1%	83.84	0.56	1%	174.60	7.21	4%	301.33	16.74	6%
Square- 400	**Square- 400 G-11**	177.22	6.62	4%	85.12	0.57	1%	177.37	4.82	3%	310.00	12.08	4%
Square- 400	**Square- 400 G-12**	166.48	6.95	4%	83.72	0.69	1%	187.97	1.72	1%	315.67	14.88	5%
Square- 400	**Square- 400 G-13**	177.22	2.78	2%	85.11	0.75	1%	178.07	4.54	3%	310.67	21.91	7%
Square- 400	**Square- 400 G-14**	175.57	9.22	5%	84.27	0.64	1%	186.20	1.14	1%	305.67	12.23	22%
Square- 400	**Square- 400 G-15**	175.42	5.98	3%	82.60	0.57	1%	193.57	2.64	1%	312.33	7.36	2%

Square- 400	**Square- 400 G-16**	178.86	7.12	4%	83.87	0.96	1%	217.53	3.14	1%	303.00	12.83	4%
	Average		8.02	5%		1.4	1.9%		4.4	2.5%		9.65	6.8%

	Brinell			**Rockwell B**			**Vickers**			**Leeb**		
	Min	**Max**	**Avg**	**Min**	**Max**	**Avg**	**Min**	**Max**	**Avg**	**Min**	**Max**	**Avg**
I - 300	129.82	165.63	149.17	70.27	79.31	75.93	149.83	172.37	161.69	290.00	350.00	316.84
Angle 300	132.79	175.82	155.74	75.21	86.29	82.42	171.03	187.47	181.35	292.00	353.33	322.00
Plate 350	142.55	159.89	149.41	69.01	76.89	75.34	148.73	159.50	154.43	374.67	387.00	383.38
Plate-II-350	154.80	175.88	164.74	69.99	81.04	77.42	194.57	217.53	206.54	342.67	393.00	375.28
Square- 400	151.02	186.70	169.53	80.60	85.75	83.88	174.60	217.53	183.96	277.33	317.67	302.58

Table 2 : Experimental results of different hardness test

	Brinnell (HBS)						Rockwell B (HRB)						micro Vickers (HV)						Leeb Hardness (HL)					
Sample	Point 1	Point 2	Point 3	Average	STDEV	Error	Point 1	Point 2	Point 3	Average	STDEV	Error	Point 1	Point2	Point 3	Average	STDEV	Error	Point 1	Point 2	Point 3	Average	STDEV	Error
1	157.93	155.79	157.45	157.06	0.92	0.58	76.37	76.47	76.37	76.40	0.05	0.06	153.2	166.9	158.4	159.50	5.65	3.54	384	370	393	382.33	9.46	2.48
2	147.47	153.48	148.94	149.96	2.56	1.71	74.89	77.36	76.72	76.32	1.05	1.37	156	149.2	160.9	155.37	4.80	3.09	378	398	385	387.00	8.29	2.14
3	158.24	161.23	160.19	159.89	1.24	0.78	76.16	76.91	76.73	76.60	0.32	0.42	150.7	153.8	152.5	152.33	1.27	0.83	374	389	390	384.33	7.32	1.90
4	134.1	139.42	159.41	144.31	10.90	7.55	75.18	75.4	78	76.19	1.28	1.68	155.1	155.4	153.6	154.70	0.79	0.51	379	383	392	384.67	5.44	1.41
5	151.78	144.77	151.34	149.30	3.21	2.15	75.16	76.38	76.43	75.99	0.59	0.77	150.1	142.4	153.7	148.73	4.71	3.17	396	378	386	386.67	7.36	1.90
6	140.07	141.39	146.94	142.80	2.98	2.08	76.14	77.13	77.4	76.89	0.54	0.70	156.7	154.1	150.6	153.80	2.50	1.63	377	393	382	384.00	6.68	1.74
7	139.08	132.68	155.9	142.55	9.79	6.87	55.57	58.32	63.13	59.01	3.12	5.29	156.4	152.8	158.7	155.97	2.43	1.56	366	381	377	374.67	6.34	1.69

Table 3

Sample	Leeb	Brinell	Rockwell B	Vickers	Calculated fy	Calculated fu	Tested fy	Tested fu	difference % fy
I - 300 - 1	321	159.33	77.43	156.53	351.63	491.33	310.04	466.95	-13%
I - 300 - 2	343.33	146.81	70.27	153.13	342.45	482.83	319.09	470.58	-7%
I - 300 - 3	350	146.31	74.76	159.43	359.46	498.58	303.00	463.74	-19%
I - 300 - 4	316	145.99	77.34	149.83	333.54	474.58	303.27	466.56	-10%
I - 300 - 5	303.33	136.38	78.34	158.20	356.14	495.50	332.98	506.61	-7%
I - 300 - 6	300.33	146.92	74.72	158.90	358.03	497.25	318.49	460.56	-12%
I - 300 - 7	306.33	156.27	75.25	162.90	368.83	507.25	329.69	468.85	-12%
I - 300 - 8	291.67	155.76	79.31	172.37	394.40	530.93	339.96	500.09	-16%
I - 300 - 9	290	165.63	77.32	168.00	382.60	520.00	327.07	582.81	-17%
I - 300 - 10	315.33	160.89	75.28	166.80	379.36	517.00	321.67	573.48	-18%
I - 300 - 11	308	143.04	77.52	159.03	358.38	497.58	336.58	512.83	-6%
I - 300 - 12	320.33	139.96	73.71	165.47	375.77	513.68	345.83	543.38	-9%
I - 300 - 13	310.67	149.26	75.32	168.73	384.57	521.83	310.22	588.25	-24%
I - 300 - 14	328	129.82	77.31	154.33	345.69	485.83	315.43	476.28	-10%
I - 300 - 15	322	159.63	78.08	169.80	387.46	524.50	315.17	569.81	-23%
I - 300 - 16	345.33	136.43	74.25	159.70	360.19	499.25	339.73	518.27	-6%
I - 300 - 17	314.67	157.49	74.62	165.53	375.93	513.83	315.83	563.37	-19%
Angle 300 - 1	311.33	163.22	86.29	181.73	419.67	554.33	329.24	559.14	-27%
Angle 300 - 2	336.67	160.03	82.37	187.17	434.36	567.93	330.80	566.73	-31%
Angle 300 - 3	307.33	132.79	80.33	184.77	427.88	561.93	320.41	576.60	-34%
Angle 300 - 4	353.33	147.63	80.31	179.73	414.27	549.33	310.32	576.41	-33%
Angle 300 - 5	313.67	163.60	82.48	187.17	434.36	567.93	363.58	578.81	-19%

Angle 300 - 6	341	175.82	84.70	179.00	412.30	547.50	306.22	579.12	-35%
Angle 300 - 7	320.33	152.87	75.21	181.10	417.97	552.75	361.55	582.71	-16%
Angle 300 - 8	314.33	156.93	83.39	177.83	409.14	544.58	338.64	562.12	-21%
Angle 300 - 9	292	138.80	85.53	171.03	390.78	527.58	320.35	591.21	-22%
Angle 300 - 10	297.67	150.47	82.65	177.23	407.52	543.08	355.89	581.80	-15%
Angle 300 - 11	325.33	171.12	82.83	187.47	435.17	568.68	331.45	566.27	-31%
Angle 300 - 12	351	155.59	82.91	182.00	420.40	555.00	327.84	574.57	-28%
Plate 350 - 1	382.33	157.06	76.40	159.50	359.65	498.75	369.44	518.57	3%
Plate 350 - 2	387	149.96	76.32	155.97	350.12	489.93	360.08	529.33	3%
Plate 350 - 3	384.33	159.89	76.60	152.33	340.29	480.83	372.22	526.55	9%
Plate 350 - 4	384.67	144.31	76.19	154.70	346.69	486.75	365.19	525.04	5%
Plate 350 - 5	386.67	149.30	75.99	148.73	330.57	471.83	365.52	521.55	10%
Plate 350 - 6	384	142.80	76.89	153.80	344.26	484.50	351.62	522.13	2%
Plate 350 - 7	374.67	142.55	69.01	155.97	350.12	489.93	368.44	525.16	5%
Plate-II-350-1	371	164.10	76.79	201.57	473.24	603.93	395.27	537.55	-20%
Plate-II-350-2	370.67	160.08	76.59	213.97	506.72	634.93	407.93	537.99	-24%
Plate-II-350-3	387.33	171.10	80.29	209.47	494.57	623.68	409.71	533.64	-21%
Plate-II-350-4	379	160.33	79.67	204.00	479.80	610.00	389.08	487.03	-23%
Plate-II-350-5	385.67	159.08	78.22	199.53	467.73	598.83	397.02	489.41	-18%
Plate-II-350-6	389.33	161.80	79.54	202.67	476.21	606.68	393.21	502.23	-21%
Plate-II-350-7	382	157.78	76.23	212.63	503.10	631.58	426.61	547.88	-18%
Plate-II-350-8	384.33	167.18	80.20	194.57	454.34	586.43	420.53	555.93	-8%
Plate-II-350-9	392	170.24	70.01	205.97	485.12	614.93	418.05	550.85	-16%
Plate-II-350-10	383.67	169.90	77.17	199.67	468.11	599.18	429.42	553.66	-9%

Plate-II-350-11	388.33	175.88	78.75	215.37	510.50	638.43	416.01	546.66	-23%
Plate-II-350-12	363.67	166.50	78.62	203.03	477.18	607.58	428.69	552.19	-11%
Plate-II-350-13	367.33	166.39	81.04	200.47	470.27	601.18	419.25	553.30	-12%
Plate-II-350-14	342.67	164.44	78.36	210.20	496.54	625.50	427.14	548.96	-16%
Plate-II-350-15	393	162.05	78.01	206.37	486.20	615.93	417.97	550.67	-16%
Plate-II-350-16	345.67	169.34	79.93	217.53	516.33	643.83	435.55	585.70	-19%
Plate-II-350-17	359.33	164.92	69.99	195.13	455.85	587.83	420.41	555.68	-8%
Plate-II-350-18	382	171.26	80.06	215.17	509.96	637.93	406.06	546.75	-26%
Plate-II-350-19	367.67	154.80	71.46	205.90	484.93	614.75	408.07	550.88	-19%
Plate-II-350-20	371	157.66	77.40	217.53	516.33	643.83	410.65	545.70	-26%
Square- 400 G-1	286.33	153.23	80.60	187.07	434.09	567.68	407.72	526.46	-6%
Square- 400 G-2	278.33	151.02	83.44	177.87	409.25	544.68	402.95	526.52	-2%
Square- 400 G-3	312.33	168.47	84.08	177.97	409.52	544.93	412.13	527.92	1%
Square- 400 G-4	277.33	157.21	82.08	187.40	434.98	568.50	424.22	531.34	-3%
Square- 400 G-5	296.67	162.15	82.99	185.20	429.04	563.00	398.02	526.80	-8%
Square- 400 G-6	301.00	184.22	85.42	180.13	415.35	550.33	405.07	521.13	-3%
Square- 400 G-7	305.00	167.31	84.37	174.87	401.15	537.18	408.16	530.08	2%
Square- 400 G-8	308.00	167.36	84.87	181.43	418.86	553.58	416.57	525.50	-1%
Square- 400 G-9	317.67	186.70	85.75	176.10	404.47	540.25	409.74	529.23	1%
Square- 400 G-10	301.33	164.08	83.84	174.60	400.42	536.50	407.81	530.27	2%
Square- 400 G-11	310.00	177.22	85.12	177.37	407.90	543.43	411.36	528.34	1%
Square- 400 G-12	315.67	166.48	83.72	187.97	436.52	569.93	424.95	520.94	-3%
Square- 400 G-13	310.67	177.22	85.11	178.07	409.79	545.18	412.26	527.85	1%
Square- 400 G-14	305.67	175.57	84.27	186.20	431.74	565.50	422.68	522.17	-2%

Square- 400 G-15	312.33	175.42	82.60	193.57	451.64	583.93	432.13	517.03	-5%
Square- 400 G-16	303.00	178.86	83.87	199.00	466.30	597.50	462.84	500.30	-1%
									-12%

Table 4

Sample	Leeb	converted Vickers	Calculated fy	Calculated fu	Tested fy	Tested fu	difference % fy	difference % fu
I - 300 - 1	321	90.33	172.89	325.82	310.04	466.95	44%	30%
I - 300 - 2	343.33	101.98	204.35	354.95	319.09	470.58	36%	25%
I - 300 - 3	350	105.80	214.65	364.49	303.00	463.74	29%	21%
I - 300 - 4	316	87.97	166.52	319.92	303.27	466.56	45%	31%
I - 300 - 5	303.33	82.43	151.56	306.07	332.98	506.61	54%	40%
I - 300 - 6	300.33	81.21	148.27	303.03	318.49	460.56	53%	34%
I - 300 - 7	306.33	83.68	154.94	309.21	329.69	468.85	53%	34%
I - 300 - 8	291.67	77.91	139.36	294.78	339.96	500.09	59%	41%
I - 300 - 9	290	77.31	137.74	293.28	327.07	582.81	58%	50%
I - 300 - 10	315.33	87.66	165.68	319.15	321.67	573.48	48%	44%
I - 300 - 11	308	84.40	156.87	310.99	336.58	512.83	53%	39%
I - 300 - 12	320.33	90.01	172.02	325.02	345.83	543.38	50%	40%
I - 300 - 13	310.67	85.56	160.01	313.90	310.22	588.25	48%	47%
I - 300 - 14	328	93.79	182.23	334.47	315.43	476.28	42%	30%

I - 300 - 15	322	90.81	174.19	327.03	315.17	569.81	45%	43%
I - 300 - 16	345.33	103.11	207.40	357.77	339.73	518.27	39%	31%
I - 300 - 17	314.67	87.36	164.87	318.40	315.83	563.37	48%	43%
Angle 300 - 1	311.33	85.85	160.80	314.63	329.24	559.14	51%	44%
Angle 300 - 2	336.67	98.32	194.47	345.81	330.80	566.73	41%	39%
Angle 300 - 3	307.33	84.11	156.09	310.27	320.41	576.60	51%	46%
Angle 300 - 4	353.33	107.76	219.94	369.39	310.32	576.41	29%	36%
Angle 300 - 5	313.67	86.90	163.64	317.26	363.58	578.81	55%	45%
Angle 300 - 6	341	100.68	200.85	351.71	306.22	579.12	34%	39%
Angle 300 - 7	320.33	90.01	172.02	325.02	361.55	582.71	52%	44%
Angle 300 - 8	314.33	87.20	164.45	318.01	338.64	562.12	51%	43%
Angle 300 - 9	292	78.03	139.68	295.08	320.35	591.21	56%	50%
Angle 300 - 10	297.67	80.16	145.44	300.41	355.89	581.80	59%	48%
Angle 300 - 11	325.33	92.45	178.61	331.12	331.45	566.27	46%	42%
Angle 300 - 12	351	106.38	216.23	365.95	327.84	574.57	34%	36%
Plate 350 - 1	382.33	126.27	269.93	415.67	369.44	518.57	27%	20%
Plate 350 - 2	387	129.48	278.60	423.70	360.08	529.33	23%	20%
Plate 350 - 3	384.33	127.64	273.62	419.09	372.22	526.55	26%	20%
Plate 350 - 4	384.67	127.87	274.25	419.68	365.19	525.04	25%	20%
Plate 350 - 5	386.67	129.25	277.98	423.13	365.52	521.55	24%	19%
Plate 350 - 6	384	127.41	273.01	418.53	351.62	522.13	22%	20%
Plate 350 - 7	374.67	121.13	256.06	402.84	368.44	525.16	31%	23%
Plate-II-350-1	371	118.74	249.59	396.84	395.27	537.55	37%	26%
Plate-II-350-2	370.67	118.52	249.01	396.30	407.93	537.99	39%	26%
Plate-II-350-3	387.33	129.71	279.22	424.28	409.71	533.64	32%	20%
Plate-II-350-4	379	124.02	263.84	410.04	389.08	487.03	32%	16%
Plate-II-350-5	385.67	128.56	276.11	421.40	397.02	489.41	30%	14%

Plate-II-350-6	389.33	131.11	282.99	427.77	393.21	502.23	28%	15%
Plate-II-350-7	382	126.04	269.32	415.11	426.61	547.88	37%	24%
Plate-II-350-8	384.33	127.64	273.62	419.09	420.53	555.93	35%	25%
Plate-II-350-9	392	132.99	288.07	432.47	418.05	550.85	31%	21%
Plate-II-350-10	383.67	127.18	272.40	417.96	429.42	553.66	37%	25%
Plate-II-350-11	388.33	130.41	281.10	426.02	416.01	546.66	32%	22%
Plate-II-350-12	363.67	114.06	236.97	385.16	428.69	552.19	45%	30%
Plate-II-350-13	367.33	116.38	243.22	390.94	419.25	553.30	42%	29%
Plate-II-350-14	342.67	101.61	203.35	354.03	427.14	548.96	52%	36%
Plate-II-350-15	393	133.70	289.98	434.24	417.97	550.67	31%	21%
Plate-II-350-16	345.67	103.30	207.92	358.26	435.55	585.70	52%	39%
Plate-II-350-17	359.33	111.38	229.71	378.44	420.41	555.68	45%	32%
Plate-II-350-18	382	126.04	269.32	415.11	406.06	546.75	34%	24%
Plate-II-350-19	367.67	116.59	243.80	391.48	408.07	550.88	40%	29%
Plate-II-350-20	371	118.74	249.59	396.84	410.65	545.70	39%	27%
Square- 400 G-1	409.67	145.92	322.99	464.80	407.72	526.46	21%	12%
Square- 400 G-2	391.67	132.75	287.44	431.89	402.95	526.52	29%	18%
Square- 400 G-3	405	142.42	313.54	456.06	412.13	527.92	24%	14%
Square- 400 G-4	405.67	142.92	314.89	457.30	424.22	531.34	26%	14%
Square- 400 G-5	396.67	136.32	297.08	440.81	398.02	526.80	25%	16%
Square- 400 G-6	397.67	137.05	299.03	442.62	405.07	521.13	26%	15%
Square- 400 G-7	411.67	147.44	327.08	468.59	408.16	530.08	20%	12%
Square- 400 G-8	398	137.29	299.67	443.21	416.57	525.50	28%	16%
Square- 400 G-9	407.67	144.42	318.92	461.04	409.74	529.23	22%	13%
Square- 400 G-10	391.33	132.51	286.79	431.28	407.81	530.27	30%	19%
Square- 400 G-11	406.67	143.67	316.90	459.17	411.36	528.34	23%	13%
Square- 400 G-12	409	145.42	321.62	463.54	424.95	520.94	24%	11%

Square- 400 G-13	397.33	136.80	298.36	442.00	412.26	527.85	28%	16%
Square- 400 G-14	409	145.42	321.62	463.54	422.68	522.17	24%	11%
Square- 400 G-15	412.33	147.94	328.44	469.85	432.13	517.03	24%	9%
Square- 400 G-16	406.33	143.41	316.22	458.53	462.84	500.30	32%	8%
							38%	**28%**

Table 5: Comparison between Charpy and hardness test

		CHARPY Impact Energy	CHARPY Impact Toughness	Brinell	STDEV	Error %	Rockwell B	STDEV	Error %	Vickers	STDEV	Error %	Leeb	STDEV	Error %
I - 300	**I - 300 - 1**	98.48	89.70	159.33	0.67	0%	77.43	0.41	1%	156.53	5.14	3%	321.00	6.98	6%
I - 300	**I - 300 - 2 F**	69.14	69.09	146.81	2.31	2%	70.27	5.77	8%	153.13	2.50	2%	343.33	2.83	6%
I - 300	**I - 300 - 3 F**	70.60	70.34	146.31	19.79	14%	74.76	3.49	5%	159.43	2.44	2%	350.00	8.16	5%
I - 300	**I - 300 - 4 F**	73.08	72.46	145.99	8.93	6%	77.34	0.42	1%	149.83	4.68	3%	316.00	9.42	4%
I - 300	**I - 300 - 5**	82.91	88.86	136.38	12.09	9%	78.34	0.42	1%	158.20	1.98	1%	303.33	7.41	6%
I - 300	**I - 300 - 6**	88.00	87.78	146.92	5.61	4%	74.72	1.39	2%	158.90	4.82	3%	300.33	6.24	11%
I - 300	**I - 300 - 7**	97.97	93.49	156.27	8.76	6%	75.25	1.18	2%	162.90	3.41	2%	306.33	9.84	9%
I - 300	**I - 300 - 8**	81.71	95.75	155.76	4.73	3%	79.31	0.94	1%	172.37	3.00	2%	291.67	5.25	8%
I - 300	**I - 300 - 9**	96.85	91.32	165.63	5.40	3%	77.32	1.05	1%	168.00	10.13	6%	290.00	4.97	7%
I - 300	**I - 300 - 10**			160.89	5.16	3%	75.28	0.86	1%	166.80	4.68	3%	315.33	8.5	11%
I - 300	**I - 300 - 11**			143.04	7.40	5%	77.52	0.44	1%	159.03	4.97	3%	308.00	2.94	5%
I - 300	**I - 300 - 12**			139.96	13.91	10%	73.71	1.74	2%	165.47	1.72	1%	320.33	8.99	7%
I - 300	**I - 300 - 13**			149.26	4.87	3%	75.32	2.15	3%	168.73	4.03	2%	310.67	9.03	11%
I - 300	**I - 300 - 14**			129.82	6.81	5%	77.31	1.14	1%	154.33	6.27	4%	328.00	8.6	9%

I - 300	**I - 300 - 15**			159.63	4.94	3%	78.08	0.23	0%	169.80	7.42	4%	322.00	3.74	11%
I - 300	**I - 300 - 16**			136.43	2.99	2%	74.25	3.23	4%	159.70	9.51	6%	345.33	8.22	10%
I - 300	**I - 300 - 17**			157.49	3.51	2%	74.62	2.71	4%	165.53	4.00	2%	314.67	9.39	11%
Angle 300	**Angle 300 - 1**	68.26	94.81	163.22	4.51	3%	86.29	1.02	1%	181.73	5.42	3%	311.33	8.65	11%
Angle 300	**Angle 300 - 2**	65.38	90.81	160.03	8.50	5%	82.37	1.81	2%	187.17	5.45	3%	336.67	8.96	8%
Angle 300	**Angle 300 - 3**	71.07	88.71	132.79	13.52	10%	80.33	2.23	3%	184.77	0.60	0%	307.33	10.5	10%
Angle 300	**Angle 300 - 4**	66.82	82.49	147.63	16.73	11%	80.31	1.65	2%	179.73	5.07	3%	353.33	9.46	7%
Angle 300	**Angle 300 - 5**	73.02	91.42	163.60	10.03	6%	82.48	0.72	1%	187.17	1.99	1%	313.67	7.41	10%
Angle 300	**Angle 300 - 6**	67.51	93.76	175.82	8.32	5%	84.70	0.63	1%	179.00	6.08	3%	341.00	10.71	11%
Angle 300	**Angle 300 - 7**	59.16	82.17	152.87	5.60	4%	75.21	4.97	7%	181.10	3.37	2%	320.33	10.66	15%
Angle 300	**Angle 300 - 8**	60.81	92.48	156.93	10.24	7%	83.39	1.47	2%	177.83	1.49	1%	314.33	5.79	13%
Angle 300	**Angle 300 - 9**			138.80	5.19	4%	85.53	0.51	1%	171.03	12.59	7%	292.00	6.68	7%
Angle 300	**Angle 300 - 10**			150.47	10.84	7%	82.65	1.11	1%	177.23	2.85	2%	297.67	6.18	11%
Angle 300	**Angle 300 - 11**			171.12	9.88	6%	82.83	1.08	1%	187.47	5.99	3%	325.33	7.93	13%
Angle 300	**Angle 300 - 12**			155.59	5.26	3%	82.91	1.64	2%	182.00	2.71	1%	351.00	8.83	6%
Plate 350	**Plate 350 - 1**	96.66	107.40	157.06	0.92	1%	76.40	0.05	0%	159.50	5.65	4%	382.33	9.46	3%
Plate 350	**Plate 350 - 2**	94.46	104.96	149.96	2.56	2%	76.32	1.05	1%	155.97	4.80	3%	387.00	8.29	7%
Plate 350	**Plate 350 - 3**	96.86	107.62	159.89	1.24	1%	76.60	0.32	0%	152.33	1.27	1%	384.33	7.32	5%
Plate 350	**Plate 350 - 4**	107.06	103.96	144.31	10.90	11%	76.19	1.28	2%	154.70	0.79	1%	384.67	5.44	5%
Plate 350	**Plate 350 - 5**	89.13	101.28	149.30	3.21	3%	75.99	0.59	1%	148.73	4.71	3%	386.67	7.36	6%

Plate 350	**Plate 350 - 6**	103.12	108.90	142.80	2.98	3%	76.89	0.54	1%	153.80	2.50	2%	384.00	6.68	3%
Plate 350	**Plate 350 - 7**	90.90	101.00	142.55	9.79	16%	69.01	3.12	5%	155.97	2.43	2%	374.67	6.34	3%
Plate-II-350	**Plate-II-350-1**	87.23	96.92	164.10	5.58	3%	76.79	0.97	1%	201.57	5.84	3%	371.00	11.05	12%
Plate-II-350	**Plate-II-350-2**	89.47	106.41	160.08	13.70	9%	76.59	3.95	5%	213.97	8.72	4%	370.67	8.99	8%
Plate-II-350	**Plate-II-350-3**	99.64	114.55	171.10	7.21	4%	80.29	0.48	1%	209.47	11.88	6%	387.33	8.65	5%
Plate-II-350	**Plate-II-350-4**	100.08	111.20	160.33	9.76	6%	79.67	1.74	2%	204.00	4.04	2%	379.00	9.9	9%
Plate-II-350	**Plate-II-350-5**	103.90	99.87	159.08	10.65	7%	78.22	1.65	2%	199.53	6.04	3%	385.67	9.46	5%
Plate-II-350	**Plate-II-350-6**	94.66	108.32	161.80	9.82	6%	79.54	0.88	1%	202.67	4.22	2%	389.33	2.62	7%
Plate-II-350	**Plate-II-350-7**	98.01	102.51	157.78	15.45	10%	76.23	2.37	3%	212.63	0.95	0%	382.00	9.93	9%
Plate-II-350	**Plate-II-350-8**	102.91	114.34	167.18	2.52	2%	80.20	1.04	1%	194.57	6.71	3%	384.33	7.72	5%
Plate-II-350	**Plate-II-350-9**			170.24	4.67	3%	70.01	3.87	6%	205.97	4.29	2%	392.00	8.64	3%
Plate-II-350	**Plate-II-350-10**			169.90	11.00	6%	77.17	2.36	3%	199.67	3.55	2%	383.67	8.65	7%
Plate-II-350	**Plate-II-350-11**			175.88	6.28	4%	78.75	1.99	3%	215.37	3.94	2%	388.33	5.56	7%
Plate-II-350	**Plate-II-350-12**			166.50	12.06	7%	78.62	1.44	2%	203.03	2.45	1%	363.67	3.77	3%
Plate-II-350	**Plate-II-350-13**			166.39	5.33	3%	81.04	0.37	0%	200.47	3.24	2%	367.33	10.34	6%
Plate-II-350	**Plate-II-350-14**			164.44	10.79	7%	78.36	0.29	0%	210.20	4.95	2%	342.67	6.02	4%
Plate-II-350	**Plate-II-350-15**			162.05	14.90	9%	78.01	1.55	2%	206.37	5.88	3%	393.00	9.2	6%
Plate-II-350	**Plate-II-350-16**			169.34	11.14	7%	79.93	1.34	2%	217.53	3.14	1%	345.67	6.65	5%
Plate-II-350	**Plate-II-350-17**			164.92	9.12	6%	69.99	1.06	2%	195.13	2.58	1%	359.33	7.41	6%
Plate-II-350	**Plate-II-350-18**			171.26	6.11	4%	80.06	1.48	2%	215.17	6.60	3%	382.00	8.52	6%

Plate-II-350	**Plate-II-350-19**			154.80	9.33	6%	71.46	5.48	8%	205.90	5.39	3%	367.67	9.46	8%
Plate-II-350	**Plate-II-350-20**			157.66	9.73	6%	77.40	3.10	4%	217.53	5.73	3%	371.00	11.52	10%
Square- 400	**Square- 400 G-1**	74.88	133.25	153.23	11.33	7%	80.60	3.41	4%	187.07	3.47	2%	286.33	13.82	5%
Square- 400	**Square- 400 G-2**	69.11	131.41	151.02	11.93	8%	83.44	0.29	0%	177.87	5.23	3%	278.33	19.60	7%
Square- 400	**Square- 400 G-3**	73.44	131.14	168.47	19.86	12%	84.08	0.03	0%	177.97	4.74	3%	312.33	15.46	5%
Square- 400	**Square- 400 G-4**	83.63	133.71	157.21	10.72	7%	82.08	1.29	2%	187.40	2.90	2%	277.33	21.06	8%
Square- 400	**Square- 400 G-5**	69.99	127.20	162.15	16.57	10%	82.99	0.67	1%	185.20	2.05	3%	296.67	22.81	8%
Square- 400	**Square- 400 G-6**	85.99	128.64	184.22	8.07	4%	85.42	0.53	1%	180.13	8.43	5%	301.00	16.31	5%
Square- 400	**Square- 400 G-7**	75.52	124.89	167.31	7.42	4%	84.37	0.22	0%	174.87	2.70	2%	305.00	19.44	6%
Square- 400	**Square- 400 G-8**	66.79	124.36	167.36	1.09	1%	84.87	0.95	1%	181.43	2.76	2%	308.00	16.87	5%
Square- 400	**Square- 400 G-9**			186.70	6.06	3%	85.75	0.36	0%	176.10	2.87	2%	317.67	14.08	4%
Square- 400	**Square- 400 G-10**			164.08	2.30	1%	83.84	0.56	1%	174.60	7.21	4%	301.33	16.74	6%
Square- 400	**Square- 400 G-11**			177.22	6.62	4%	85.12	0.57	1%	177.37	4.82	3%	310.00	12.08	4%
Square- 400	**Square- 400 G-12**			166.48	6.95	4%	83.72	0.69	1%	187.97	1.72	1%	315.67	14.88	5%
Square- 400	**Square- 400 G-13**			177.22	2.78	2%	85.11	0.75	1%	178.07	4.54	3%	310.67	21.91	7%
Square- 400	**Square- 400 G-14**			175.57	9.22	5%	84.27	0.64	1%	186.20	1.14	1%	305.67	12.23	22%
Square- 400	**Square- 400 G-15**			175.42	5.98	3%	82.60	0.57	1%	193.57	2.64	1%	312.33	7.36	2%
Square- 400	**Square- 400 G-16**			178.86	7.12	4%	83.87	0.96	1%	217.53	3.14	1%	303.00	12.83	4%
	Average				8.02	5%		1.4	1.9%		4.4	2.5%		9.65	6.8%